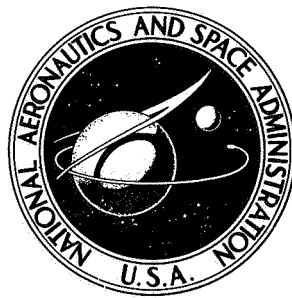


NASA TECHNICAL NOTE



NASA TN D-7539

NASA TN D-7539

FLUTTER ANALYSIS OF
SWEPT-WING SUBSONIC AIRCRAFT
WITH PARAMETER STUDIES
OF COMPOSITE WINGS

by J. M. Housner and Manuel Stein

Langley Research Center

Hampton, Va. 23665



NATIONAL AERONAUTICS AND SPACE ADMINISTRATION • WASHINGTON, D. C. • SEPTEMBER 1974

FLUTTER ANALYSIS OF SWEEP-WING SUBSONIC AIRCRAFT WITH PARAMETER STUDIES OF COMPOSITE WINGS

By J. M. Housner and Manuel Stein
Langley Research Center

SUMMARY

This paper presents a computer program which has been developed for the flutter analysis, including the effects of rigid-body roll, pitch, and plunge, of swept-wing subsonic aircraft with a flexible fuselage and engines mounted on flexible pylons. The program utilizes a direct flutter solution in which the flutter determinant is derived by using finite differences, and the root locus branches of the determinant are searched for the lowest flutter speed. In addition, a preprocessing subroutine is included which evaluates the variable bending and twisting stiffness properties of the wing by using a laminated, balanced ply, filamentary composite plate theory. The program has been substantiated by comparisons with existing flutter solutions.

The program has been applied to parameter studies which examine the effect of filament orientation upon the flutter behavior of wings belonging to the following three classes: wings having different angles of sweep, wings having different mass ratios, and wings having variable skin thicknesses. These studies demonstrated that the program can perform a complete parameter study in one computer run. The program is designed to detect abrupt changes in the lowest flutter speed and mode shape as the parameters are varied.

INTRODUCTION

The use of filamentary composite materials in aircraft structures offers a great potential for weight savings over conventional (all-metal) construction. Composites also introduce added versatility into the design process by allowing the structure to be better tailored to meet the design criteria. One such criterion is the prevention of flutter in a designated flight regime. The flutter speed can be quite sensitive to the distribution of structural stiffness. With the added versatility of composite material, the stiffness distribution can be tailored to avoid flutter by controlling the filament orientation in each lamina of the structural wing box.

Flutter is a complex phenomenon and the designer and analyst may have little intuitive feel for flutter even in all-metal airplanes since, in addition to the stiffness

distribution, the flutter speed may be highly dependent upon the mass distribution, especially the placement of engines, the flexibility of their supporting pylons, the rigid-body degrees of freedom of the plane, and the flexibility and mass of the fuselage. Furthermore, it is the lowest flutter speed which is critical to the design and this speed can be significantly different in two seemingly similar designs since the lowest flutter speed may be associated with a different flutter mode in each design. Consequently, it would be desirable to have a computer program capable of analyzing the flutter behavior of composite-wing aircraft and determining the influence on the lowest flutter speed of composite structural parameters (such as filament orientation and lamina thickness) as well as other structural parameters (such as engine mass and fuselage stiffness).

The purpose of this paper is to present a flutter analysis program applicable to parametric studies of swept-wing aircraft and to apply it to study some of the flutter characteristics of composite wings. The program, which is written in FORTRAN IV, includes the effects of rigid-body roll, pitch, and plunge and is applicable to both symmetric and antisymmetric flutter modes. In addition, the effects of engines mounted on flexible pylons and a flexible fuselage are incorporated into the program.

The wing is modeled as a bending-twisting beam and the aerodynamic loads are modeled from modified swept-wing strip theory (refs. 1 to 3) in which finite aspect ratio and compressibility effects may be approximately accounted for. The program uses a direct flutter analysis approach in which the flutter determinant is derived from energy considerations using finite differences. The root locus branches of the determinant are searched for the lowest flutter speed.

The program contains a preprocessing subroutine which evaluates the variable bending and twisting stiffness properties of the wing by using a laminated, balanced ply, elementary composite plate theory. The program also allows a parameter of interest (e.g., filament orientation, lamina thickness, and fuselage stiffness) to be automatically incremented over a user specified range, and the critical flutter speed is found at each parameter value. The program is demonstrated by studying the effect of filament orientation on the lowest flutter speed of wings belonging to the following three classes: (1) wings having different angles of sweep, (2) wings having different mass ratios, and (3) wings having variable lamina thickness.

The program has been verified by comparison with examples found in the literature (refs. 4 to 6) and with the SADSAM computer program (ref. 7). The difficulty of determining the lowest flutter speed is illustrated by discussing an example reported in reference 5. The present program predicted the same flutter speed as reference 5 but in addition found two lower flutter speeds.

SYMBOLS

A_r	coefficients of superimposed displacement field as defined in equation (D3)
$a_{11}, a_{12}, a_{22}, a_{33}$	elements of elastic matrix as defined by equations (9) to (11)
\bar{a}, a	local dimensional and nondimensional offsets of elastic axis from midchord, respectively (positive towards trailing edge), $a = \frac{\bar{a}}{b_r}$
\bar{a}_c, a_c	local dimensional and nondimensional offsets of aerodynamic center from midchord, respectively (positive towards trailing edge), $a_c = \frac{\bar{a}_c}{b_r}$
b_r	reference value of semichord
\bar{b}, b	local dimensional and nondimensional semichords of airfoil normal to elastic axis, respectively, $b = \frac{\bar{b}}{b_r}$
\bar{b}^*	local semichord of wing box
$C(k)$	Theodorsen's circulation function
c_{l_α}	local lift-curve slope
D	complex flutter determinant
\bar{d}, d	dimensional and nondimensional fuselage diameter, respectively, $d = \frac{\bar{d}}{\bar{l}}$
E_l, E_t	Young's moduli parallel and transverse to filaments, respectively
$(EI)_p$	pylon and/or fuselage bending stiffness
$(EI)_r$	reference value of wing bending stiffness
\bar{EI}, EI	local dimensional and nondimensional wing bending stiffness, respectively, $EI = \frac{\bar{EI}}{(EI)_r}$
e	elements of flutter determinant defined by equation (D4)

- G_{zt} composite shear modulus
- $(GJ)_p$ pylon and/or fuselage torsional stiffnesses
- \bar{GJ}, GJ local dimensional and nondimensional torsional stiffnesses of wing,
 respectively, $GJ = \frac{\bar{GJ}}{(EI)_r}$
- h_p upward vertical displacement of any point along pylon
- \bar{h}, h local dimensional and nondimensional upward vertical displacements of
 elastic axis, respectively, $h = \frac{\bar{h}}{b_r}$
- J_c Jacobian of flutter determinant defined by equation (D2)
- k reduced frequency, $\frac{b_r \omega}{V}$
- $k_n = \frac{k}{\cos \Lambda}$
- \bar{L}, L dimensional and nondimensional lengths of pylons, respectively, $L = \frac{\bar{L}}{b_r}$
- \bar{l} length of wing along elastic axis
- M_p bending moment on pylon at root
- m_r reference mass per unit length along wing elastic axis
- \bar{m}, m local dimensional and nondimensional mass distributions per unit length along
 elastic axis, respectively, $m = \frac{\bar{m}}{m_r}$
- \bar{m}_e, m_e dimensional and nondimensional mass of engines, respectively, $m_e = \frac{\bar{m}_e}{m_r \bar{l}}$
- $\bar{m}_e \bar{J}_e, m_e J_e$ dimensional and nondimensional rotational inertias of engine masses,
 respectively, $m_e J_e = \frac{\bar{m}_e \bar{J}_e}{m_r \bar{l}^3}$
- N number of finite-difference stations

N_L	number of composite reinforced laminas in each cover face
$Q_{11}, Q_{12}, Q_{22}, Q_{66}$	elements of reduced stiffness matrix defined in equations (12) to (15)
\bar{Q}_h, Q_h	local dimensional and nondimensional upward aerodynamic lifts per unit length of elastic axis on wings, respectively, $Q_h = \frac{\bar{Q}_h \bar{l}^4}{b_r (EI)_r}$
\bar{Q}_α, Q_α	local dimensional and nondimensional aerodynamic torques on wings, respectively, $Q_\alpha = \frac{\bar{Q}_\alpha \bar{l}^2}{(EI)_r}$
\bar{q}_h, q_h	dimensional and nondimensional upward vertical loads, respectively, applied to wings by pylons, $q_h = \frac{\bar{q}_h \bar{l}^4}{b_r (EI)_r}$
\bar{q}_m, q_m	dimensional and nondimensional bending moments, respectively, applied to wings by pylons, $q_m = \frac{\bar{q}_m \bar{l}^3}{b_r (EI)_r}$
\bar{q}_α, q_α	dimensional and nondimensional torques, respectively, applied to wings by pylons, $q_\alpha = \frac{\bar{q}_\alpha \bar{l}^2}{(EI)_r}$
R	ratio of wing length along elastic axis to reference semichord, $\frac{\bar{l}}{b_r}$
\bar{r}_α, r_α	local dimensional and nondimensional radii of gyration, respectively, of wing about elastic axis, $r_\alpha = \frac{\bar{r}_\alpha}{b_r}$
T	kinetic energy of wings
T_p	torque applied to pylon at its root
U	strain energy of wings
\bar{u}	wing displacements along elastic axis

V	airspeed
\bar{v}	chordwise wing displacement, positive towards trailing edge
\bar{w}	upward vertical displacement of wing
$\delta W_a, \delta W_e$	virtual work of air loads and engine masses, respectively
x,y,z	aircraft coordinate system as shown in figure 1
x_p	axial coordinate of pylon
\bar{x}_α, x_α	local dimensional and dimensionless offsets of wing center of gravity from elastic axis, $x_\alpha = \frac{\bar{x}_\alpha}{b_r}$
α	twist of wing, positive leading edge up
β	quantity defined by equation (E11)
$\bar{\epsilon}, \epsilon$	dimensional and nondimensional distances, respectively, between adjacent finite-difference stations, $\epsilon = \frac{\bar{\epsilon}}{\bar{l}}$
ζ_j	thickness coordinate of jth lamina
$\bar{\eta}$	coordinate of wing along elastic axis
Θ	pitch about Y-axis
θ	angle of filament orientation, measured from $\bar{\eta}$ axis
κ	reference wing mass ratio, $\frac{\pi \rho b_r^2}{m_r}$
Λ	sweep angle
λ	nondimensional dynamic pressure, $\frac{\rho b_r \bar{l}^3 V^2}{(EI)_r}$

ν_{zt}, ν_{tz}	Poisson's ratios for the composite material
$\bar{\xi}$	chordwise coordinate of wing, positive towards trailing edge
ρ	air density
$\sigma_{\eta}, \sigma_{\xi}, \sigma_{\eta\xi}$	stress components in wing
ϕ	roll angle about X-axis
Ω	nondimensional frequency, $\omega \bar{t}^2 \left[\frac{m_r}{(EI)_r} \right]^{1/2}$
ω	circular frequency

ANALYSIS

Assumptions and Governing Equations

Consider the model of a swept-wing subsonic aircraft with engines and flexible fuselage as shown in figure 1. The following assumptions concerning this model have been made:

(1) All deformations are sufficiently small so that the governing dynamic equations are linear.

(2) In-plane motions of the airplane are neglected; hence, only roll, pitch, and plunge of any point of the plane are allowed.

(3) The tapered, variable-thickness wings are modeled as beams having an arbitrary distribution of bending and twisting stiffnesses.

(4) The engines are modeled as lumped masses (having rolling and plunging inertias) extended out in the plane of the wings mounted on flexible, massless pylons. The pylons are modeled as bending-twisting beams rigidly attached to the wings at the elastic axis.

(5) A rigid carry-through beam joins the two wings and is rigidly attached to the elastic axes.

(6) The fuselage is modeled as two flexible, massless, bending-twisting beams, one extending fore and the other aft of the wings. Each beam has a lumped mass at its tip with rolling and plunging inertia. The fuselage beams are rigidly attached to the carry-through beam.

The aerodynamic loads are provided from modified swept-wing strip theory as given in references 1 to 3 and repeated for completeness in appendix A. Air loads which do not act on the wings themselves are neglected. Due to the symmetry of the problem only symmetric and antisymmetric flutter modes need be investigated; however, the limiting case of cantilever wing flutter is also considered.

For harmonic motion, the lateral and torsional deflections of the wing may be expressed as

$$\bar{h} = \bar{h}_0 e^{i\omega t} \quad (1)$$

$$\alpha = \alpha_0 e^{i\omega t} \quad (2)$$

where \bar{h}_0 and α_0 are complex amplitudes, ω is circular frequency, and t is time. The governing equations which are valid for symmetric, antisymmetric, and cantilever wing harmonic motions are derived in finite-difference form in appendices B and C. They may be expressed as

$$\left\{ [\mathbf{S}] - \Omega^2 [\mathbf{M}] - [\mathbf{A}(\lambda, \Omega)] \right\} [\mathbf{q}] = 0 \quad (3)$$

where $[\mathbf{S}]$, $[\mathbf{M}]$, and $[\mathbf{A}]$ are the stiffness, mass, and aerodynamic load matrices, respectively. (The complex matrix $[\mathbf{A}]$ does not include the mass effects of the air surrounding the wing; these effects are incorporated into matrix $[\mathbf{M}]$.) Also in equation (3), $[\mathbf{q}]$ is the column of generalized displacements of the model, λ is the dimensionless dynamic pressure, and Ω is the dimensionless complex frequency.

For a given value of λ , equation (3) represents a complex eigenvalue problem, for which a set of eigenvalues $\Omega = \Omega_R + i\Omega_I$ and eigenvectors $[\mathbf{q}]$ exist. Each pair of values (λ, Ω) represent a root of the flutter determinant associated with equation (3) and the loci of all such roots constitute the root locus branches of equation (3) as shown in figure 2. Stable roots of equation (3) are those for which $\Omega_I > 0$. Consequently, flutter is indicated by a change in sign of Ω_I from positive to negative and may be found by tracing the root locus branches.

Numerical Procedure for Tracing the Root Locus Branches and Determining Flutter

The root locus branches are searched for flutter in the following manner:

(1) At zero airspeed, $\lambda = 0$, all the branches emanate from the natural frequencies of the system when the effective mass of the air is taken into account because

$$\lim_{\lambda \rightarrow 0} [A(\lambda, \Omega)] = 0 \quad (4)$$

For this reason the natural frequencies are found first; in the computer program, these frequencies are found with a determinant plotting routine.

(2) The branches are then traced by incrementing λ from zero with the natural frequencies, determined in step (1), as starting points.

(3) For each value of λ , the complex eigenvalue Ω is found by driving the flutter determinant to zero by using a Newton-Raphson scheme whose iterative steps are given in appendix D.

(4) A flutter instability is indicated by the vanishing of the imaginary part of the complex frequency; hence, each branch is traced out until flutter is indicated or a maximum airspeed is attained. (As discussed in a subsequent section, traces need not necessarily start at $\lambda = 0$.)

Preprocessing the Wing Stiffness Distributions

In this section, the bending and twisting stiffness distributions of the wing are presented for a laminated, balanced ply, elementary composite wing box as shown in figure 3.

The cover of each box contains N_L layers and each layer contains an equal number of filaments oriented in the plus and minus θ_j directions ($j = 1, 2, \dots, N_L$). The filament orientation angle θ_j and the lamina thickness t_j may be variable along the span and different in each lamina; however, complete symmetry is assumed to exist between the top and bottom covers of the box.

It is assumed that the deformations of the wing obey the usual thin-plate Bernoulli-Euler assumptions and that chordwise bending may be neglected. On this basis, the bending and twisting stiffnesses of the wings, as derived in appendix E for cross sections normal to the elastic axis, are

$$\overline{EI} = \frac{4}{3} \bar{b}^* \sum_{j=1}^{N_L} (\zeta_j^3 - \zeta_{j-1}^3) a_{11,j} \quad (5)$$

$$\overline{GJ} = \frac{16}{3} \bar{b}^* \sum_{j=1}^{N_L} (\zeta_j^3 - \zeta_{j-1}^3) a_{33,j} \quad (6)$$

where \bar{b}^* is the semichord of the structural wing box as shown in figure 3 and

$$\zeta_0 = z_T \quad (7)$$

$$\zeta_j = \zeta_{j-1} + t_j \quad (j = 1, \dots, N_L) \quad (8)$$

in which z_T is the distance of the upper and lower covers of the box from the middle surface of the box. (See fig. 3.) In addition $a_{11,j}$ and $a_{33,j}$ are coefficients of the following elastic matrix which defines the orthotropic stress-strain law (ref. 8) in the j th lamina with filaments oriented in the plus and minus θ_j directions:

$$\begin{bmatrix} \sigma_{\eta,j} \\ \sigma_{\xi,j} \\ \sigma_{\eta\xi,j} \end{bmatrix} = \begin{bmatrix} a_{11,j} & a_{12,j} & 0 \\ a_{12,j} & a_{22,j} & 0 \\ 0 & 0 & 2a_{33,j} \end{bmatrix} \begin{bmatrix} \epsilon_{\eta} \\ \epsilon_{\xi} \\ \epsilon_{\eta\xi} \end{bmatrix} \quad (9)$$

From reference 8 the coefficients of the elastic matrix are given by

$$a_{11,j} = 2 \left[Q_{11} \cos^4 \theta_j + 2(Q_{12} + 2Q_{66}) \sin^2 \theta_j \cos^2 \theta_j + Q_{22} \sin^4 \theta_j \right] \quad (10)$$

$$a_{33,j} = 2 \left[(Q_{11} + Q_{22} - 2Q_{12} - 2Q_{66}) \sin^2 \theta_j \cos^2 \theta_j + Q_{66} (\sin^4 \theta_j + \cos^4 \theta_j) \right] \quad (11)$$

where $[Q]$ is the reduced stiffness matrix whose elements are

$$Q_{11} = \frac{E_l}{1 - \nu_{lt}\nu_{tl}} \quad (12)$$

$$Q_{22} = \frac{E_t}{1 - \nu_{lt}\nu_{tl}} \quad (13)$$

$$Q_{12} = \frac{\nu_{lt}E_t}{1 - \nu_{lt}\nu_{tl}} \quad (14)$$

$$Q_{66} = G_{zt} \quad (15)$$

In equations (12) to (15), E_l and E_t are the Young's moduli parallel and transverse to the filaments, respectively, and G_{zt} is the shear modulus. Equations (5) and (6) may be readily reduced to the case of an isotropic wing and to the case of a solid wing.

COMPUTER PROGRAM

Description

A computer program denoted COMBOF (Composite Box Beam Flutter) has been developed for the flutter analysis of swept-wing subsonic aircraft. The aircraft model contains a flexible fuselage and allows the engines to be mounted on flexible pylons. In addition the program takes into account the effects of rigid-body roll, pitch, and plunge.

The user has the option of either supplying the bending and twisting stiffness distributions of the wing or supplying the reduced stiffness matrix, filament orientation, and lamina thickness of a composite wing and allowing the program to automatically calculate the stiffness distribution of the wing by using a preprocessing subroutine governed by equations (5) to (15). When the preprocessor option is used, the program can perform a complete parameter study in one computer run, consecutively incrementing a parameter (e.g., fiber orientation, lamina thickness) over a range of interest. When calculating the flutter speed in such parameter studies, it may be possible to start from the flutter speed and frequency corresponding to the previous value of the parameter and to trace only the previous critical branch. Use of the previous lowest flutter speed in such a manner is reasonable so long as the lowest flutter speed or its associated frequency does not change discontinuously as the parameter is incremented. However, it may happen that as the parameter is incremented, a lower flutter speed may appear whose associated mode shape is different from that at the previous parameter value. This situation implies that the lowest flutter speed and/or its associated frequency have changed discontinuously with the parameter increment. In order to avoid such discontinuities, periodic searches of all the branches, starting from $\lambda = 0$, are automatically performed by the program.

The flow diagram of figure 4 shows the logic in COMBOF for finding the lowest flutter speed during a parameter study. Once the parameter of interest is chosen, the study proceeds as follows:

- ① After the input of aircraft geometry, aerodynamics, and program control information, the program finds a user specified number of lowest natural frequencies.
- ② A subroutine named RLF traces each branch, starting from the natural frequencies found in step ①, till a flutter speed is found or a specified maximum airspeed is obtained.

③ The lowest flutter speed is chosen, or, if no flutter speeds have been found, the program may terminate.

④ The parameter of interest is incremented, and the preprocessor computes new wing bending and twisting stiffness distributions. A count is kept so that after a specified number of increments a complete search of all branches is again initiated from $\lambda = 0$. Consequently, discontinuities in the lowest flutter speed are checked for periodically during the parameter study.

⑤ If the count has not been exceeded, subroutine RLF traces the branch on which the lowest flutter speed occurred for the previous parameter value while testing

① the first and second derivatives of λ with respect to Ω_1 along the branch to see if flutter is imminent

② the number of airspeed increments made along the branch

③ the maximum airspeed limitation

These tests may indicate that, for the parameter value, flutter is not likely to occur on the same branch as it occurred for the previous parameter value and a complete search of all branches is initiated.

⑥ The procedure continues until the specified number of parameter iterations is fulfilled or an internal decision is made to terminate the study. A description of the user input and options, an example computer output and a listing of the program are provided in appendix F.

Validation

In order to verify the accuracy of the flutter analysis, several comparisons were made with examples found in the literature (refs. 4 to 6) and with the SADSAM (ref. 7) computer program. The results of these comparisons are given in tables I, II, and III. In order to agree with references 4 to 6, the aerodynamic coefficient $\left[c_{l\alpha} \right]$ and the aerodynamic center a_c were set equal to 2π and -0.5 , respectively.

In table I, a uniform cantilever rectangular straight wing (with aspect ratio of 6.67) as given by Goland in reference 4 (with later correction of results in ref. 5) is considered. The table shows that COMBOF gives good agreement with Goland's exact solution both in flutter speed and frequency even when as few as 10 finite difference stations are used. The SADSAM solution, although not doing as well in this example as COMBOF, also gives good results. The small differences between COMBOF or SADSAM and Goland's solution is probably due to the approximation of Theodorsen's circulation function used in both COMBOF and SADSAM instead of the exact Bessel Function form used by Goland. For all the calculations in table I, the branch on which flutter occurs is the first torsional branch;

this is not meant to imply that only torsion is associated with the flutter mode. The designation of any root locus branch is derived from the designation of the natural frequency from which it emanates.

An example of an aircraft having a rigid fuselage and in symmetric flutter is presented in table II. The aircraft has uniform rectangular straight wings of aspect ratio 6.67 and has weights attached to the wing tips. A solution to this problem is given by Goland and Luke in reference 5. They considered two cases in this investigation as described in the table. In each case, both COMBOF and SADSAM were in good agreement with reference 5 for the flutter speed and frequencies of the first torsional branch. However, in tracing out other root locus branches, COMBOF predicted that even lower flutter speeds existed for case 1 on the first and second bending branches. These speeds were later confirmed by SADSAM. This example serves to point out the ease with which the lowest flutter speed can be missed.

Finally, a comparison with reference 6 for a uniform cantilever rectangular swept wing of aspect ratio 12.4 is presented in table III. Since reference 6 contains analytical and experimental results, comparisons were made with both. As in tables I and II, the comparisons show good agreement in all cases.

DISCUSSION OF RESULTS FOR COMPOSITE-WING BOX PARAMETER STUDIES

The program has been applied to parameter studies in which the effect of filament orientation upon flutter behavior has been examined for wings belonging to the following three classes: wings having different angles of sweep, wings having different mass ratios, and wings having variable lamina thicknesses. In each class, a cantilever wing was considered whose filament orientation angle was the same in each lamina and was uniform along the span (i.e., $\theta_j = \theta = \text{Constant}$).

The studies were carried out by using the program logic shown in figure 4 (previously described). For the cases presented herein the composite material was boron-epoxy and the appropriate moduli and other wing properties are given in table IV.

In each case, the filament angle θ was incremented in 101 steps from 0° to 90° . Among the relevant information output by the program was the variation of EI and GJ with θ . These data are shown in figure 5. Notice that while GJ is symmetric about 45° , EI is asymmetric, decreasing with increasing θ .

The variation of the dimensionless dynamic pressure λ with θ is shown in figure 6 for three swept wings. Values of λ above the flutter boundary are unstable, whereas those below are stable. The figure indicates that for $\theta < 55^\circ$ the effect of

sweeping the wing is to raise the flutter speed by a factor between $1/\sqrt{\cos \Lambda}$ and $1/\cos \Lambda$. This effect is about the same as that recorded in references 6 and 9 for all-metal wings. However, when $\theta > 55^\circ$ sweeping the wing seems to have no definite effect on flutter. Moreover, in general, it appears that the effect of wing sweep is of secondary importance to the effect of fiber orientation, and, as anticipated, the maximum flutter speeds are attained when GJ is maximum or near $\theta = 45^\circ$. This general shape of the curve bears much similarity to that presented in reference 10.

As discussed in a previous section, COMBOF is designed to find the lowest value of the flutter parameter λ (which corresponds to the lowest flutter speed) even if λ is discontinuous. Such a situation occurs in figure 7 for a relatively high-mass-ratio wing (a heavy wing or low-air-density—high-altitude flight, $m/m_{TK} = 64$) as the filament orientation angle θ is varied. The solid line in the figure represents the lowest flutter speed and in general follows the shape of GJ in figure 5. The curve contains two discontinuities: one at $\theta = 36^\circ$ and one at 81° . However, the flutter boundary or boundaries must be continuous and in the vicinity of such a discontinuity are usually multivalued. COMBOF may also be used to predict these multivalued curves. (See appendix F for program option.) Hence the dashed curve in figure 7 completes the flutter boundary between $\theta = 36^\circ$ and 45° .

Further details of the nature of the flutter boundary in the vicinity of the discontinuity at $\theta = 36^\circ$ are shown in figure 8. The figure indicates the change in flutter mode from the first torsional branch (dashed curves) to the second bending branch (solid curves) as θ increases from 35.1° to 45.0° . Flutter is indicated by a change in sign (from plus to minus) of the imaginary part of Ω . Notice that at 35.1° the second bending branch almost goes unstable near $\lambda = 4$ while at the same value of θ the first torsional branch is unstable near $\lambda = 6.5$. When $\theta = 43.2^\circ$ the second bending branch becomes unstable near $\lambda = 5$, while the first torsional branch is also unstable but at $\lambda = 7.3$. With further increase in θ to 45° , the second bending branch is still unstable while the first torsional branch has become stable.

Apparently the discontinuities in the curves of figure 7 are highly dependent upon the mass ratio of the wing. Figure 9 shows that, for mass ratios below that shown in figure 8, the discontinuity decreases as the mass ratio decreases. This trend is in agreement with results presented in references 11 and 12. When $m/m_{TK} = 8$ no discontinuity appears. Again the curves generally follow the variation of GJ .

The variation of λ with θ for variable thickness lamina is shown in figure 10. The thickness of the lamina varied linearly along the span from the root to the tip. The figure indicates that the discontinuity in λ decreases in size as the lamina taper increases, and as anticipated, the flutter speed generally decreases with taper as well.

CONCLUDING REMARKS

A computer program has been developed for the flutter analysis of composite swept-wing subsonic aircraft with a flexible fuselage and engines mounted on flexible pylons including the effects of rigid-body roll, pitch, and plunge. The program uses a direct flutter solution in which the flutter determinant is derived by using finite differences and the root locus branches of the determinant are searched for the lowest flutter speed. The air loads are generated internally by using modified swept-wing strip theory. In addition a preprocessing subroutine is included which can be used to evaluate the variable bending and twisting stiffness properties of the wing using a laminated, balanced ply, elementary composite plate theory. The program has been substantiated by comparison with existing flutter solutions.

The program has been applied to parameter studies in which the effect of filament orientation upon flutter behavior has been examined for wings belonging to the following three classes: wings having different angles of sweep, wings having different mass ratios, and wings having variable lamina thicknesses. These studies demonstrated that the program can perform a complete parameter study in one computer run. Such studies make it possible to use the lowest flutter speed, for one parameter value, in obtaining the lowest flutter speed at the next parameter value while making periodic checks for the occurrence of abrupt changes in the lowest flutter speed and/or frequency as the parameter is varied. The occurrence of these abrupt changes is associated with the lowest flutter speed shifting from one flutter mode to another with a relatively small structural change.

In addition, the studies indicated that, as anticipated, the highest critical flutter speed for swept and unswept wings occurred when the filament orientation was near $\pm 45^\circ$. However, for wings having high mass ratios, the critical flutter speed changed abruptly with small changes in filament angle when the filament orientation was near $\pm 45^\circ$.

Langley Research Center,
National Aeronautics and Space Administration,
Hampton, Va., May 22, 1974.

APPENDIX A

AERODYNAMIC WING LOADS

In this analysis the aerodynamic loads are provided by modified strip theory (refs. 1 to 3) valid for constant amplitude harmonic motion of the form $e^{i\omega t}$. This theory represents an improvement of elementary strip theory in that it includes effects due to finite aspect ratio and compressibility. The theory employs a variable section lift-curve slope $c_{l\alpha}(\eta)$ instead of 2π , a variable section aerodynamic center $a_c(\eta)$ instead of $-1/2$ (the quarter-chord), and a modified Theodorsen circulation function $C(k)$, which accounts for compressibility effects on the magnitude of the lift and pitching moment. Appropriate spanwise distributions for $c_{l\alpha}(\eta)$ and $a_c(\eta)$ are those for the particular planform and Mach number of interest. (See refs. 1 to 3.)

The lift and pitching moment per unit span at the i th finite-difference station may be expressed in dimensionless form as

$$\begin{aligned}
 Q_{h,i} = & b_i \left[b_i k \Omega^2 - i (c_{l\alpha})_i R C_i(k_n) \lambda_n k_n \right] h_i + b_i^2 \left(\Omega^2 k \alpha_i \right. \\
 & + i \pi \lambda_n k_n R \left\{ 1 + \left[\frac{(c_{l\alpha})_i}{2\pi} + \frac{a_{c,i} - a_i}{b_i} \right] (c_{l\alpha})_i \frac{C_i(k_n)}{\pi} \right\} \\
 & \left. + (c_{l\alpha})_i \lambda_n R b_i C_i(k_n) \right) \alpha_i - \left[(c_{l\alpha})_i C_i(k_n) \right. \\
 & \left. + i \pi k_n b_i \right] b_i \lambda_n \frac{dh_i}{d\eta} \tan \Lambda + \left\{ (c_{l\alpha})_i \left[\frac{(c_{l\alpha})_i}{2\pi} \right. \right. \\
 & \left. \left. + \frac{a_{c,i} - a_i}{b_i} \right] C_i(k_n) - i \pi k_n a_i \right\} b_i^2 \lambda_n \frac{d\alpha_i}{d\eta} \tan \Lambda
 \end{aligned} \tag{A1}$$

APPENDIX A

$$\begin{aligned}
 Q_{\alpha,i} = & b_i^2 \left[\frac{a_i \kappa \Omega^2}{R} - i k_n \lambda_n (a_i - a_{c,i}) (c_{l\alpha})_i \frac{C_i(k_n)}{b_i} \right] \frac{h_i}{R} + b_i^2 \left\{ \kappa b_i^2 \left(\frac{1}{8} + \frac{a_i^2}{b_i^2} \right) \frac{\Omega^2}{R} \right. \\
 & - 2 \pi i k_n \lambda_n b_i \left[\frac{1}{2} - (a_i - a_{c,i}) (c_{l\alpha})_i \frac{C_i(k_n)}{2 \pi b_i} \right] \left[\frac{(c_{l\alpha})_i}{2 \pi} + \frac{a_{c,i} - a_i}{b_i} \right] \\
 & + (a_i - a_{c,i}) (c_{l\alpha})_i C_i(k_n) \lambda_n \left. \right\} \frac{\alpha_i}{R} - \left[i \pi k_n a_i + (a_i - a_{c,i}) (c_{l\alpha})_i \frac{C_i(k_n)}{b_i} \right] \\
 & \times b_i^2 \lambda_n \frac{d h_i \tan \Lambda}{d \eta} \frac{1}{R^2} - b_i^2 \tan \Lambda \left\{ i k_n \left(\frac{1}{8} + \frac{a_i^2}{b_i^2} \right) + a_i + \left[1 - (a_i - a_{c,i}) (c_{l\alpha})_i \frac{C_i(k_n)}{\pi b_i} \right] \right. \\
 & \left. \times \left[\frac{(c_{l\alpha})_i}{2 \pi} + \frac{a_{c,i} - a_i}{b_i} \right] \right\} \frac{\pi \lambda_n}{R^2} \frac{d \alpha_i}{d \eta} \quad (i = 1, 2, \dots, N) \quad (A2)
 \end{aligned}$$

where the dimensionless (unbarred) loads are related to the dimensional (barred) loads by

$$\left. \begin{aligned}
 Q_{h,i} &= \frac{\bar{Q}_{h,i} \bar{l}^4}{b_r (EI)_r} \\
 Q_{\alpha,i} &= \frac{\bar{Q}_{\alpha,i} \bar{l}^2}{(EI)_r}
 \end{aligned} \right\} \quad (A3)$$

in which \bar{l} is the wing span (tip to root), b_r is a reference semichord and $(EI)_r$ is a reference bending stiffness. Also,

$$b_i = \frac{\bar{b}_i}{b_r} \quad a_i = \frac{\bar{a}_i}{b_r} \quad a_{c,i} = \frac{\bar{a}_{c,i}}{b_r} \quad R = \frac{\bar{l}}{b_r} \quad h_i = \frac{\bar{h}_i}{b_r}$$

and Λ is the sweep angle. Furthermore,

APPENDIX A

$$\lambda_n = \lambda \cos^2 \Lambda = \rho b_r \bar{l}^{-3} V^2 \frac{\cos^2 \Lambda}{(EI)_r}$$

$$k_n = \frac{k}{\cos \Lambda} = \frac{b_r \omega}{V \cos \Lambda}$$

$$\kappa = \frac{\pi \rho b_r^2}{m_r}$$

$$\Omega = \omega \bar{l}^2 \sqrt{m_r / (EI)_r}$$

An approximate form of Theodorsen's circulation function, due to reference 7, is used in place of the exact Bessel function form; that is,

$$C_j(k_n) = \frac{(1 + 10.61ik_n b_j)(1 + 1.774ik_n b_j)}{(1 + 13.51ik_n b_j)(1 + 2.745ik_n b_j)} \quad (j = 1, \dots, N) \quad (A4)$$

Moreover, to correct for compressibility effects, $C_j(k_n)$ may be modified in magnitude by the choice of an appropriate factor. (See ref. 3 for additional details.)

APPENDIX B

GOVERNING EQUATIONS

Since the aircraft is geometrically and structurally symmetric, only the symmetric and antisymmetric oscillations of the aircraft need be considered. Hence, the total elastic energy stored in both wings may be expressed as

$$U = \int_0^{\bar{l}} \left[\overline{EI} (\bar{h}'')^2 + \overline{GJ} (\alpha')^2 \right] d\bar{\eta} \quad (B1)$$

where a prime denotes differentiation with respect to $\bar{\eta}$, the coordinate along the elastic axis of the wing. The variation of equation (B1) may be expressed as

$$\begin{aligned} \frac{1}{2} \delta U = & \frac{1}{2} \bar{\epsilon} (\overline{EI})_1 h_1'' \delta h_1'' + \bar{\epsilon} \sum_{i=2}^{N-1} (\overline{EI})_i \bar{h}_i'' \delta \bar{h}_i'' + \frac{1}{2} \bar{\epsilon} (\overline{EI})_N \bar{h}_N'' \delta \bar{h}_N'' \\ & + \bar{\epsilon} \sum_{i=2}^N (\overline{GJ})_{i-1/2} \alpha'_{i-1/2} \delta \alpha'_{i-1/2} \end{aligned} \quad (B2)$$

where the elastic axis of the wing has been subdivided into $N-1$ equal segments of length $\bar{\epsilon}$ and the subscripts denote the finite-difference stations numbered as shown in figure 1.

The kinetic energy of both wings may be expressed as

$$T = \int_0^{\bar{l}} \left[\bar{m} \left(\dot{\bar{h}}^2 - 2\dot{\alpha} \dot{\bar{h}} x_\alpha \right) + \bar{m} \bar{r}_\alpha^2 \dot{\alpha}^2 \right] d\eta \quad (B3)$$

where

\bar{m} mass of wing per unit span

\bar{r}_α radius of gyration of cross section about elastic axis

\bar{x}_α offset of center of gravity from elastic axis (positive towards the trailing edge)

APPENDIX B

and a dot signifies differentiation with respect to time. The variation of equation (B3) may be expressed as

$$\begin{aligned}
 \frac{1}{2} \delta T = & \frac{1}{2} \bar{\epsilon} \bar{m}_1 \left[\left(\dot{\bar{h}}_1 - \dot{\alpha}_1 \bar{x}_{\alpha,1} \right) \delta \dot{\bar{h}}_1 + \left(\dot{\alpha}_1 \bar{r}_{\alpha,1}^2 - \dot{\bar{h}}_1 \bar{x}_{\alpha,1} \right) \delta \dot{\alpha}_1 \right] \\
 & + \bar{\epsilon} \sum_{i=2}^{N-1} \bar{m}_i \left[\left(\dot{\bar{h}}_i - \dot{\alpha}_i \bar{x}_{\alpha,i} \right) \delta \dot{\bar{h}}_i + \left(\dot{\alpha}_i \bar{r}_{\alpha,i}^2 - \dot{\bar{h}}_i \bar{x}_{\alpha,i} \right) \delta \dot{\alpha}_i \right] \\
 & + \frac{1}{2} \bar{\epsilon} \bar{m}_N \left[\left(\dot{\bar{h}}_N - \dot{\alpha}_N \bar{x}_{\alpha,N} \right) \delta \dot{\bar{h}}_N + \left(\dot{\alpha}_N \bar{r}_{\alpha,N}^2 - \dot{\bar{h}}_N \bar{x}_{\alpha,N} \right) \delta \dot{\alpha}_N \right] \tag{B4}
 \end{aligned}$$

The variation of the work done by the engines and fuselage may be expressed as

$$\begin{aligned}
 \frac{1}{2} \delta W_e = & \frac{1}{2} \bar{\epsilon} \left(\bar{q}_{h,1} \delta \bar{h}_1 + \bar{q}_{m,1} \delta \bar{h}'_1 + \bar{q}_{\alpha,1} \delta \alpha_1 \right) \\
 & + \bar{\epsilon} \sum_{i=2}^{N-1} \left(\bar{q}_{h,i} \delta \bar{h}_i + \bar{q}_{m,i} \delta \bar{h}'_i + \bar{q}_{\alpha,i} \delta \alpha_i \right) \\
 & + \frac{1}{2} \bar{\epsilon} \left(\bar{q}_{h,N} \delta \bar{h}_N + \bar{q}_{m,N} \delta \bar{h}'_N + \bar{q}_{\alpha,N} \delta \alpha_N \right) \tag{B5}
 \end{aligned}$$

where $\bar{q}_{h,i}$, $\bar{q}_{m,i}$, and $\bar{q}_{\alpha,i}$ are the vertical upward loads, torques, and moments (positive as shown in fig. 11) applied to the wings at the i th finite-difference station by the engines and fuselage. These loads are evaluated in appendix E, and are taken to be zero at the finite-difference stations where no engines are attached.

The variation of the work done by the aerodynamic loads may be expressed as

APPENDIX B

$$\begin{aligned} \frac{1}{2} \delta W_a = & \frac{1}{2} \bar{\epsilon} \left(\bar{Q}_{h,i} \delta \bar{h}_1 + \bar{Q}_{\alpha,1} \delta \alpha_1 \right) + \bar{\epsilon} \sum_{i=2}^{N-1} \left(\bar{Q}_{h,i} \delta \bar{h}_i + \bar{Q}_{\alpha,i} \delta \alpha_i \right) \\ & + \frac{1}{2} \bar{\epsilon} \left(\bar{Q}_{h,N} \delta \bar{h}_N + \bar{Q}_{\alpha,N} \delta \alpha_N \right) \end{aligned} \quad (B6)$$

Substituting equations (B2), (B4), (B5), and (B6) into Hamilton's principle,

$$\int_{t_1}^{t_2} \left(\delta U - \delta T - \delta W_e - \delta W_a \right) dt = 0 \quad (B7)$$

with harmonic motion of the form $e^{i\omega t}$ being assumed, and using the following finite-difference expressions for derivatives of \bar{h}_i and α_i and their respective variations

$$\bar{h}'_i = \frac{1}{2\bar{\epsilon}} \left(\bar{h}_{i+1} - \bar{h}_{i-1} \right) \quad (B8)$$

$$\bar{h}''_i = \frac{1}{\bar{\epsilon}^2} \left(\bar{h}_{i+1} - 2\bar{h}_i + \bar{h}_{i-1} \right) \quad (B9)$$

$$\alpha'_{i-1/2} = \frac{1}{\bar{\epsilon}} \left(\alpha_i - \alpha_{i-1} \right) \quad (B10)$$

yield

$$\begin{aligned} 0 = & \int_{t_1}^{t_2} \left\{ \left[\frac{1}{2} (EI)_1 (h_2 - 2h_1 + h_0) + \frac{1}{4} \epsilon^3 q_{m,1} \right] \frac{(EI)_r \delta h_0}{\epsilon 3\bar{l}R^2} + \left[-(EI)_1 (h_2 - 2h_1 + h_0) \right. \right. \\ & \left. \left. + (EI)_2 (h_3 - 2h_2 + h_1) - \frac{1}{2} \epsilon^4 m_1 \Omega^2 (h_1 - \alpha_1^x \alpha,1) - \frac{1}{2} \epsilon^4 (Q_{h,1} + q_{h,1}) \right. \right. \\ & \left. \left. + \frac{1}{2} \epsilon^3 q_{m,2} \right] \frac{(EI)_r \delta h_1}{\epsilon 3\bar{l}R^2} + \left[\frac{1}{2} (EI)_1 (h_2 - 2h_1 + h_0) - 2(EI)_2 (h_3 - 2h_2 + h_1) \right. \right. \\ & \left. \left. + (EI)_3 (h_4 - 2h_3 + h_2) - \epsilon^4 m_2 \Omega^2 (h_2 - \alpha_2^x \alpha,2) - \epsilon^4 (Q_{h,2} + q_{h,2}) \right. \right. \end{aligned}$$

(Equation continued on next page)

APPENDIX B

$$\begin{aligned}
& + \frac{1}{2} \epsilon^3 \left(q_{m,3} - \frac{1}{2} q_{m,1} \right) \left[\frac{(EI)_r \delta h_2}{\epsilon^3 \bar{l} R^2} + \sum_{i=3}^{N-2} \left[(EI)_{i+1} (h_{i+2} - 2h_{i+1} + h_i) \right. \right. \\
& - 2(EI)_i (h_{i+1} - 2h_i + h_{i-1}) + (EI)_{i-1} (h_i - 2h_{i-1} + h_{i-2}) - \epsilon^4 m_i \Omega^2 (h_i - \alpha_i x_{\alpha,i}) \\
& - \epsilon^4 (Q_{h,i} + q_{h,i}) + \left. \left. \frac{1}{2} \epsilon^3 (q_{m,i+1} - q_{m,i-1}) \right] \frac{(EI)_r \delta h_i}{\epsilon^3 \bar{l} R^2} + \left[(EI)_{N-2} (h_{N-1} - 2h_{N-2} + h_{N-3}) \right. \right. \\
& - 2(EI)_{N-1} (h_N - 2h_{N-1} + h_{N-2}) + \left. \left. \frac{1}{2} (EI)_N (h_{N+1} - 2h_N + h_{N-1}) \right] \right. \\
& - \epsilon^4 m_{N-1} \Omega^2 (h_{N-1} - \alpha_{N-1} x_{\alpha,N-1}) - \epsilon^4 (Q_{h,N-1} + q_{h,N-1}) \\
& - \left. \frac{1}{2} \epsilon^3 \left(q_{m,N-2} - \frac{1}{2} q_{m,N} \right) \right] \frac{(EI)_r \delta h_{N-1}}{\epsilon^3 \bar{l} R^2} + \left[(EI)_{N-1} (h_N - 2h_{N-1} + h_{N-2}) \right. \\
& - (EI)_N (h_{N+1} - 2h_N + h_{N-1}) - \frac{1}{2} \epsilon^4 m_N \Omega^2 (h_N - \alpha_N x_{\alpha,N}) - \frac{1}{2} \epsilon^4 (Q_{h,N} + q_{h,N}) \\
& - \left. \frac{1}{2} \epsilon^3 q_{m,N-1} \right] \frac{(EI)_r \delta h_N}{\epsilon^3 \bar{l} R^2} + \left[\frac{1}{2} (EI)_N (h_{N+1} - 2h_N + h_{N-1}) - \frac{1}{4} \epsilon^3 q_{m,N} \right] \frac{(EI)_r \delta h_{N+1}}{\epsilon^3 \bar{l} R^2} \\
& + \left[-(GJ)_{3/2} (\alpha_2 - \alpha_1) - \frac{1}{2R^2} \epsilon^2 \Omega^2 m_1 (\alpha_1 r_{\alpha,1}^2 - x_{\alpha,1} h_1) - \frac{1}{2} \epsilon^4 (Q_{\alpha,1} + q_{\alpha,1}) \right] \frac{(EI)_r \delta \alpha_1}{\epsilon \bar{l}} \\
& + \sum_{i=2}^{N-1} \left[-(GJ)_{i+1/2} (\alpha_{i+1} - \alpha_i) + (GJ)_{i-1/2} (\alpha_i - \alpha_{i-1}) - \frac{\epsilon^4 m_i \Omega^2}{R^2} (\alpha_i r_{\alpha,i} - x_{\alpha,i} h_i) \right]
\end{aligned}$$

(Equation continued on next page)

APPENDIX B

$$\begin{aligned}
 & -\epsilon^2 \left(Q_{\alpha,i} + q_{\alpha,i} \right) \left[\frac{(EI)_r \delta \alpha_i}{\epsilon \bar{l}} + \left[(GJ)_{N-1/2} (\alpha_N - \alpha_{N-1}) + \frac{1}{2} \frac{\epsilon^2 m_N \Omega^2}{R^2} (\alpha_N r_{\alpha,N}^2 - x_{\alpha,N} h_N) \right. \right. \\
 & \left. \left. - \frac{1}{2} \epsilon^2 \left(Q_{\alpha,N} + q_{\alpha,N} \right) \right] \frac{(EI)_r \delta \alpha_N}{\epsilon \bar{l}} \right] dt \tag{B11}
 \end{aligned}$$

In deriving equation (B11) the variation of the kinetic energy has been integrated once by parts and the following dimensionless quantities have been introduced:

$$\begin{aligned}
 \epsilon &= \frac{\bar{\epsilon}}{\bar{l}} & x_{\alpha,i} &= \frac{\bar{x}_{\alpha,i}}{b_r} & r_{\alpha,i} &= \frac{\bar{r}_{\alpha,i}}{b_r} \\
 (EI)_i &= \frac{(\overline{EI})_i}{(EI)_r} & (GJ)_i &= \frac{(\overline{GJ})_i}{(EI)_r} & q_{h,i} &= \frac{\bar{q}_{h,i} \bar{l}^4}{b_r (EI)_r} \\
 q_{\alpha,i} &= \frac{\bar{q}_{\alpha,i} \bar{l}^2}{(EI)_r} & q_{m,i} &= \frac{\bar{q}_{m,i} \bar{l}^3}{(EI)_r} & m_i &= \frac{\bar{m}_i}{m_r}
 \end{aligned}$$

Not all the variations in equation (B11) are independent of one another; some are constrained by the requirement of either symmetric or antisymmetric motion.

Symmetric Modes

For symmetric modes,

$$\phi_F = 0 \tag{B12}$$

where ϕ_F is the roll of the fuselage. However, since the wings are attached to the fuselage via a rigid carry-through beam, ϕ_F is also the roll of the wings at the first finite-difference station, hence

$$0 = \phi_F = \phi_1 = \bar{h}_1' \cos \Lambda + \alpha_1 \sin \Lambda \tag{B13}$$

Expressing equation (B13) in finite-difference form, with dimensionless quantities introduced, gives

APPENDIX B

$$h_0 = h_2 + 2\epsilon R \alpha_1 \tan \Lambda \quad (\text{B14})$$

whose variation is

$$\delta h_0 = \delta h_2 + 2\epsilon R \delta \alpha_1 \tan \Lambda \quad (\text{B15})$$

Inasmuch as equation (B11) must be valid for all independent variations of h_i and α_i which satisfy equation (B15), the governing finite-difference equations for symmetric flutter may be obtained by setting the coefficients of each variation equal to zero. The resulting equations are

$$\begin{aligned} 0 = & -(GJ)_{3/2}(\alpha_2 - \alpha_1) - \frac{1}{2} \frac{\epsilon^2 \Omega^2 m_1}{R^2} (r_{\alpha,1}^2 \alpha_1 - \beta_1 h_1) - \frac{1}{2} \epsilon^2 (Q_{\alpha,1} + q_{\alpha,1}) \\ & + 2 \left[(EI)_1 (h_2 - h_1 + \epsilon R \alpha_1 \tan \Lambda) + \frac{1}{4} \epsilon^3 q_{m,1} \right] \frac{\tan \Lambda}{\epsilon R} \end{aligned} \quad (\text{B16})$$

$$\begin{aligned} 0 = & -2(EI)_1 (h_2 - h_1) + (EI)_2 (h_3 - 2h_2 + h_1) - \frac{1}{2} \epsilon^4 m_1 \Omega^2 (h_1 - \alpha_1 x_{\alpha,1}) \\ & - \frac{1}{2} \epsilon^4 (Q_{h,1} + q_{h,1}) + \frac{1}{2} \epsilon^3 q_{m,2} - 2\epsilon R (EI)_1 \alpha_1 \tan \Lambda \end{aligned} \quad (\text{B17})$$

$$\begin{aligned} 0 = & -(GJ)_{5/2}(\alpha_3 - \alpha_2) + (GJ)_{3/2}(\alpha_2 - \alpha_1) - \frac{\epsilon^2 m_2 \Omega^2}{R^2} (\alpha r_{\alpha,2}^2 - \beta_2 h_2) \\ & - \epsilon^2 (Q_{\alpha,2} + q_{\alpha,2}) \end{aligned} \quad (\text{B18})$$

$$\begin{aligned} 0 = & 2(EI)_1 (h_2 - h_1 + \epsilon R \alpha_1 \tan \Lambda) - 2(EI)_2 (h_3 - 2h_2 + h_1) \\ & + (EI)_1 (h_4 - 2h_3 + h_2) - \epsilon^4 m_2 \Omega^2 (h_2 - \alpha_2 x_{\alpha,2}) \\ & - \epsilon^4 (Q_{h,2} + q_{h,3}) + \frac{1}{2} \epsilon^3 q_{m,3} \end{aligned} \quad (\text{B19})$$

APPENDIX B

$$\begin{aligned}
 0 = & -(GJ)_{i-1}/2(\alpha_{i+1} - \alpha_i) + (GJ)_{i-1}/2(\alpha_i - \alpha_{i-1}) \\
 & - \frac{\epsilon^2 m_i \Omega^2}{R^2} (\alpha_i r_{\alpha,i}^2 - x_{\alpha,i} h_i) - \epsilon^2 (Q_{\alpha,i} + q_{h,i}) \quad (i = 3, 4, \dots, N-2) \quad (B20)
 \end{aligned}$$

$$\begin{aligned}
 0 = & (EI)_{i+1}(h_{i+2} - 2h_{i+1} + h_i) - 2(EI)_i(h_{i+1} - 2h_i + h_{i-1}) \\
 & + (EI)_{i-1}(h_i - 2h_{i-1} + h_{i-2}) - \epsilon^4 m_i \Omega^2 (h_i - \alpha_i x_{\alpha,i}) \\
 & - \epsilon^4 (Q_{h,i} + q_{h,i}) - \frac{1}{2} \epsilon^3 (q_{m,i-1} - q_{m,i+1}) \quad (i = 3, 4, \dots, N-2) \quad (B21)
 \end{aligned}$$

$$\begin{aligned}
 0 = & -(GJ)_{N-1}/2(\alpha_N - \alpha_{N-1}) + (GJ)_{N-3}/2(\alpha_{N-1} - \alpha_{N-2}) \\
 & - \frac{\epsilon^2 m_{N-1} \Omega^2}{R^2} (\alpha_{N-1} r_{\alpha,N-1}^2 - h_{N-1} x_{\alpha,N-1}) - \epsilon^2 (Q_{\alpha,N-1} + q_{\alpha,N-1}) \quad (B22)
 \end{aligned}$$

$$\begin{aligned}
 0 = & (EI)_{N-2}(h_{N-1} - 2h_{N-2} + h_{N-3}) - 2(EI)_{N-1}(h_N - 2h_{N-1} + h_{N-2}) \\
 & - \epsilon^4 m_{N-1} \Omega^2 (h_{N-1} - \alpha_{N-1} x_{\alpha,N-1}) - \epsilon^4 (Q_{h,N-1} + q_{h,N-1}) \\
 & - \frac{1}{2} \epsilon^3 (q_{m,N-2} - q_{m,N}) \quad (B23)
 \end{aligned}$$

$$\begin{aligned}
 0 = & (GJ)_{N-1}/2(\alpha_N - \alpha_{N-1}) - \frac{1}{2} \frac{\epsilon^2 m_N \Omega^2}{R^2} (\alpha_N r_{\alpha,N}^2 - x_{\alpha,N} h_N) \\
 & - \frac{1}{2} \epsilon^2 (Q_{\alpha,N} + q_{\alpha,N}) \quad (B24)
 \end{aligned}$$

APPENDIX B

$$\begin{aligned}
 0 = (EI)_{N-1} (h_N - 2h_{N-1} + h_{N-2}) - \frac{1}{2} \epsilon^4 m_N \Omega^2 (h_N - \alpha_{N^x} \alpha_{,N}) \\
 - \frac{1}{2} \epsilon^4 (Q_{h,N} + q_{h,N}) - \frac{1}{2} \epsilon^3 (q_{m,N} + q_{m,N-1})
 \end{aligned} \tag{B25}$$

In addition the following equation, which results from equation (B11), was used to eliminate h_{N+1} from equations (B23) and (B25).

$$0 = (EI)_N (h_{N+1} - 2h_N + h_{N-1}) - \frac{1}{2} \epsilon^3 q_{m,N} \tag{B26}$$

Antisymmetric Modes

In the antisymmetric case the constraints on the motion are

$$\Theta_F = h_F = 0 \tag{B27}$$

where Θ_F and h_F are the pitch and plunge of the fuselage, respectively. Since the wings are rigidly attached to the fuselage,

$$\bar{h}_1 = \frac{1}{2} \bar{d} \phi_F \tag{B28}$$

where \bar{d} is the fuselage diameter. Then as a consequence of equations (B27) and (B28) and assumption (6), the antisymmetric constraints take the following form:

$$0 = \Theta_F = \alpha_1 \cos \Lambda - (h_2 - h_0) \frac{\sin \Lambda}{2\epsilon R} \tag{B29}$$

$$h_1 = \frac{1}{2} d \left[R \alpha_1 \sin \Lambda + (h_2 - h_0) \frac{\cos \Lambda}{2\epsilon} \right] \tag{B30}$$

where

$$d = \frac{\bar{d}}{\bar{l}} \tag{B31}$$

Equations (B29) and (B30) together imply

$$\alpha_1 = \frac{1}{2} (h_2 - h_0) \frac{\tan \Lambda}{\epsilon R} \tag{B32}$$

APPENDIX B

$$h_1 = \frac{1}{4} \frac{d(h_2 - h_0)}{\epsilon \cos \Lambda} \quad (\text{B33})$$

and their variation gives

$$\delta \alpha_1 = \frac{1}{2} (\delta h_2 - \delta h_0) \frac{\tan \Lambda}{\epsilon R} \quad (\text{B34})$$

$$\delta h_1 = \frac{1}{4} \frac{d(\delta h_2 - \delta h_0)}{\epsilon \cos \Lambda} \quad (\text{B35})$$

Again, equation (B11) must be valid for all independent variations of h_i and α_i which satisfy equations (B34) and (B35); hence, the governing finite-difference equations for antisymmetric flutter are obtained as follows:

$$\begin{aligned} 0 = & \left[\frac{1}{2} (EI)_1 + \frac{1}{4} (EI)_1 \frac{d}{\epsilon} \cos \Lambda + \frac{1}{4} (GJ)_{3/2} \tan^2 \Lambda - \frac{1}{8} r_{\alpha,1}^2 \epsilon^2 \Omega^2 m_1 \frac{\tan^2 \Lambda}{R^2} \right. \\ & + \frac{1}{16} m_1 x_{\alpha,1} d \epsilon^2 \Omega^2 \frac{\tan \Lambda}{R \cos \Lambda} + \frac{1}{8} \frac{(EI)_1}{\cos^2 \Lambda} \left(\frac{d}{\epsilon} \right)^2 + \frac{1}{4} \frac{(EI)_1}{\cos \Lambda} \frac{d}{\epsilon} + \frac{1}{16} \frac{(EI)_2}{\cos^2 \Lambda} \left(\frac{d}{\epsilon} \right)^2 \\ & \left. - \frac{1}{32} m_1 \frac{d \epsilon^2 \Omega^2}{\cos^2 \Lambda} + \frac{1}{16} m_1 x_{\alpha,1} \epsilon^2 \Omega^2 d \frac{\tan \Lambda}{R \cos \Lambda} \right] h_0 + \left[\frac{1}{2} (EI)_1 - \frac{1}{4} \frac{(EI)_1}{\cos \Lambda} \frac{d}{\epsilon} \right. \\ & - \frac{1}{4} (GJ)_{3/2} \tan^2 \Lambda + \frac{1}{8} r_{\alpha,1}^2 \epsilon^2 \Omega^2 m_1 \frac{\tan^2 \Lambda}{R^2} - \frac{1}{16} m_1 x_{\alpha,1} d \epsilon^2 \Omega^2 \frac{\tan^2 \Lambda}{R \cos \Lambda} \\ & + \frac{1}{4} \frac{(EI)_1}{\cos \Lambda} \frac{d}{\epsilon} - \frac{1}{8} \frac{(EI)_2}{\cos^2 \Lambda} \left(\frac{d}{\epsilon} \right)^2 + \frac{1}{2} \frac{(EI)_2}{\cos \Lambda} \frac{d}{\epsilon} - \frac{1}{16} \frac{(EI)_2}{\cos^2 \Lambda} \frac{d}{\epsilon} + \frac{1}{32} \frac{m_1 d^2 \epsilon^2 \Omega^2}{\cos^2 \Lambda} \\ & \left. - \frac{1}{16} m_1 d_1 x_{\alpha,1} \epsilon^2 \Omega^2 \frac{\tan \Lambda}{R \cos \Lambda} \right] h_2 - \frac{1}{4} (EI)_2 \frac{d}{\epsilon} h_3 \cos \Lambda + \frac{1}{4} \epsilon^3 q_{m,1} \\ & + \frac{1}{2} \epsilon^3 (Q_{\alpha,1} + q_{\alpha,1}) \frac{\tan \Lambda}{R} + \frac{1}{8} \frac{\epsilon^3 d}{\cos \Lambda} (Q_{h,1} + q_{h,1}) - \frac{1}{8} \epsilon^2 q_{m,2} d \cos \Lambda \\ & + \frac{1}{2} (GJ)_{3/2} \alpha_2 \frac{\tan \Lambda}{\epsilon R} \end{aligned} \quad (\text{B36})$$

APPENDIX B

$$0 = -(GJ)_{5/2}(\alpha_3 - \alpha_2) + (GJ)_{3/2} \left[\alpha_2 - \frac{1}{2}(h_2 - h_0) \frac{\tan \Lambda}{\epsilon R} \right] - \frac{\epsilon^2 m_2 \Omega^2}{R^2} (\alpha_2 r_{\alpha,2}^2 - x_{\alpha,2} h_2) - \epsilon^2 (Q_{\alpha,2} + q_{\alpha,2}) \quad (B37)$$

$$0 = \frac{1}{2} (EI)_1 \left(h_2 - \frac{1}{2} \frac{d}{\epsilon} \frac{h_2 - h_0}{\cos \Lambda} + h_0 \right) - 2(EI)_2 \left(h_3 - 2h_2 + \frac{1}{4} \frac{d}{\epsilon} \frac{h_2 - h_0}{\cos \Lambda} \right) + (EI)_3 (h_4 - 2h_3 + h_2) - \epsilon^4 \Omega^2 m_2 (h_2 - \alpha_2 x_{\alpha,2}) - \epsilon^4 (Q_{h,2} + q_{h,2}) + \frac{1}{2} \epsilon^3 q_{m,3} - \frac{q_{m,1}}{2} - \frac{1}{2} \left\{ (GJ)_{3/2} \left[\alpha_2 - \frac{1}{2}(h_2 - h_0) \frac{\tan \Lambda}{\epsilon R} \right] + \frac{1}{2} \epsilon^4 \Omega^2 m_1 \left(r_{\alpha,1}^2 \frac{\tan \Lambda}{\epsilon R} - \frac{1}{4} \frac{x_{\alpha,1}}{\cos \Lambda} \frac{d}{\epsilon} \right) \frac{h_2 - h_0}{\epsilon^2 R^2} + \frac{1}{2} (Q_{\alpha,1} + q_{\alpha,1}) \right\} \epsilon R \tan \Lambda + \frac{1}{4} \left[-(EI)_1 \left(h_2 - \frac{1}{2} \frac{d}{\epsilon} \frac{h_2 - h_0}{\cos \Lambda} + h_0 \right) + (EI)_2 \left(h_3 - 2h_2 + \frac{1}{4} \frac{d}{\epsilon} \frac{h_2 - h_0}{\cos \Lambda} \right) - \frac{1}{4} \epsilon^4 \Omega^2 m_1 \left(\frac{1}{2} \frac{d}{\epsilon \cos \Lambda} - x_{\alpha,1} \frac{\tan \Lambda}{\epsilon R} \right) (h_2 - h_0) - \frac{1}{2} \epsilon^4 (Q_{h,1} + q_{h,1}) + \frac{1}{2} \epsilon^3 q_{m,2} \right] \frac{d}{\epsilon \cos \Lambda} \quad (B38)$$

In addition, equations (B20) to (B25) are valid for antisymmetric modes.

Cantilever Wing

It is often assumed that the flutter behavior of an aircraft can be approximated by neglecting the rigid-body motion of the aircraft and any effect of fuselage flexibility. With these assumptions, the constraints on the fuselage are

$$\Theta_F = \phi_F = h_F = 0 \quad (B39)$$

APPENDIX B

By using equations (B13), (B29), (B30), and (B39), the constraints take the form

$$\alpha_1 = h_1 = 0 \quad (B40)$$

and

$$h_2 = h_0 \quad (B41)$$

The wing is, therefore, cantilevered along a root normal to the elastic axis. Taking the variation of equations (B40) and (B41) yields

$$\delta h_1 = \delta h_1 = 0 \quad (B42)$$

and

$$\delta h_2 = \delta h_0 \quad (B43)$$

Equations (B11) must be valid for all independent variations of α_i and h_i which satisfy equations (B42) and (B43); hence, the governing equations for flutter of a cantilever wing are

$$\begin{aligned} 0 = & -(GJ)_{5/2} (\alpha_3 - \alpha_2) + (GJ)_{3/2} \alpha_2 - \frac{\epsilon^2 \Omega^2}{R^2} m_2 (\alpha_2 r_{\alpha,2}^2 - x_{\alpha,2} h_2) \\ & - \epsilon^2 (Q_{\alpha,2} + q_{\alpha,2}) \end{aligned} \quad (B44)$$

$$\begin{aligned} 0 = & 2(EI)_1 h_2 - 2(EI)_2 (h_3 - 2h_2) + (EI)_3 (h_4 - 2h_3 + h_2) \\ & - \epsilon^4 \Omega^2 m_2 (h_2 - x_{\alpha,2} \alpha_2) - \epsilon^4 (Q_{h,2} + q_{h,2}) + \frac{1}{2} \epsilon^3 q_{m,3} \end{aligned} \quad (B45)$$

In addition, equations (B20) to (B25) are valid for cantilever wing flutter.

APPENDIX C

EVALUATION OF ENGINE AND FUSELAGE LOADS

A free-body diagram of the pylon-engine model is shown in figure 11. It is assumed that the pylon is rigidly attached to the wing at the i th finite-difference station. The bending and twisting deformations of the pylon are assumed to be uncoupled and hence may be treated separately.

Pylon Bending

From elementary beam theory, bending deformations of the pylon are governed by

$$(EI)_p \frac{d^2 h_p}{dx_p^2} = \omega^2 \bar{m}_e x_p h_p(0) \quad (C1)$$

where $(EI)_p$ is the bending stiffness of the pylon, \bar{m}_e is the mass of the engine, and h_p is the upward vertical displacement of the pylon. Integrating equation (C1) twice yields

$$h_p = \bar{m}_e \omega^2 h_p(0) \int_{\bar{L}}^{x_p} \frac{x(x_p - x)}{(EI)_p} dx + \Theta_p(\bar{L})(\bar{L} - x_p) + h_p(\bar{L}) \quad (C2)$$

where \bar{L} is the length of the pylon.

Evaluating equation (C2) at the engine yields

$$h_p(0) = \frac{\bar{L}\Theta_p(\bar{L}) + h_p(\bar{L})}{1 - \bar{m}_e \omega^2 \int_0^{\bar{L}} \frac{x^2 dx}{(EI)_p}} \quad (C3)$$

Then, from the equilibrium of the pylon,

$$P_p = \omega^2 \bar{m}_e h_p(0) = \frac{\omega^2 \bar{m}_e}{1 - (\omega^2/\omega_B^2)} \left[\bar{L}\Theta_p(\bar{L}) - h_p(\bar{L}) \right] \quad (C4)$$

APPENDIX C

and

$$M_p = \frac{\omega^2 \bar{L} \bar{m}_e [\bar{L} \theta_p(\bar{L}) - h_p(\bar{L})]}{1 - (\omega^2 / \omega_B^2)} \quad (C5)$$

where

$$\frac{1}{\omega_B^2} = \bar{m}_e \int_0^{\bar{L}} \frac{x^2 dx}{(EI)_p} \quad (C6)$$

and P_p is the downward vertical force at the pylon root and M_p is the moment at the pylon root. (See fig. 11.) For a uniform pylon,

$$\omega_B^2 = \frac{3(EI)_p}{\bar{m}_e \bar{L}^3} \quad (C7)$$

Pylon Twist

From elementary beam theory, torsional deformations of the pylon are governed by

$$(GJ)_p \frac{d\phi_p}{dx_p} = -\bar{m}_e \bar{J}_e \omega^2 \phi_p(0) \quad (C8)$$

where $\bar{m}_e \bar{J}_e$ represents the torsional inertia of the engine. Integrating equation (C8) and evaluating the result at the engine yield

$$\phi_p(0) = \frac{\phi_p(\bar{L})}{1 - (\omega^2 / \omega_T^2)} \quad (C9)$$

where

$$\frac{1}{\omega_T^2} = \bar{m}_e \bar{J}_e \int_0^{\bar{L}} \frac{dx}{(GJ)_p} \quad (C10)$$

For a uniform pylon,

APPENDIX C

$$\omega_T^2 = \frac{(GJ)_p}{\bar{L} \bar{m}_e \bar{J}_e} \quad (C11)$$

Hence from equilibrium, the torque at the pylon root is

$$T_p = \frac{\bar{m}_e \bar{J}_e \omega^2 \phi_p(\bar{L})}{1 - (\omega^2 / \omega_T^2)} \quad (C12)$$

Continuity of Displacements, Forces, and Moments at Pylon Root

Enforcing the continuity of displacements and rotations at the i th finite-difference station where the pylon is rigidly attached to the wing's elastic axis implies

$$\Theta_p(\bar{L}) = \alpha_i \cos \Lambda - \bar{h}_i' \sin \Lambda \quad (C13)$$

$$\phi_p(\bar{L}) = \alpha_i \sin \Lambda + \bar{h}_i' \cos \Lambda \quad (C14)$$

$$h_p(\bar{L}) = -\bar{h}_i \quad (C15)$$

Moreover, from figure 11

$$\bar{\epsilon} \bar{q}_{h,i} = P_p \quad (C16)$$

$$\bar{\epsilon} \bar{q}_{\alpha,i} = M_p \cos \Lambda + T_p \sin \Lambda \quad (C17)$$

$$\bar{\epsilon} \bar{q}_{m,i} = T_p \cos \Lambda - M_p \sin \Lambda \quad (C18)$$

except for $i = N$ where $\bar{\epsilon}/2$ should replace $\bar{\epsilon}$. Finally, substituting equations (C13) to (C15) into equations (C4), (C5), and (C12) and then substituting the resulting equation into equations (C16) to (C18) yields, in dimensionless quantities,

$$q_{h,i} = \frac{\Omega^2}{1 - (\Omega/\Omega_B)^2} \frac{m_e}{\epsilon} \left[\left(\alpha_i \cos \Lambda - \frac{dh_i}{d\eta} \frac{\sin \Lambda}{R} \right) L + h_i \right] \quad (C19)$$

APPENDIX C

$$q_{\alpha,i} = \Omega^2 \frac{m_e}{\epsilon R^2} \left[\left(\alpha_i \cos \Lambda - \frac{dh_i}{d\eta} \frac{\sin \Lambda}{R} \right) L + h_i \right] \frac{L \cos \Lambda}{1 - (\Omega/\Omega_B)^2} + J_e \frac{m_e}{\epsilon} \Omega^2 \left(\alpha_i \sin \Lambda + \frac{dh_i}{d\eta} \frac{\cos \Lambda}{R} \right) \frac{\sin \Lambda}{1 - (\Omega/\Omega_T)^2} \quad (C20)$$

$$q_{m,i} = J_e \frac{m_e}{\epsilon} \Omega^2 R \left(\alpha_i \sin \Lambda + \frac{dh_i}{d\eta} \frac{\cos \Lambda}{R} \right) \frac{\cos \Lambda}{1 - (\Omega/\Omega_T)^2} - \Omega^2 \frac{m_e L}{\epsilon R} \left[\left(\alpha_i \cos \Lambda - \frac{dh_i}{d\eta} \frac{\sin \Lambda}{R} \right) L + h_i \right] \frac{\sin \Lambda}{1 - (\Omega/\Omega_B)^2} \quad (C21)$$

where

$$L = \frac{\bar{L}}{b_r} \quad m_e = \frac{\bar{m}_e}{\bar{l} m_r} \quad J_e = \frac{\bar{J}_e}{\bar{l}^2}$$

$$\Omega_B^2 = \frac{m_r \omega_B^2 \bar{l}^4}{(EI)_r} \quad \Omega_T^2 = \frac{m_r \omega_T^2 \bar{l}^4}{(EI)_r}$$

In numerically evaluating the engine loads, the following finite-difference equations were employed for symmetric flutter modes:

$$\frac{dh_i}{d\eta} = \left\{ \begin{array}{ll} -R\alpha_i \tan \Lambda & (i = 1) \\ \frac{h_{i+1} - h_{i-1}}{2\epsilon} & (i = 2, 3, \dots, N-1) \\ \frac{1}{2 \left[(EI)_N - (1/4) \epsilon^4 \Omega^2 q_3^* \right]} \epsilon \left\{ \left[2(EI)_N + \frac{1}{2} \epsilon^4 \Omega^2 q_2^* \right] \right. \\ \left. \times h_N - (EI)_N h_{N-1} + \frac{1}{2} q_1^* \epsilon^4 \Omega^2 \alpha_N \right\} & (i = N) \end{array} \right\} \quad (C22)$$

APPENDIX C

where

$$q_1^* = \frac{1}{2}(m_e)_N \left\{ \frac{(J_e)_N^R}{\epsilon^2 \left[1 - \left(\Omega^2 / \Omega_T^2 \right) \right]_N} - \frac{L_N^2}{\epsilon^2 R \left[1 - \left(\Omega^2 / \Omega_B^2 \right) \right]_N} \right\} \sin 2\Lambda \quad (C23)$$

$$q_2^* = -\frac{1}{2} \frac{(m_e)_N L_N^2 \sin 2\Lambda}{\epsilon^2 \left[1 - \left(\Omega^2 / \Omega_B^2 \right) \right]_N} \quad (C24)$$

$$q_3^* = (m_e)_N \left\{ \frac{(J_e)_N \cos^2 \Lambda}{\epsilon^2 \left[1 - \left(\Omega^2 / \Omega_T^2 \right) \right]_N} + \frac{L_N^2 \sin^2 \Lambda}{\epsilon^3 R^2 \left[1 - \left(\Omega^2 / \Omega_B^2 \right) \right]_N} \right\} \quad (C25)$$

and the subscript N designates the properties of an engine/pylon attached to the tip of the wing. The value of $dh_N/d\eta$ as expressed in equation (C22) was found from equation (B26) and (C21). In addition

$$\frac{d\alpha_i}{d\eta} = \left\{ \begin{array}{ll} \frac{\alpha_2 - \alpha_1}{\epsilon} & (i = 1) \\ \frac{\alpha_{i+1} - \alpha_{i-1}}{2\epsilon} & (i = 2, 3, \dots, N-1) \\ \frac{\alpha_N - \alpha_{N-1}}{\epsilon} & (i = N) \end{array} \right\} \quad (C26)$$

For the case of antisymmetric flutter modes,

$$\frac{dh_i}{d\eta} = \left\{ \begin{array}{ll} \frac{h_2 - h_0}{2\epsilon} & (i = 1) \\ \left[h_3 - \frac{1}{4} \frac{d(h_2 - h_0)}{\epsilon \cos \Lambda} \right] \frac{1}{\epsilon} & (i = 2) \end{array} \right\} \quad (C27)$$

APPENDIX C

$$\frac{d\alpha_i}{d\eta} = \left\{ \begin{array}{l} \left[\alpha_2 - \frac{1}{2}(h_2 - h_0) \frac{\tan \Lambda}{\epsilon R} \right] \frac{1}{\epsilon} \quad (i = 1) \\ \left[\alpha_3 - \frac{1}{2}(h_2 - h_0) \frac{\tan \Lambda}{\epsilon R} \right] \frac{1}{2\epsilon} \quad (i = 2) \end{array} \right\} \quad (C28)$$

Equations (C22) and (C26) are valid for $i > 2$. For the case of a cantilever wing

$$\frac{dh_i}{d\eta} = \left\{ \begin{array}{l} 0 \quad (i = 1) \\ \frac{h_3}{2\epsilon} \quad (i = 2) \end{array} \right\} \quad (C29)$$

$$\frac{d\alpha_i}{d\eta} = \left\{ \begin{array}{l} \frac{\alpha_2}{\epsilon} \quad (i = 1) \\ \frac{\alpha_3}{2\epsilon} \quad (i = 2) \end{array} \right\} \quad (C30)$$

For $i > 2$ the expressions for $dh_i/d\eta$ and $d\alpha_i/d\eta$ may be obtained from equations (C22) and (C26).

Fuselage Loads

Because of the similarity between the engine-pylon and fuselage models (compare assumptions (4) and (6)), the derivation of the fuselage loads may be readily obtained from equations (C19) to (C21) evaluated at $i = 1$. Consider the fuselage to be composed of two engine-pylon combinations, one extending forward and the other aft of the carry-through beam to which they are rigidly attached. Inasmuch as, for the case of symmetric or cantilever flutter modes, the roll, pitch, and plunge of the fuselage at the carry-through beam are the same as those at the first finite-difference station, equations (C19) to (C21) with $i = 1$ provide the fuselage loads. For antisymmetric flutter modes, the roll and pitch of the fuselage and the carry-through beam are still the same; however, the plunge of the fuselage at the carry-through beam is zero, and that at the first finite-difference station is given by equation (B28).

APPENDIX D

EVALUATION OF THE FLUTTER DETERMINANT AND THE EXTRACTION OF ITS EIGENVALUES

The value of the complex eigenvalue (frequency), Ω , at a value of λ , is determined from a Newton-Raphson iteration technique whose iterative steps are

$$\Omega_{j+1} = \Omega_j \frac{1}{J_{c,j}} \left[(D_j)_I \frac{\partial (D_j)_R}{\partial \Omega_I} - (D_j)_R \frac{\partial (D_j)_I}{\partial \Omega_I} \right] + \frac{i}{J_{c,j}} \left[(D_j)_R \frac{\partial (D_j)_I}{\partial \Omega_R} - (D_j)_I \frac{\partial (D_j)_R}{\partial \Omega_R} \right] \quad (D1)$$

$$J_{c,j} = \frac{\partial (D_j)_R}{\partial \Omega_R} \frac{\partial (D_j)_R}{\partial \Omega_I} - \frac{\partial (D_j)_R}{\partial \Omega_I} \frac{\partial (D_j)_I}{\partial \Omega_R} \quad (D2)$$

and $(D_j)_R$ and $(D_j)_I$ are the real and imaginary parts, respectively, of the flutter determinant D_j whose roots are sought on the j th iterative step. The partial derivatives appearing in equations (D1) and (D2) are computed by finite-difference approximations. To reduce the amount of computation a marching technique, subsequently described, is used to reduce the flutter determinant solved by equation (D1) to order three.

In this marching method, values of two displacements and one angle near the root of the wing are assumed. Through simultaneous application of all but three of the governing equations the displacements throughout the aircraft can be calculated from the assumed values. (The number of displacements and angles which must be assumed at the root is determined by the number of boundary conditions at the root and hence by the order of the governing equations, which is fourth order in h and second order in α .) The remaining three governing equations, valid at the wing tip, provide the reduced flutter determinant. The method proceeds as follows.

Symmetric Flutter Modes

For symmetric flutter modes, the following procedure is used:

- (1) Set $h_{11} = 1$, $h_{21} = \alpha_{11} = 0$, where the first subscript refers to the finite-difference station and the second to one of three assumed solutions
- (2) With the values set in step (1), solve for α_{21} from equation (B16)
- (3) With the values set in step (1) and derived in step (2), solve for h_{31} from equation (B17)

APPENDIX D

- (4) Continue, using equations (B18) to (B28) to solve for $\alpha_{31}, h_{41}, \alpha_{41}, h_{51}, \dots, h_{N1}, \alpha_{N1}$ in that order
- (5) Set $h_{12} = \alpha_{12} = 0$ and $h_{22} = 1$
- (6) Perform steps (2) to (4) calculating $\alpha_{22}, h_{32}, \alpha_{32}, h_{42}, \dots, h_{N2}, \alpha_{N2}$
- (7) Set $h_{13} = h_{23} = 0$ and $\alpha_{13} = 1$
- (8) Perform steps (2) to (4) calculating $\alpha_{33}, h_{33}, \dots, h_{N3}, \alpha_{N3}$

The total solution is a linear superposition of the three assumed sets of displacements as

$$h_i = \sum_{r=1}^3 A_r h_{ir} \qquad \alpha_i = \sum_{r=1}^3 A_r \alpha_{ir} \qquad (D3)$$

The total solution must satisfy the three remaining governing equations (eqs. (B23) to (B25)). Hence at a value of $\Omega = \Omega_j$, one has

$$\begin{bmatrix} e_1^{(23)} & e_2^{(23)} & e_3^{(23)} \\ e_2^{(24)} & e_2^{(24)} & e_3^{(24)} \\ e_3^{(25)} & e_2^{(25)} & e_3^{(25)} \end{bmatrix} \begin{bmatrix} A_1 \\ A_2 \\ A_3 \end{bmatrix} = 0 \qquad (D4)$$

where $e_r^{(23)}$, $e_r^{(24)}$, and $e_r^{(25)}$ ($r = 1, 2, 3$) are the complex values of the left-hand side of equations (B23), (B24), and (B25), respectively, for the r th set of trial solutions. For a nontrivial solution of equation (D4), the determinant of the coefficients must vanish; hence, the determinant of the matrix e is the reduced flutter determinant

$$D_j = |e|_{\Omega=\Omega_j} \qquad (D5)$$

Antisymmetric Flutter Modes

For antisymmetric flutter modes, the following procedure is used:

- (1) Set $h_{21} = 1$ and $h_{31} = \alpha_{21} = 0$
- (2) Solve for h_{01} from equation (B36), α_{31} from equation (B37), and h_{41} from equation (B38)

APPENDIX D

- (3) Continue using equations (B20) to (B22) to solve for $\alpha_{41}, h_{51}, \dots, h_{N1}, \alpha_{N1}$ in that order
- (4) Set $h_{22} = \alpha_{22} = 0$ and $h_{32} = 1$
- (5) Perform steps (2) to (4)
- (6) Set $h_{23} = h_{33} = 0$ and $\alpha_{23} = 1$
- (7) Perform steps (2) to (4)

The flutter determinant is then given by equation (D4).

Cantilever Flutter Modes

The same trial solutions are used for the cantilever flutter modes as for the anti-symmetric case in conjunction with equations (B44), (B45), and (B20) to (B25).

APPENDIX E

EVALUATION OF $\bar{E}I$ AND $\bar{G}J$ OF LAMINATED, BALANCED PLY, FILAMENTARY COMPOSITE WING BOX

By employing the usual thin-plate Bernoulli-Euler assumptions and neglecting chordwise bending of the wing, the displacements \bar{w} , \bar{u} , and \bar{v} take the form

$$\bar{w}(\bar{\eta}, \bar{\xi}) = \bar{h}(\bar{\eta}) - \bar{\xi}\alpha(\bar{\eta}) \quad (\text{E1})$$

$$\bar{u}(\bar{\eta}, \bar{\xi}) = -z \left[\bar{h}'(\bar{\eta}) - \bar{\xi}\alpha'(\bar{\eta}) \right] \quad (\text{E2})$$

$$\bar{v}(\bar{\eta}, \bar{\xi}) = -z\alpha(\bar{\eta}) \quad (\text{E3})$$

Consequently, the strains are

$$\epsilon_{\eta} = \frac{\partial \bar{u}}{\partial \bar{\eta}} = -z \left(\bar{h}'' - \bar{\xi}\alpha'' \right) \quad (\text{E4})$$

$$\epsilon_{\eta\xi} = \frac{1}{2} \left(\frac{\partial \bar{u}}{\partial \bar{\xi}} + \frac{\partial \bar{v}}{\partial \bar{\eta}} \right) = -z\alpha' \quad (\text{E5})$$

$$\epsilon_{\xi} = \epsilon_{\eta z} = \epsilon_{\xi z} = 0 \quad (\text{E6})$$

If only the energy associated with the upper and lower covers of the box is considered, the strain energy per unit length along the elastic axis is

$$U_{\eta} = \frac{1}{2} \int_{-\bar{b}^*}^{\bar{b}^*} \int_{-z_0}^{z_0} \left(\sigma_{\eta} \epsilon_{\eta} + \sigma_{\xi} \epsilon_{\xi} + 2\sigma_{\eta\xi} \epsilon_{\eta\xi} \right) dz d\bar{\xi} \quad (\text{E7})$$

where z_0 is the distance from the middle surface of the box ($z = 0$) to the outer face of either the top or bottom cover of the box. Substituting equations (E1) to (E3) into equation (E4) yields

$$U_{\eta} = \frac{1}{2} \int_{-\bar{b}^*}^{\bar{b}^*} \int_{-z_0}^{z_0} \left[-z\sigma_{\eta} \left(\bar{h}'' - \bar{\xi}\alpha'' \right) - 2z\sigma_{\eta\xi} \alpha' \right] dz d\bar{\xi} \quad (\text{E8})$$

APPENDIX E

and substituting equations (10), (11), (E4), (E5), and (E6) into equation (E8) yields,

$$U_\eta = \int_{-\bar{b}^*}^{\bar{b}^*} \left\{ \sum_{j=1}^{N_L} \int_{\xi_{j-1}}^{\xi_j} \left[z^2 a_{11,j} (\bar{h}'' - \bar{\xi} \alpha'')^2 + 4z^2 a_{33,j} (\alpha')^2 \right] dz \right\} d\bar{\xi} \quad (E9)$$

Integrating through z gives

$$U_\eta = \int_{-\bar{b}^*}^{\bar{b}^*} \sum_{j=1}^{N_L} \beta_j \left[a_{11,j} (\bar{h}'' - \bar{\xi} \alpha'')^2 + 4a_{33,j} (\alpha')^2 \right] d\bar{\xi} \quad (E10)$$

where

$$\beta_j = \frac{1}{3} (\xi_j^3 - \xi_{j-1}^3) \quad (E11)$$

and integrating through $\bar{\xi}$ gives,

$$U_\eta = \sum_{j=1}^{N_L} \beta_j \left[2a_{11,j} \bar{b}^* (\bar{h}'')^2 + \frac{2}{3} (\bar{b}^*)^3 (\alpha'')^2 + 8\bar{b}^* a_{33,j} (\alpha')^2 \right] \quad (E12)$$

Then introducing nondimensional quantities yields

$$U_\eta = \frac{2}{\bar{l} R^3} \sum_{j=1}^{N_L} \beta_j \left[a_{11,j} b^* \frac{d^2 h}{d\eta^2} + 4a_{33,j} b^* R^2 \left(\frac{d\alpha}{d\eta} \right)^2 + \frac{1}{3} (b^*)^3 a_{11,j} \left(\frac{d^2 \alpha}{d\eta^2} \right)^2 \right] \quad (E13)$$

where \bar{b}^* has been replaced by $b_r b^*$. For high-aspect-ratio wings it is assumed that the last term on the right-hand side of equation (E13) may be neglected compared with the next to the last term (see ref. 13 for further explanation); hence,

$$U_\eta \approx \frac{2}{\bar{l} R^3} \sum_{j=1}^{N_L} \beta_j \left[a_{11,j} b^* \left(\frac{d^2 h}{d\eta^2} \right)^2 + 4a_{33,j} b^* R^2 \left(\frac{d\alpha}{d\eta} \right)^2 \right] \quad (E14)$$

Furthermore, for a beam,

$$U_\eta = \frac{L}{2\bar{l} R^3} \left[\frac{EI}{b_r} \left(\frac{d^2 h}{d\eta^2} \right)^2 + R^2 \frac{GJ}{b_r} \left(\frac{d\alpha}{d\eta} \right)^2 \right] \quad (E15)$$

Comparison of equations (E11) and (E12) indicates that

APPENDIX E

$$\overline{EI} = 4b^* \sum_{j=1}^{N_L} a_{11,j}^{\beta_j} \quad (\text{E16})$$

and

$$\overline{GJ} = 16b^* \sum_{j=1}^{N_L} a_{33,j}^{\beta_j} \quad (\text{E17})$$

It is readily shown that equation (E16) is the same result derived from laminated plate theory and that equation (E17) reduces to Bredt's formula for a thin-walled isotropic tube with a rectangular cross section in which

$$\sum_{j=1}^{N_L} \frac{t_j}{z_T} \ll 1 \quad (\text{E18})$$

and

$$\frac{z_T}{b^*} \ll 1 \quad (\text{E19})$$

APPENDIX F

COMPUTER PROGRAM

The computer program COMBOF was written in FORTRAN IV on a SCOPE 3.1 system modified for Langley Research Center and executes and loads with a field length specification of 60000 octal. The program is applicable to the flutter analysis (including rigid-body roll, pitch, and plunge) of composite swept-wing subsonic aircraft. To aid the user, a brief description of the input (which is supplied in Namelist format), an example problem showing input and output, a program flow diagram (fig. 4), and a complete program listing are provided.

Input Description

NAMELIST /OPTION/

ISYM = 1	cantilever flutter modes
= 2	symmetric flutter modes
= 3	antisymmetric flutter modes
KOPT = 1	option for tracing each root locus branch up to a maximum value of λ (DAMMAX) while ignoring the occurrence of flutter
= 2	normal running option for parametric studies in which the root locus branches are traced up to flutter or a maximum value of λ (DAMMAX)
ISHAPE = 1	flutter mode shapes are computed and printed
= 2	flutter mode shapes are not computed
ILMAX	maximum number of branches to be traced (also, number of natural frequencies calculated)
IMORDER	one-dimensional array specifying order in which branches are to be searched (e.g., 2, 3, 1, 4, 5) where the branch number is determined by the order of the natural frequency from which it emanates

NAMELIST /TRACE/

DAM	λ increment used in tracing each branch
IPROC = 1	trace of branch will continue even if Newton-Raphson method fails to converge within specified number of iterations

APPENDIX F

IPROC = 2 search of branch terminates if Newton-Raphson method fails to converge within specified number of iterations
 ITMAX maximum number of iterations for convergence of Newton-Raphson method when IPROC = 2
 ISTOP maximum number of λ increments along any branch
 DAMMAX maximum value of λ above which no search for flutter is made
 DOM1 increment used in the finite difference evaluation of the partial derivatives appearing in the Newton-Raphson method

NAMELIST /INOUT/

IX or JX = 1 display of two separately controlled sets of intermediate output
 = 2 no display of two separately controlled sets of intermediate output
 IY = 1 multiple parameter studies on one computer run
 $\neq 1$ single parameter study

NAMELIST /PLAN/

SPAN = \bar{l}

The following six symbols denote one-dimensional arrays which prescribe wing properties at each finite-difference station on the wing:

A = \bar{a}

B = \bar{b}

SW = \bar{x}_α

RGSQ = \bar{r}_α^2

BCH = $2\bar{b}^*$

ZT = z_T

Q reduced stiffness matrix supplied by column

SWEEP sweep angle Λ of elastic axis in radians

N number of finite-difference stations along elastic axis

CL one-dimensional array prescribing c_{l_α} at each finite-difference station

AC one-dimensional array prescribing a_c at each finite-difference station

APPENDIX F

NAMELIST /ENGINE/

The following six symbols denote one-dimensional arrays prescribing engine, pylon, or fuselage properties of each engine or fuselage:

$$\text{ENEI} = \frac{\bar{L}^3}{3 \int_0^{\bar{L}} \xi^2 \frac{d\xi}{(EI)_p}}$$

$$\text{ENGJ} = \frac{\bar{L}}{\int_0^{\bar{L}} d\xi / (GJ)_p}$$

$$\text{ENJ} = \bar{J}_e$$

$$\text{ENM} = \bar{m}_e$$

$$\text{PYL} = \bar{L}$$

LOC finite-difference stations at which pylons are attached. As discussed in appendix C, the fuselage is simulated by two engine-pylon combinations, both having LOC = 1 but one extending fore and the other aft of the carry-through beam.

NENG total number of engines (including the number of fuselage lumped masses)

NAMELIST /DESIGN/

$$\text{EIREF} = (EI)_r$$

$$\text{EMREF} = m_r$$

$$\text{RHO} = \rho$$

RHOBAR mass density of composite material

$$\text{BREF} = b_r$$

WTI one-dimensional array prescribing nonstructural weight per unit length of wing along elastic axis

LOW during a parameter study, periodic checks are made for discontinuities in lowest flutter speed by tracing all root locus branches starting from $\lambda = 0$; a count is kept of number of successive parameter increments for which no check is made and a check is initiated when this count equals integer value of LOW

APPENDIX F

NL	number of layers of composite material in top or bottom covers of wing box
DB	diameter of fuselage
G	acceleration due to gravity

NAMELIST/ PARAM/

Two types of automatic parameter studies are available to the user. In the first option, $ISTIFF = 1$, the program internally calculates \overline{EI} , \overline{GJ} , and \overline{m} of the wing. The user supplies the engine properties in NAMELIST /ENGINE/ and the initial thickness distribution and filament orientation as functions of η in a rectangular array AA; that is,

$$t_j = (AA)_{1,j} + \eta(AA)_{2,j} + (AA)_{3,j} \sin \eta(AA)_{4,j} \quad (F1)$$

$$\theta_j = (AA)_{5,j} + \eta(AA)_{6,j} + (AA)_{7,j} \sin \eta(AA)_{8,j} \quad (F2)$$

Equations (F1) and (F2) are employed in calculating \overline{EI} , \overline{GJ} , and \overline{m} . During the parameter study, specified elements of AA are incremented causing \overline{EI} , \overline{GJ} , and \overline{m} to be incremented.

In the second option, $ISTIFF = 2$, the program increments engine, pylon, or fuselage properties and the user supplies \overline{EI} , \overline{GJ} , and \overline{m} in NAMELIST /STIFF/ and the initial engine-pylon or fuselage properties in array AA. (See listing of subroutine EVAL2 for details.)

KVT	number of elements of array AA which will be simultaneously incremented during study
KV1,KV2	two one-dimensional arrays providing row and column designation, respectively, of elements of AA which are to be incremented during study
DEL	one-dimensional array providing increment size of each element of AA specified by KV1, KV2
MAX	maximum number of parameter increments to be performed during study

NAMELIST /STIFF/ (To be used only if $ISTIFF = 2$)

EM,EI,GJ	one-dimensional arrays which provide \overline{m} , \overline{EI} , and \overline{GJ} at each finite-difference station
----------	---

APPENDIX F

NAMELIST /NATFQ/

OS	starting value of Ω_R , used to search for natural frequencies of aircraft
OE	maximum value of Ω_R during natural frequency search
ODEL	step size of Ω_R used in natural frequency search

APPENDIX F

Program Listing

	PROGRAM COMBOF(INPUT,OUTPUT,TAPE5=INPUT,TAPE6=OUTPUT)	A	1
C		A	2
C	COMPOSITE WING BOX FLUTTER	A	3
C		A	4
C	NASA LANGLEY RESEARCH CENTER PROGRAM A3788	A	5
C	WING IN SUBSONIC FLIGHT	A	6
C		A	7
C	RHO=AIR DENSITY	A	8
C	WING PLANFORM - INPUT	A	9
C		A	10
C	SPAN	A	11
C	A=OFFSET OF ELASTIC AXIS FROM SEMI-CHORD	A	12
C	BOX BEAM CHORD - BCH(NODAL POINT)	A	13
C	RGSQ=RADIUS OF GYRATION ABOUT ELASTIC AXIS	A	14
C	SW=OFFSET OF C.G. FROM ELASTIC AXIS	A	15
C	EM=WING MASS PER UNIT SPAN	A	16
C	EI=WING BENDING STIFFNESS	A	17
C	GJ=WING TORSIONAL STIFFNESS	A	18
C	EIREF,EMREF=REFERENCE BENDING STIFFNESS AND WING MASS RESPECTIVELY	A	19
C	BREF=REFERENCE WING SEMI-CHORD	A	20
C	ZT= ONE HALF THE DISTANCE BETWEEN TOP AND BOTTOM COVERS	A	21
C	RHOBAR=WING BOX COMPOSITE MATERIAL DENSITY	A	22
C	NL=NUMBER OF LAMINAS IN TOP OR BOTTOM WING BOX COVERS	A	23
C	WTI=WEIGHT OF WING PER UNIT SPAN (NOT INCLUDING COMPOSITE WEIGHT)	A	24
C	G=ACCELERATION DUE TO GRAVITY IN APPROPRIATE UNITS	A	25
C	DB=DIAMETER OF FUSELAGE	A	26
C	Q=REDUCED STIFFNESS MATRIX	A	27
C		A	28
C	ENGINE DATA - INPUT	A	29
C	ENEI=BENDING STIFFNESSES OF PYLONS	A	30
C	ENGJ=TORSIONAL STIFFNESSES OF PYLONS	A	31
C	ENJ=TORSIONAL INERTIA OF ENGINE	A	32
C	NENG=NUMBER OF ENGINES (INCLUDE FUSELAGE IN COUNT)	A	33
C	LOC=NODAL LOCATION OF ENGINE	A	34
C	PYL=PYLON LENGTH	A	35
C	ENM=ENGINE MASSES	A	36
C		A	37
C	MATRIX AA CONTAINS INFORMATION RELATING TO THE LAMINA THICKNESS	A	38
C	AND FILAMENT ORIENTATION WHEN ISTIFF=1 AND RELATES TO ENGINE/PYLON	A	39
C	INFORMATION WHEN ISTIFF=2. (SEE EVAL1 AND EVAL2)	A	40
C		A	41
C	COMMON // IX,JX,IERROR,KOPT/CUM/OM,LAMBDA,RHO,EM(60),EI(61),GJ(61)	A	42
	1,A(60),B(60),SW(60),AR,RGSQ(60),MU,E(3,3),W(60),AL(60),NN,SWEEP,IP	A	43
	2ROCD,ITMAX,ISYM,CL(90),AC(90)/STATIC/IST,ALO,CMAC,EL,ISHAPE/PYLON/	A	44
	3BPY(10),CPY(10),DPY(10),ENJ(10),ENM(10),ENEI(10),ENGJ(10),PYL(10),	A	45
	4LOC(10),NENG/BLK1/RHOBAR,SPAN,BCH(60),G/BLK2/Q(3,3),ZT(60),EIREF,E	A	46
	5MREF,OBEGIN,LBEGIN/FREQ/OM1(5),DOM1,DAM,OMMAX1,TOAM,DAMMAX	A	47
	DIMENSION AA(8,4), IMORDER(5), WTI(60), KV1(4), KV2(4), DEL(4)	A	48
	REAL LAMBDA,LBEGIN	A	49
	COMPLEX OM,W,AL,E,OBEGIN	A	50

APPENDIX F

C		A	51
C	INOUT DATA IS IN NAMELIST FORM	A	52
C		A	53
	NAMELIST /OPTION/ ISYM,KOPT,ISHAPE,ILMAX,IMORDER	A	54
	NAMELIST /TRACE/ DAM,IPROC,ITMAX,ISTOP,DAMMAX,DOM1	A	55
	NAMELIST /INOUT/ IX,JX,IY	A	56
	NAMELIST /PLAN/ SPAN,A,B,SW,RGSQ,BCH,ZT,Q,SWEEP,N,CL,AC	A	57
	NAMELIST /ENGINE/ ENEI,ENGJ,ENJ,ENM,PYL,LOC,NENG	A	58
	NAMELIST /DESIGN/ EIREF,EMREF,RHO,RHOBAR,BREF,WTI,LDW,NL,DB,G	A	59
	NAMELIST /PARAM/ ISTIFF,AA,KVT,KV1,KV2,DEL,MAX	A	60
	NAMELIST /STIFF/ EM,EI,GJ	A	61
	NAMELIST /START/ OBEGIN,LBEGIN	A	62
	NAMELIST /NATFQ/ OS,OE,ODEL	A	63
1	READ OPTION	A	64
	READ TRACE	A	65
	READ INOUT	A	66
	READ PLAN	A	67
	READ ENGINE	A	68
	READ DESIGN	A	69
	READ PARAM	A	70
	IF (ISTIFF.EQ.2) READ STIFF	A	71
	IF (ISTIFF.EQ.1.AND.NL.EQ.0) READ STIFF	A	72
C		A	73
C	FOR FLUTTER SET (FORD=1	A	74
	IFORD=1	A	75
	IST=IFORD	A	76
	IM=0	A	77
	ISTART=3	A	78
	DBAR=.5*DB	A	79
	MU=N	A	80
	EL=N-1	A	81
	LBEGIN=0.	A	82
	OBEGIN=0.	A	83
	IF (ISTART.EQ.2) READ START	A	84
	READ NATFQ	A	85
	PRINT 26	A	86
	PRINT 34	A	87
	PRINT 27, IX,JX,N,IFORD,MAX,SPAN,SWEEP,(KV1(I),KV2(I),DEL(I),I=1,K	A	88
	1VT)	A	89
	PRINT 41, IPROC,ITMAX,ISTOP,ISHAPE,ISYM,ISTART,ILMAX,KOPT	A	90
	PRINT 38	A	91
	PRINT 28, (I,A(I),B(I),SW(I),RGSQ(I),I=1,MU)	A	92
	PRINT 49	A	93
	PRINT 50, (I,BCH(I),ZT(I),WTI(I),I=1,MU)	A	94
	PRINT 29, ((Q(I,J),J=1,3),I=1,3)	A	95
	PRINT 30, COM1,DAM,DAMMAX	A	96
	PRINT 32, RHO,RHOBAR,EIREF,EMREF,BREF	A	97
	IF (NENG.EQ.0) GO TO 2	A	98
	PRINT 31, (LOC(I),ENEI(I),ENGJ(I),ENJ(I),ENM(I),PYL(I),I=1,NENG)	A	99
	GO TO 3	A	100
2	PRINT 43	A	101
3	IF (ISTIFF.EQ.2) GO TO 5	A	102
	IF (NL.EQ.0) PRINT 47	A	103
	IF (NL.EQ.0) GO TO 7	A	104
	PRINT 44	A	105
	DO 4 I=1,8	A	106
4	PRINT 33, (AA(I,J),J=1,NL)	A	107
	GO TO 7	A	108
5	PRINT 45	A	109
	DO 6 I=1,5	A	110
6	PRINT 33, (AA(I,J),J=1,NENG)	A	111
7	CONTINUE	A	112
	IF (ISTART.EQ.2) PRINT 40, OBEGIN,LBEGIN	A	113
	IERROR=0	A	114
	IERRS=0	A	115

APPENDIX F

C		A 116
C	NON-DIMENSIONALIZE	A 117
C		A 118
	RBREF=1./BREF	A 119
	AR=SPAN*RBREF	A 120
	REIREF=1./EIREF	A 121
	DBAR=DBAR/SPAN	A 122
	RHO=3.141592658979*BREF*BREF*RHO/EMREF	A 123
	REMREF=1./EMREF	A 124
	DO 8 I=1,MU	A 125
	B(I)=B(I)*RBREF	A 126
	A(I)=A(I)*RBREF	A 127
	SW(I)=SW(I)*RBREF	A 128
8	RGSQ(I)=RGSQ(I)*RBREF*RBREF	A 129
	PRINT 35	A 130
	PRINT 38	A 131
	PRINT 28, (I,A(I),B(I),SW(I),RGSQ(I),I=1,MU)	A 132
	IF (NENG.EQ.0) GO TO 10	A 133
	DO 9 I=1,NENG	A 134
	ENEI(I)=ENEI(I)*REIREF	A 135
	ENGJ(I)=ENGJ(I)*REIREF	A 136
	ENJ(I)=ENJ(I)/(SPAN*SPAN)	A 137
	ENM(I)=ENM(I)*REMREF/SPAN	A 138
9	PYL(I)=PYL(I)*RBREF	A 139
	PRINT 31, (LOC(I),ENEI(I),ENGJ(I),ENJ(I),ENM(I),PYL(I),I=1,NENG)	A 140
10	IF (ISTIFF.EQ.1.AND.NL.GT.0) GO TO 12	A 141
	DO 11 I=1,MU	A 142
	EI(I)=EI(I)*REIREF	A 143
	GJ(I)=GJ(I)*REIREF	A 144
11	EM(I)=EM(I)*REMREF	A 145
12	CONTINUE	A 146
	RKAPPA=1./RHO	A 147
	PRINT 39, AR,RKAPPA	A 148
	PRINT 51	A 149
	AR=AR/EL	A 150
	DOM1=DOM1/EL**2	A 151
	DAM=DAM/EL**3	A 152
	DBAR=DBAR*EL	A 153
C	PRE CALCULATIONS FOR ENGINES	A 154
	IF (NENG.EQ.0) GO TO 14	A 155
	DO 13 IJ=1,NENG	A 156
	ENM(IJ)=ENM(IJ)*EL	A 157
	ENJ(IJ)=ENJ(IJ)*EL*EL	A 158
C	1/BPY = FIRST BENDING FREQ. OF PYLON	A 159
C	1/DPY = FIRST TORSIONAL FREQ. OF PYLON	A 160
	BPY(IJ)=PYL(IJ)*PYL(IJ)*PYL(IJ)*ENM(IJ)/(3.*ENEI(IJ))/(AR*AR*AR)	A 161
	CPY(IJ)=ENJ(IJ)*ENM(IJ)	A 162
13	DPY(IJ)=CPY(IJ)*PYL(IJ)/(ENGJ(IJ)*AR)	A 163
14	CONTINUE	A 164
C		A 165
C	CALL EVAL1 TO PREPROCESS EI,GJ AND EM IF ISTIFF=1	A 166
C	CALL EVAL2 TO PREPROCESS ENGINE DATA IF ISTIFF=2	A 167
C		A 168
	IF (ISTIFF.EQ.1) CALL EVAL1 (AA,WTI,NL)	A 169
	IF (ISTIFF.EQ.2) CALL EVAL2 (AA)	A 170
	PRINT 36	A 171

APPENDIX F

	MU1=MU+1	A 172
	PRINT 37, (I,EI(I),GJ(I),EM(I),CL(I),AC(I),I=1,MU)	A 173
	IF (ISTART.NE.3) GO TO 15	A 174
	CALL NATRL (ILMAX,OS,OE,ODEL)	A 175
	PRINT 42, (OM1(I),I=1,ILMAX)	A 176
	IM=0	A 177
15	CALL RLF (QBEGIN,LBEGIN,ISTART,ILMAX,IM,IMORDER)	A 178
	V=SQRT(LBEGIN*EIREF/(SPAN**3)/BREF*3.141592658979*(BREF*BREF)/(EMR	A 179
	IEF*RHO))	A 180
	IF (IERROR.EQ.0) PRINT 46, V	A 181
	PRINT 51	A 182
	IT=1	A 183
	KX=1	A 184
	IF (MAX.EQ.0) GO TO 25	A 185
C		A 186
C	INCREMENT PARAMETER	A 187
C		A 188
	DO 24 KZ=1,MAX	A 189
	IF (IERRS.GT.2.AND.KOPT.EQ.1) GO TO 24	A 190
	IERRS=0	A 191
	CALL VARY (AA,KV1,KV2,KVT,DEL,WTI,NL,ISTIFF)	A 192
	IF (ISTIFF.EQ.2) PRINT 48, (LOC(I),ENEI(I),ENGJ(I),ENJ(I),ENM(I),P	A 193
	IYL(I),I=1,NENG)	A 194
	IF (ISTIFF.EQ.1) PRINT 36	A 195
	IF (ISTIFF.EQ.1) PRINT 37, (I,EI(I),GJ(I),EM(I),CL(I),AC(I),I=1,MU	A 196
	1)	A 197
	IF (ISTIFF.EQ.2) GO TO 17	A 198
	PRINT 44	A 199
	DO 16 I=1,8	A 200
16	PRINT 33, (AA(I,J),J=1,NL)	A 201
	GO TO 19	A 202
17	PRINT 45	A 203
	DO 18 I=1,5	A 204
18	PRINT 33, (AA(I,J),J=1,NENG)	A 205
19	CONTINUE	A 206
	IF (KX.LT.LOW) GO TO 20	A 207
	ISTART=3	A 208
	KX=0	A 209
20	IF (ISTART.EQ.2) GO TO 22	A 210
21	CALL NATRL (ILMAX,OS,OE,ODEL)	A 211
	PRINT 42, (OM1(I),I=1,ILMAX)	A 212
22	CALL RLF (QBEGIN,LBEGIN,ISTART,ILMAX,IM,IMORDER)	A 213
	V=SQRT(LBEGIN*EIREF/(SPAN**3)/BREF*3.141592658979*(BREF*BREF)/(EMR	A 214
	IEF*RHO))	A 215
	PRINT 46, V	A 216
	PRINT 51	A 217
	KX=KX+1	A 218
	IF (IOPT.EQ.1) GO TO 23	A 219
23	IERRS=IERRS+IERROR	A 220
	IF (IERRS.GT.2) GO TO 24	A 221
	IF (IERROR.GT.0) GO TO 21	A 222
24	CONTINUE	A 223
25	IF (IY.EQ.1) GO TO 1	A 224
	STOP	A 225

APPENDIX F

C		A 226
26	FORMAT (1H1,35X,6HCOMBOF,3X,28H(COMPOSITE WING BOX FLUTTER),/,35X, 142(1H*),///)	A 227 A 228
27	FORMAT (10X,3HIX=,I1,5X,3HJX=,I1,5X,2HN=,I2,5X,6HIFORD=,I2,5X,4HMA 1X=,I3,5X,5HSPAN=,E16.8,6X,6HSWEEP=,E16.8//,(10X,11HKV1,KV2,DEL,2X, 2I2,3X,I2,3X,E16.8),/)	A 229 A 230 A 231
28	FORMAT (5X,I2,6X,4(E14.6,4X))	A 232
29	FORMAT (//,15X,24HREDUCED STIFFNESS MATRIX,/, (3(2X,E16.8)))	A 233
30	FORMAT (//,15X,5HDOM1=,E16.8,5X,4HDAM=,E16.8,5X,7HDAMMAX=,E16.8//)	A 234
31	FORMAT (//,40X,11HENGINE DATA,//,3X,4HNODE,6X,4HENEI,12X,4HENGJ,12 1X,3HENJ,17X,3HENM,14X,3HPLY,/, (1X,I4,1X,E16.8,2X,E16.8,2X,E16.8,,2 2X,E16.8,2X,E16.8))	A 235 A 236 A 237
32	FORMAT (//,15X,4HRHO=,E16.8,10X,7HRHOBAR=,E16.8,//,15X,6HEIREF=,E1 16.8,8X,6HEMREF=,E16.8,8X,5HBREF=,E16.8//)	A 238 A 239
33	FORMAT (8(2X,E15.8))	A 240
34	FORMAT (//,20X,17HDIMENSIONAL INPUT,/,20X,17(1H*),//)	A 241
35	FORMAT (//,20X,21HNON-DIMENSIONAL INPUT,/,20X,21(1H*),///)	A 242
36	FORMAT (//,1X,9HNODAL PT.,10X,2HEI,16X,2HGJ,16X,2HEM,16X,2HCL,,16X 1,2HAC)	A 243 A 244
37	FORMAT (5X,I2,4X,E16.8,2X,E16.8,2X,E16.8,2X,E16.8,2X,E16.8)	A 245
38	FORMAT (1X,9HNODAL PT.,10X,1HA,17X,1HB,17X,2HSW,15X,4HRGSQ)	A 246
39	FORMAT (//,35X,13HASPECT RATIO=,E16.8,5X,19HMASS RATIO=1/KAPPA=,E1 16.8//)	A 247 A 248
40	FORMAT (/,5X,7HOBEGIN=,2E20.8,5X,7HLBEGIN=,E20.8/)	A 249
41	FORMAT (/,4X,6HIPROCD,2X,53HITMAX ISTOP ISHAPE ISYM ISTART 1 ILMAX KOPT,/,8(4X,I4),/)	A 250 A 251
42	FORMAT (/,5X,23HESTIMATES OF NAT. FREQ.,2(3X,E16.8),/, (3(3X,E16.8) 1))	A 252 A 253
43	FORMAT (///,20X,23HNO ENGINES ON THE WINGS,//)	A 254
44	FORMAT (//,25X,62HELEMENTS OF MATRIX AA (ISTIFF=1, ONE LAMINA PER 1MATRIX COLUMN),//)	A 255 A 256
45	FORMAT (//,40X,21HELEMENTS OF MATRIX AA,/,10X,88H(ISTIFF=2, ONE EN 1GINE/PYLON OR FUSELAGE PER MATRIX COLUMN, WHEN NODE=1 FUSELAGE IMP 2LIED),//)	A 257 A 258 A 259
46	FORMAT (/,30X,14HFLUTTER SPEED=,E16.8/,30X,14(1H*))	A 260
47	FORMAT (//,20X,30HNUMBER OF COMPOSITE LAYERS = 0,/))	A 261
48	FORMAT (//,40X,11HENGINE DATA,//,3X,4HNODE,6X,4HENEI,12X,4HENGJ,12 1X,3HENJ,17X,8HENM(N-1),9X,3HPYL,/, (1X,I4,1X,E16.8,2X,E16.8,2X,E16. 28,2X,E16.8,2X,E16.8))	A 262 A 263 A 264
49	FORMAT (1X,9HNODAL PT.,10X,3HBCH,16X,2HZT,15X,3HWT I)	A 265
50	FORMAT (5X,I2,6X,3(E14.6,4X))	A 266
51	FORMAT (//,1X,110(1H*),//)	A 267
	END	A 268-

APPENDIX F

	SUBROUTINE EVALI (AA,WTI,NL)	B	1
	COMPLEX OM,AL,W,E,OBEGIN	B	2
	REAL LAMBDA,LBEGIN	B	3
C		B	4
C	CUMPUTES WEIGHT OF WING,MASS AND PREPROCESSES EI AND GJ	B	5
C		B	6
C	T=THICKNESS OF WING COVERS	B	7
C	TJ=THICKNESS OF EACH LAMINA	B	8
C	WT=WEIGHT OF WING	B	9
C	THETA=ANGLE OF FILAMENT ORIENTATION	B	10
C		B	11
	COMMON // IX,JX,IERROR,KOPT/CUM/CM,LAMBDA,RHO,EM(60),EI(61),GJ(61)	B	12
	1,A(60),B(60),SW(60),AR,RGSQ(60),MU,E(3,3),W(60),AL(60),NN,SWEEP,IP	B	13
	ZROCD,ITMAX,ISYM,CL(90),AC(90)/BLK1/RHOBAR,SPAN,BCH(60),G/BLK2/D(3,	B	14
	33),ZT(60),EIREF,EMREF,OBEGIN,LBEGIN	B	15
	DIMENSION AA(8,4),WTI(60)	B	16
	IF (NL.EQ.0) RETURN	B	17
	O3=1./3.	B	18
	SMU=SPAN/(MU-1)	B	19
	WT=.0	B	20
	IF (JX.EQ.2) GO TO 1	B	21
	PRINT 7	B	22
1	DO 6 I=1,MU	B	23
	X=(I-1)*SMU/SPAN	B	24
	X1=(I-2)*SMU/SPAN	B	25
	X12=X-.5*SMU/SPAN	B	26
	CHORD=BCH(I)	B	27
	CH1=CHORD	B	28
	IF (I.GT.1) CH1=BCH(I-1)	B	29
	B22=.0	B	30
	B33=.0	B	31
	ZJM12=ZJM1=ZT(I)	B	32
	T=.0	B	33
	IF (I.EQ.1) GO TO 2	B	34
	ZJM12=(ZT(I)+ZT(I-1))*0.5	B	35
2	T12=.0	B	36
	DO 4 IA=1,NL	B	37
	TJ=AA(1,IA)*(1.+X*AA(2,IA))+AA(3,IA)*SIN(AA(4,IA)*X)	B	38
	TJ12=AA(1,IA)*(1.+X12*AA(2,IA))+AA(3,IA)*SIN(AA(4,IA)*X12)	B	39
	THETA=AA(5,IA)*(1.+X*AA(6,IA))+AA(7,IA)*SIN(AA(8,IA)*X)	B	40
	THETA12=AA(5,IA)*(1.+X12*AA(6,IA))+AA(7,IA)*SIN(AA(8,IA)*X12)	B	41
	IF (JX.EQ.2) GO TO 3	B	42

APPENDIX F

	PRINT B, X, T, THETA	B	43
3	CALL TRANS (THETA, A11, A33)	B	44
	ZJ=ZJM1+TJ	B	45
	ZJ12=ZJM12+TJ12	B	46
	BETA=03*(ZJ**3-ZJM1**3)	B	47
	BETA12=03*(ZJ12**3-ZJM12**3)	B	48
C	MULTIPLY BY 2 FOR SYMMETRIC SECTION	B	49
	B22=B22+2.*A11*BETA	B	50
	B33=B33+2.*A33*BETA12	B	51
	ZJM1=ZJ	B	52
	ZJM12=ZJ12	B	53
	T12=T12+TJ12	B	54
4	T=T+TJ	B	55
C	COMPUTE STIFFNESSES OF WING	B	56
	EI(I)=B22*CHORD/EIREF	B	57
	CH12=.5*(CHORD+CH1)	B	58
	GJ(I)=4.*B33*CH12/EIREF	B	59
	IF (I.EQ.1) GO TO 5	B	60
	WT=WT+SMU*(CHORD*T+CH1*TP)*RHOBAR*G+SMU*(WTI(I)+WTI(I-1))*5	B	61
5	TP=T	B	62
6	EM(I)=CHORD*RHOBAR*2.*T/EMREF+WTI(I)/G/EMREF	B	63
C	PRINT 1, WT	B	64
	RETURN	B	65
C		B	66
7	FORMAT (/ , 10X, 1HX, 15X, 2HT1, 15X, 6HTHETA1, 15X, 2HT2, 15X, 6HTHETA2, /)	B	67
8	FORMAT (3X, E16.8, 4(2X, E16.8))	B	68
	END	B	69-

	SUBROUTINE EVAL2 (AA)	C	1
	DIMENSION AA(8,4)	C	2
	COMMON /CUP/ OM, LAMBDA, RHO, EM(60), EI(61), GJ(61), A(60), B(60), SW(60)	C	3
	1, AR, RGSQ(60), MU, E(3,3), W(60), AL(60), NN, SWEEP, IPROCD, ITMAX, ISYM, CL(C	4
	290), AC(90)/PYLON/BPY(10), CPY(10), DPY(10), ENJ(10), ENM(10), ENEI(10),	C	5
	3ENGJ(10), PYL(10), LOC(10), NENG	C	6
	COMPLEX OM, W, AL, E	C	7
C		C	8
C	PREPROCESSOR OF ENGINE PROPERTIES	C	9
C		C	10
	IF (NENG.EQ.0) RETURN	C	11
	DO 1 IJ=1, NENG	C	12
	ENEI(IJ)=AA(1, IJ)	C	13
	ENGJ(IJ)=AA(2, IJ)	C	14
	ENJ(IJ)=AA(3, IJ)	C	15
	ENM(IJ)=AA(4, IJ)	C	16
	PYL(IJ)=AA(5, IJ)	C	17
	BPY(IJ)=PYL(IJ)**3*ENM(IJ)/(3.*ENEI(IJ))/(AR**3)	C	18
	CPY(IJ)=ENJ(IJ)*ENM(IJ)	C	19
1	DPY(IJ)=CPY(IJ)*PYL(IJ)/(ENGJ(IJ)*AR)	C	20
	RETURN	C	21
	END	C	22-

APPENDIX F

	SUBROUTINE TRANS (THETA,A11,A33)	D	1
	COMMON // IX,JX,IERROR,IOPT/BLK2/D(3,3),ZT(60),EIREF,EMREF,OBEGIN,	D	2
	1LBEGIN	D	3
	DIMENSION A(3,3), T(3,3), TI(3,3), ST(3,3)	D	4
	CT=COS(THETA)	D	5
	SIT=SIN(THETA)	D	6
	T(1,1)=CT*CT	D	7
	T(1,2)=SIT*SIT	D	8
	T(1,3)=2.*CT*SIT	D	9
	T(2,1)=T(1,2)	D	10
	T(2,2)=T(1,1)	D	11
	T(2,3)=-T(1,3)	D	12
	T(3,1)=-CT*SIT	D	13
	T(3,2)=-T(3,1)	D	14
	T(3,3)=T(1,1)-T(1,2)	D	15
	IF (IX.EQ.2) GO TO 1	D	16
	PRINT 8, ((T(I,J),J=1,3),I=1,3)	D	17
1	DO 2 I=1,3	D	18
	DO 2 J=1,3	D	19
	A(I,J)=0.	D	20
2	ST(I,J)=.0	D	21
	DO 3 I=1,3	D	22
	DO 3 K=1,3	D	23
	DO 3 J=1,3	D	24
3	ST(I,K)=ST(I,K)+D(I,J)*T(J,K)	D	25
C		D	26
C	NOTE --- TI=T(-THETA)	D	27
C		D	28
	TI(1,1)=T(1,1)	D	29
	TI(1,2)=T(1,2)	D	30
	TI(1,3)=-T(1,3)	D	31
	TI(2,1)=T(2,1)	D	32
	TI(2,2)=T(2,2)	D	33
	TI(2,3)=-T(2,3)	D	34
	TI(3,1)=-T(3,1)	D	35
	TI(3,2)=-T(3,2)	D	36
	TI(3,3)=T(3,3)	D	37
	IF (IX.EQ.2) GO TO 4	D	38
	PRINT 8, ((TI(I,J),J=1,3),I=1,3)	D	39
4	CONTINUE	D	40
	DO 5 L=1,3	D	41
	DO 5 K=1,3	D	42
	DO 5 I=1,3	D	43
5	A(L,K)=A(L,K)+TI(L,I)*ST(I,K)	D	44
	A11=A(1,1)*2.	D	45
	A33=A(3,3)	D	46
C		D	47
	IF (IX.EQ.2) RETURN	D	48
	DO 6 I=1,3	D	49
6	PRINT 7, (A(I,J),J=1,3)	D	50
	RETURN	D	51
C		D	52
7	FORMAT (/ ,3(3X,E16.8))	D	53
8	FORMAT (/ ,3X,(3(E16.8,2X)))	D	54
	END	D	55-

APPENDIX F

SUBROUTINE VARY (AA,KV1,KV2,KVT,DEL,WTI,NL,ISTIFF)	E	1
DIMENSION AA(8,4), WTI(60), KV1(4), KV2(4), DEL(4)	E	2
DO 1 I=1,KVT	E	3
I1=KV1(I)	E	4
I2=KV2(I)	E	5
1 AA(I1,I2)=AA(I1,I2)+DEL(I)	E	6
IF (ISTIFF.EQ.1) CALL EVAL1 (AA,WTI,NL)	E	7
IF (ISTIFF.EQ.2) CALL EVAL2 (AA)	E	8
RETURN	E	9
END	E	10-

APPENDIX F

	SUBROUTINE RLF (OBEGIN,LBEGIN,ISTART,ILMAX,IM,IMORDER)	F	1
C	SUBSONIC FLUTTER OF EI - GJ WING	F	2
	COMPLEX E,OM,HOLD,CDET,CSDET,DCM,W,AL,WW(60),AAL(60),BBDI,BB(3),QW	F	3
	1W,QAL,O,OBEGIN	F	4
	REAL LAMBDA,LBEGIN,LAM	F	5
	DIMENSION X(3),Y(3),OMI(200),OMR(200),LAM(200),BDA(5),ODA(5)	F	6
	1,IMORDER(5)	F	7
	COMMON // IX,JX,IERROR,KOPT/CUM/OM,LAMBDA,RHO,EM(60),EI(61),GJ(61)	F	8
	1,A(60),B(60),SW(60),AR,RGSQ(60),MU,E(3,3),W(60),AL(60),NN,SWEEP,IP	F	9
	2RQCD,ITMAX,ISYM,CL(90),AC(90)/STATIC/IST,ALO,CMAC,EL,ISHAPE/PYLON/	F	10
	3BPY(10),CPY(10),DPY(10),ENJ(10),ENM(10),ENEI(10),ENGJ(10),PYL(10),	F	11
	4LOC(10),NENG/FREQ/OM1(5),DOM1,DAM,OMMAX1,TDAM,DAMMAX	F	12
C		F	13
	NAMelist /DEBUG1/ X,Y	F	14
C		F	15
C	A=OFFSET OF ELASTIC AXIS FROM SEMI CHORD/SEMI CHORD	F	16
C	AK=REDUCED FREQ.=SEMI CHORD*FREQ./VELOCITY	F	17
C	AL=POS. LEADING EDGE UP WING TWIST	F	18
C	B=SEMI CHORD/WING SPAN	F	19
C	C= THEODORSEN LAG FUNCTION	F	20
C	DYNAMIC PRESSURE=ONE HALF THE AIR DENSITY*VEL. SQD.	F	21
C	EI=BENDING STIFFNESS OF WING/REFERENCE EI	F	22
C	EL=SPAN/FINITE DIFF. SPACING	F	23
C	EM=MASS PER LENGTH OF SPAN/REFERENCE MASS PER LENGTH OF SPAN	F	24
C	GJ=TORSIONAL STIFFNESS OF WING/REFERENCE EI	F	25
C	LAMBDA=2*DYNAMIC PRESSURE*SPAN CUBED*SEMI CHORD/REF. EI	F	26
C	MU=NO. OF FINITE DIFF. NODES	F	27
C	RGSQ=SQ. OF THE RADIUS OF GYRATION ABOUT EL. AXIS/SEMI CHORD SQD.	F	28
C	RHO=PI*SEMI CHORD SQUARED*AIR DENSITY/REF. MASS PER UNIT SPAN	F	29
C	SW=OFFSET OF C.G. FROM EL. AXIS/SEMI CHORD	F	30
C	SWEEP=ANGLE OF WING SWEEP (RADIAN)	F	31
C	W=POS. UPWARD WING DEFLECTION	F	32
C		F	33
C	WING MAY HAVE TWO ENGINES	F	34
C	ENEI=BENDING STIFFNESS OF PYLON/REFERENCE EI	F	35
C	ENGS=TORSIONAL STIFFNESS OF PYLONS/REFERENCE EI	F	36
C	ENJ=TORSIONAL INERTIA OF ENGINE/(SPAN*SPAN)	F	37
C	ENM=ENGINE MASS/WING MASS	F	38
C	PYL=LENGTH OF PYLON/SEMI CHORD	F	39
	ABSCISA(X3,X2,X1,Y3,Y2,Y1)=X3+((Y1*Y3-Y2*Y3)*(X3-X1)*(X2-X3))/(Y1*	F	40
	Y2*(X1-X2)+Y1*Y3*(X3-X1)+Y2*Y3*(X2-X3))	F	41
	ILL=0	F	42
	IF (ISTART.NE.2) GO TO 2	F	43
	OM=OBEGIN/(EL*EL)	F	44
	LAMBDA=LBEGIN/(EL*EL*EL)	F	45
	IF (LAMBDA.GT.0.) GO TO 1	F	46
	IERROR=4	F	47
	RETURN	F	48
1	HOLD=OM	F	49
	DAMMAX1=DAMMAX/(EL*EL*EL)	F	50
	GO TO 9	F	51
2	IMO=1	F	52
	IL=IMORDER(IMO)	F	53
	DAMMAX1=DAMMAX/(EL*EL*EL)	F	54
3	IF (IMO.GT.ILMAX) GO TO 4	F	55
	IL=IMCRDER(IMO)	F	56
	OM2=OM1(IL)	F	57
	CM2=OM2/(EL*EL)	F	58
	GO TO 9	F	59

APPENDIX F

4	IF (ILL.EQ.0) GO TO 8	F 60
	BMIN=BDA(1)	F 61
	IM=1	F 62
	IF (ILMAX.EQ.1) GO TO 6	F 63
	CO 5 IL=2,ILMAX	F 64
	IF (BDA(IL).LT.BMIN) IM=IL	F 65
5	IF (BDA(IL).LT.BMIN) BMIN=BDA(IL)	F 66
6	OO=ODA(IM)*EL*EL	F 67
	AMDA=BDA(IM)*EL*EL*EL	F 68
	PRINT 58,AMDA,OO,IM	F 69
	LAMBDA=BDA(IM)	F 70
	OMEGA=ODA(IM)	F 71
	IF (ISHAPE.EQ.2) GO TO 7	F 72
	CALL CFI	F 73
	GO TO 35	F 74
7	IF (KOPT.EQ.2) ISTART=2	F 75
	IERROR=0	F 76
	LBEGIN=AMDA	F 77
	OBEGIN=OO	F 78
	RETURN	F 79
8	PRINT 59	F 80
	IERROR=1	F 81
	RETURN	F 82
9	INSTAB=0	F 83
	PRINT 50	F 84
	ICOUNT=0	F 85
	KOUNT=0	F 86
	NN=3	F 87
	IF (IST.EQ.3) GO TO 42	F 88
	IF (ISTART.EQ.2) GO TO 17	F 89
	CM=CMLX(OM2,.0)	F 90
	HOLD=OM	F 91
	DOM=CMLX(DOM1,0.)	F 92
	LAMBDA=0.	F 93
	DO 10 I=1,3	F 94
	IF (I.GE.2) CM=OM+DOM	F 95
	CALL CFI	F 96
	CALL DEUPPS (E,3,CDET,3)	F 97
	X(I)=REAL(CDET)	F 98
	Y(I)=REAL(OM)	F 99
	IF (IX.EQ.2) GO TO 10	F 100
	PRINT DEBUG1	F 101
10	CONTINUE	F 102
11	CISSA=ABSCISA(Y(3),Y(2),Y(1),X(3),X(2),X(1))	F 103
	CM=CMLX(CISSA,0.)	F 104
	IF (KCOUNT.EQ.0) XO=X(1)	F 105
	KCOUNT=KCOUNT+1	F 106
	IF (ABS(X(1))/ABS(XO).LE.5.E-4) GO TO 15	F 107
	IF (KCOUNT.GE.ITMAX) GO TO 14	F 108
	CALL CFI	F 109
	CALL DEUPPS (E,3,CDET,3)	F 110
	CSDET=CDET	F 111
	X(1)=REAL(CDET)	F 112
	Y(1)=REAL(OM)	F 113
	IF (IX.EQ.2) GO TO 12	F 114
	PRINT DEBUG1	F 115

APPENDIX F

12	CONTINUE	F 116
	DOM=DOM/4.	F 117
	DO 13 I=2,3	F 118
	CM=OM+DOM	F 119
	CALL CFI	F 120
	CALL DEUPPS (E,3,CDET,3)	F 121
	X(I)=REAL(CDET)	F 122
	Y(I)=REAL(OM)	F 123
	IF (IX.EQ.2) GO TO 13	F 124
	PRINT DEBUG1	F 125
13	CONTINUE	F 126
	GO TO 11	F 127
14	G=OM*EL**2	F 128
	AMDA=LAMBDA*EL**3	F 129
	PRINT 51, G,AMDA,CSDET,KCUNT	F 130
	PRINT 52	F 131
	IF (IPROCD.EQ.2) GO TO 43	F 132
15	O=OM*EL**2	F 133
	AMDA=LAMBDA*EL**3	F 134
	PRINT 51, O,AMDA,CDET,KCUNT	F 135
	ICOUNT=1	F 136
	LAM(1)=O.	F 137
	OMR(1)=OM	F 138
	OMI(1)=.0	F 139
16	DAMIN=DAM*((-1.)**INSTAB)	F 140
	LAMBDA=LAMBDA+DAMIN	F 141
	IF (LAMBDA.GT.DAMMAX1.AND.ISTART.NE.2) GO TO 28	F 142
17	LAMBDA=LAMBDA*COS(SWEEP)*COS(SWEEP)	F 143
	ICOUNT=ICOUNT+1	F 144
	IF (ICOUNT.GE.ISTOP) GO TO 43	F 145
	HOLD=OM	F 146
	KOUNT=0	F 147
18	CALL CFI	F 148
	CALL DEUPPS (E,3,CDET,3)	F 149
	CSDET=CDET	F 150
	A0=REAL(CDET)	F 151
	A00=A0	F 152
	B0=AIMAG(CDET)	F 153
	IF (IX.EQ.2) GO TO 19	F 154
	PRINT 49, CDET	F 155
19	CONTINUE	F 156
	OM=OM+CMPLX(DOM1,0.)	F 157
	CALL CFI	F 158
	CALL DEUPPS (E,3,CDET,3)	F 159
	A1=REAL(CDET)	F 160
	B1=AIMAG(CDET)	F 161
	PRWOMR=(A1-A0)/DOM1	F 162
	PIWOMR=(B1-B0)/DOM1	F 163
	OMIM=-DOM1	F 164
	OM=OM+CMPLX(CMIM,DOM1)	F 165
	CALL CFI	F 166
	CALL DEUPPS (E,3,CDET,3)	F 167
	A2=REAL(CDET)	F 168
	B2=AIMAG(CDET)	F 169
	PRWOMI=(A2-A0)/DOM1	F 170
	PIWOMI=(B2-B0)/DOM1	F 171

APPENDIX F

	AJACOBI=PRWOMR*PIWOMI-PRWOMI*PIWOMR	F 172
	DOMR=(BO*PRWOMI-AO*PIWOMI)/AJACOBI	F 173
	DOMI=(AO*PIWOMR-BO*PRWOMR)/AJACOBI	F 174
	OM=HOLD+CMPLX(DOMR,DOMI)	F 175
	HOLD=CM	F 176
	IF (IX.EQ.2) GO TO 20	F 177
	PRINT 47, PRWOMR,PIWOMR,PRWOMI,PIWOMI	F 178
	PRINT 48, DOMR,DOMI,CM	F 179
20	CONTINUE	F 180
	ROM=REAL(OM)	F 181
	AOM=AIMAG(OM)	F 182
	KOUNT=KOUNT+1	F 183
	IF (RCM.EQ.0.) GO TO 22	F 184
	IF (AOM.EQ.0.) GO TO 21	F 185
	IF (ABS(DCMR/ROM).LT.5.E-3.AND.ABS(DOMI/AOM).LT.5.E-3) GO TO 24	F 186
	GO TO 23	F 187
21	IF (ABS(DOMR/ROM).LT.1.E-5) GO TO 24	F 188
	GO TO 23	F 189
22	IF (ABS(DOMI/AOM).LT.1.E-5) GO TO 24	F 190
23	CONTINUE	F 191
	IF (KOUNT.GE.(2*ITMAX)) PRINT 52	F 192
	IF (KOUNT.GE.(2*ITMAX).AND.IPROCD.EQ.2) GO TO 29	F 193
	IF (KOUNT.GE.(2*ITMAX).AND.IPROCD.EQ.1) GO TO 24	F 194
	GO TO 18	F 195
C	ROOT LOCUS POINT FOUND	F 196
24	O=OM*EL**2	F 197
	LAMBDA=LAMBDA/(COS(SWEEP)*COS(SWEEP))	F 198
	LAM(ICOUNT)=LAMBDA	F 199
	OMR(ICOUNT)=ROM	F 200
	OMI(ICOUNT)=AOM	F 201
	AMDA=LAMBDA*EL**3	F 202
	PRINT 51, O,AMDA,CSDET,KCUNT	F 203
	IF (AOM.LT.0..AND.ICOUNT.EQ.1) INSTAB=1	F 204
	IF (INSTAB.EQ.1) GO TO 27	F 205
	IF (KOPT.EQ.2) GO TO 25	F 206
C		F 207
C	TRACE OUT V - G DIAGRAM DO NOT STOP AT FLUTTER	F 208
C		F 209
	GO TO 26	F 210
25	IF (AOM.LT.0..AND.INSTAB.EQ.0) GO TO 30	F 211
26	CONTINUE	F 212
	IF (ICOUNT.LT.2) GO TO 16	F 213
	ROM=2.*OMR(ICOUNT)-OMR(ICOUNT-1)	F 214
	AOM=2.*OMI(ICOUNT)-OMI(ICOUNT-1)	F 215
	CM=CMPLX(RCM,AOM)	F 216
	IF (ISTART.NE.2) GO TO 16	F 217
	IF (ICOUNT.LT.3) GO TO 16	F 218
	CURV=OMI(ICOUNT)-2.*OMI(ICOUNT-1)+OMI(ICOUNT-2)	F 219
	IF (CURV.GT..0.AND.INSTAB.EQ.0) GO TO 44	F 220
	IF (ICOUNT.GT.12.AND.ISTART.EQ.2) GO TO 46	F 221
	GO TO 16	F 222
27	IF (AOM.GT.0.) GO TO 30	F 223
	IF (ICOUNT.EQ.1) GO TO 16	F 224
	ROM=2.*OMR(ICOUNT)-OMR(ICOUNT-1)	F 225
	AOM=2.*OMI(ICOUNT)-OMI(ICOUNT-1)	F 226
	OM=CMPLX(ROM,AOM)	F 227
	GO TO 16	F 228

APPENDIX F

28	DAMMAX2=DAMMAX1*EL*EL*EL	F 231
	PRINT 55, DAMMAX2	F 232
	IF (ICPT.EQ.2.AND.ISTART.EQ.2) GO TO 45	F 233
29	IF (ISTART.EQ.2) RETURN	F 234
	BDA(IL)=DAMMAX1	F 235
	ODA(IL)=0.	F 236
	IMO=IMO+1	F 237
	IF (ISTART.NE.2) GO TO 3	F 238
	GO TO 43	F 239
C	FLUTTER ENCOUNTERED	F 240
C	USE ABCISA TO FIND A BETTER ROOT	F 241
30	IF (ICOUNT.LT.3) GO TO 31	F 242
31	ROOT=LAM(ICOUNT-1)-DAMIN*OMI(ICOUNT-1)/(OMI(ICOUNT)-OMI(ICOUNT-1))	F 243
	LAMBDA=ROOT	F 244
	IF (ICOUNT.LT.3) GO TO 33	F 245
	DO 32 IV=1,3	F 246
32	Y(IV)=OMR(ICCUNT-3+IV)	F 247
	ROOT=ABSCISA(Y(3),Y(2),Y(1),X(3),X(2),X(1))	F 248
	GO TO 34	F 249
33	ROOT=OMR(ICOUNT-1)-(OMR(ICOUNT)-OMR(ICOUNT-1))*OMI(ICOUNT-1)/(OMI(ICOUNT)-OMI(ICOUNT-1))	F 250
	IICOUNT=ICOUNT-1	F 251
34	ROM=ROOT	F 252
	RO=ROM*EL*EL	F 253
	AMDA=LAMBDA*EL*EL*EL	F 254
	PRINT 54, AMDA, RO	F 255
	IERROR=0	F 256
	LBEGIN=AMDA	F 257
	OBEGIN=CMPLX(RO,0.)	F 258
	IF (ISTART.EQ.2.AND.ISHAPE.EQ.2) GO TO 42	F 259
	IF (ISTART.EQ.2.AND.ISHAPE.EQ.1) GO TO 35	F 260
	BDA(IL)=LAMBDA	F 261
	ODA(IL)=RCM	F 262
	ILL=1	F 263
	IMO=IMO+1	F 264
	IF (ISTART.NE.2) DAMMAX1=LAMBDA+DAM	F 265
	IF (ISTART.NE.2.AND.IST.EQ.1) GO TO 3	F 266
	IF (ISHAPE.EQ.2) GO TO 42	F 267
C		F 268
C	MODE SHAPE	F 269
35	BBDI=1./(E(2,1)*E(3,3)-E(2,3)*E(3,1))	F 270
	BB(1)=(-E(2,2)*E(3,3)+E(3,2)*E(2,3))*BBDI	F 271
	BB(2)=1.	F 272
	BB(3)=(-E(2,1)*E(3,2)+E(3,1)*E(2,2))*BBDI	F 273
	LAMBDA=LAMBDA*COS(SWEEP)*COS(SWEEP)	F 274
	DO 36 I=1,MU	F 275
	J=I	F 276
	WW(J)=0.	F 277
36	AAL(J)=0.	F 278
	DO 37 NN=1,3	F 279
	CALL CFI	F 280
	DO 37 I=1,MU	F 281
	J=I	F 282
	WW(J)=WW(J)+BB(NN)*W(I)	F 283

APPENDIX F

37	AAL(J)=AAL(J)+BB(NN)*AL(I)	F 284
	PRINT 56	F 285
	MUJ=(MU+1)/2	F 286
	DO 41 J=1,MU	F 287
	I=J	F 288
	IF (REAL(WW(J)).EQ.0..AND.AIMAG(WW(J)).EQ.0.) GO TO 38	F 289
	CWW=CABS(WW(J))	F 290
	QWW=CLOG(WW(J))	F 291
	PWW=AIMAG(QWW)	F 292
	GO TO 39	F 293
38	CWW=0.	F 294
	PWW=0.	F 295
39	IF (REAL(AAL(J)).EQ.0..AND.AIMAG(AAL(J)).EQ.0.) GO TO 40	F 296
	CAL=CABS(AAL(J))	F 297
	QAL=CLOG(AAL(J))	F 298
	PAL=AIMAG(QAL)	F 299
	GO TO 41	F 300
40	CAL=0.	F 301
	PAL=0.	F 302
41	PRINT 57, I,CWW,PWW,CAL,PAL	F 303
42	IF (IST.LT.3.AND.ISTART.EQ.2) RETURN	F 304
	IF (IST.LT.3.AND.ISTART.EQ.3) GO TO 7	F 305
	IF (ILL.EQ.2) RETURN	F 306
C		F 307
C	DIVERGENCE TEST IS PERFORMED ONLY IF IFORD=2 OR 3	F 308
C		F 309
	CALL DIV	F 310
	ILL=2	F 311
	IF (ISHAPE.EQ.1) GO TO 35	F 312
	RETURN	F 313
43	PRINT 60	F 314
C		F 315
44	IF (OMI(ICOUNT).LT.OMI(ICOUNT-1)) GO TO 16	F 316
	AMDA=LAMBDA*EL*EL*EL	F 317
	PRINT 61, AMDA	F 318
C		F 319
C	TROUBLE ENCOUNTERED ON A BRANCH CURVE CHECK OUT ALL BRANCHES	F 320
C		F 321
45	ISTART=3	F 322
	IERROR=1	F 323
	RETURN	F 324
46	IF (OMI(ICOUNT).LT.OMI(ICOUNT-1)) GO TO 16	F 325
	AMDA=LAMBDA*EL*EL*EL	F 326
	PRINT 62, AMDA	F 327
	IERROR=2	F 328
	ISTART=3	F 329
	RETURN	F 330
C		F 332

APPENDIX F

47	FORMAT (/ ,2X,19HPARTIAL DERIVATIVES,/,4(1X,E16.8))	F 333
48	FORMAT (3X,5HDOMR=,E16.8,3X,5HDOMI=,E16.8,3X,3HOM=,2(E16.8,1X))	F 334
49	FORMAT (/ ,5X,5HCDET=,2(E16.8,1X))	F 335
50	FORMAT (///16X,5HOMEGA23X,6HLAMBDA26X,11HDETERMINANT23X,13HNO.ITER LATIONS/5X,9HREAL PART11X,14HIMAGINARY PART23X,9HREAL PART11X,14HIM 2AGINARY PART/)	F 336 F 337
51	FORMAT (5E20.8,15X18)	F 338 F 339
52	FORMAT (1X,102HNO CONVERGENCE AT THE FOLLOWING BRANCH PT. - PROGRA 1M WILL PROCEED TO NEXT BRANCH PT. PROVIDED IPROC=1)	F 340 F 341
53	FORMAT (/ ,5X,20HTHE MAGNITUDE OF OM=,E16.8,2H+I,E16.8,2X,8HEXCEEDS 1 ,E16.8/,5X,37HPROGRAM WILL PROCEED TO THE NEXT CASE)	F 342 F 343
54	FORMAT (/ ,30X,42HFLUTTER INSTABILITY ENCOUNTERED AT LAMBDA=,F8.5,5 1X,6HOMEGA=,F8.4/,30X,42H***** 2,/)	F 344 F 345 F 346
55	FORMAT (/ ,5X,14HLAMBDA EXCEEDS,F10.5)	F 347
56	FORMAT (///,50X,17HDEFORMATION SHAPE,///,1X,8HPOSITION,25X,10HDEFLEC TION,40X,5HTWIST,/,23X,9HMAGNITUDE,20X,5HPHASE,15X,9HMAGNITUDE,15X 2,5HPHASE,/)	F 348 F 349 F 350
57	FORMAT (3X,13,10X,E16.8,8X,E16.8,10X,E16.8,8X,E16.8)	F 351
58	FORMAT (///,10X,62HMINIMUM FLUTTER SPEED FOR PRELIMINARY DESIGN OCC URS AT LAMBDA=,E16.8,10HAND OMEGA=,E16.8,1X,13HON BRANCH NO.,I2/,1 20X,51(1H*),/)	F 352 F 353 F 354
59	FORMAT (///,5X,75HALL BRANCHES SEARCHED OUT BUT NO FLUTTER SPEED FO LUND FOR PRELIMINARY DESIGN)	F 355 F 356
60	FORMAT (///,5X,16HSTOPPED ON ISTOP)	F 357
61	FORMAT (///,5X,73HCURV IS POSITIVE AND INSTAB=0 THEREFORE IERROR=1 1 TEST OUT ALL BRANCHES/,5X,21HOCCURANCE AT LAMBDA=,E16.8/)	F 358 F 359
62	FORMAT (///,5X,74HCOUNT EXCEEDS 12 WHILE ISTART=2 SET IERROR=2 AN 1D SEARCH OUT ALL BRANCHES,/,5X,20HOCCURANCE AT LAMBDA=,E16.8/)	F 360 F 361
	END	F 362-

APPENDIX F

	SUBROUTINE CFI	G	1
C		G	2
C	TO DETERMINE THE REDUCED FLUTTER DETERMINANT	G	3
C		G	4
C	ISYM=1, CLAMPED ROOT	G	5
C	ISYM=2, SYMMETRIC WING FLUTTER AND/OR DIVERGENCE	G	6
C	ISYM=3, ANTI-SYMMETRIC WING FLUTTER AND/OR DIVERGENCE	G	7
	REAL LAMBDA	G	8
	COMPLEX CM,W,AL,E,OM2,AK,II,C,D1,D2,QM1(10),QH(10),QAL(10),QMA(10)	G	9
	1,QMB(10),AQH,AQAL,AQAL1,QMA1(10),QMMU(10),SH,SAL,SHP,AQH1,AK2,S,T,	G	10
	2,QMA2(10),QH1(10),QAL1(10),QM2(10),QMAA,QMBB,Q1,Q2,A0,A1,A2,A3,AH1,	G	11
	3,AH2,AH3,AH4,AAL1,AAL2,AAL3,AAL4,WO	G	12
	COMMON // IX,JX,IERRCR,KOPT/CUM/OM,LAMBDA,RHO,EM(60),EI(61),GJ(61)	G	13
	1,A(60),B(60),SW(60),AR,RGSQ(60),MU,E(3,3),W(60),AL(60),NN,SWEEP,IP	G	14
	2,ROCD,ITMAX,ISYM,CL(90),AC(90)/STATIC/IST,ALO,CMAC,EL,ISHAPE/PYLON/	G	15
	3BPY(10),CPY(10),DPY(10),ENJ(10),ENM(10),ENEI(10),ENGJ(10),PYL(10),	G	16
	4LOC(10),NENG	G	17
	NAMelist /DEBUG2/ E	G	18
	ALOS=CMACS=0.	G	19
	IF (IST.EQ.4) ALOS=ALO	G	20
	IF (IST.EQ.4) CMACS=CMAC	G	21
	BRHO=RHO	G	22
	BLAM=LAMBDA	G	23
	PI=3.141592653589793238	G	24
	II=CMPLX(0.,1.)	G	25
	IF (IST.GE.2) OM=OM2=0.	G	26
	CM2=OM*CM	G	27
	IF (LAMBDA.EQ.0.) GO TO 1	G	28
	AK=CM*SQRT(RHO/(PI*LAMBDA*AR))	G	29
	GO TO 2	G	30
1	AK=0.	G	31
2	DO 36 N=1,NN	G	32
	MN=0	G	33
	AL(1)=AL(2)=W(1)=W(2)=W(3)=0.	G	34
	IF (ISYM.EQ.2) GO TO 3	G	35
	IF (N.NE.3.AND.IST.NE.4) W(N+1)=1.	G	36
	IF (N.EQ.3.AND.IST.NE.4) AL(2)=1.	G	37
	IMU=2	G	38
	GO TO 4	G	39
3	IF (N.NE.3) W(N)=1.	G	40
	IF (N.EQ.3) AL(1)=1.	G	41
	IMU=1	G	42
4	CONTINUE	G	43
	MU1=MU-1	G	44
	MU2=MU-2	G	45
	MU3=MU-3	G	46
	CS=COS(SWEEP)	G	47
	SN=SIN(SWEEP)	G	48
	TN=SN/CS	G	49
	O8=1./8.	G	50
	PI2=2.*PI	G	51
	AR2=AR*AR	G	52
	RJ2=B(1)*B(1)	G	53
	IF (ISYM.NE.3) GO TO 8	G	54
C	CALCULATE WO	G	55
	A0=.5*EI(1)+.25*EI(1)*DBAR*CS+.25*GJ(2)*TN*TN-O8*EM(1)*OM2*RGSQ(1)	G	56
	1*TN*TN/(AR*AR)+O8*EM(1)*SW(1)*DBAR*OM2*TN/CS/AR-.5*EI(1)*DBAR2/CS2	G	57
	2+.5*EI(1)*DBAR/CS+.25*EI(2)*DBAR2/CS2-O8*EM(1)*OM2*DBAR2/CS2+O8*EM	G	58
	3(1)*SW(1)*OM2*DBAR/AR/CS*TN	G	59
	A2=.5*EI(1)-.5*EI(1)*DBAR/CS-.25*GJ(2)*TN2+O8*EM(1)*OM2*TN2*RGSQ(1	G	60
	1)/AR2-O8*EM(1)*SW(1)*DBAR*OM2*TN/CS/AR+.5*EI(1)*DBAR/CS-.25*EI(2)*	G	61
	2DBAR2/CS+EI(2)*DBAR/CS-.25*EI(2)*DBAR2/CS2+O8*EM(1)*OM2*DBAR2/CS2-	G	62
	3O8*EM(1)*OM2*SW(1)*DBAR*TN/AR/CS	G	63
	A3=-.5*EI(2)*DBAR/CS	G	64

APPENDIX F

C	ADD ON AERODYNAMIC LOADS	G 65
	AH1=B(1)*(B(1)*OM2*RHO-II*CL(1)*AR*C*LAMBDA*AK)*DBAR/CS	G 66
	AH2=B(1)*B(1)*(OM2*RHO+II*PI*LAMBDA*AK*AR*(1.+CL(1)/PI*(CL(1)/PI2+ACMA/B(1))*C)+CL(1)*LAMBDA*AR*B(1)*C)*TN/AR	G 67
	AH3=-((CL(1)*C+II*PI*AK*B(1))*B(1)*LAMBDA*TN	G 68
	AH4=(CL(1)*(CL(1)/PI2+ACMA/B(1))*C-II*PI*AK*A(1))*BJ2*LAMBDA	G 69
	AAL1=BJ2/AR*(A(1)*RHC/AR*OM2+II*PI*AK*LAMBDA*ACMA/PI/B(1)*CL(1)*C)	G 70
	1*DBAR/CS	G 71
	AAL2=BJ2/AR*(RHO*BJ2/AR*(O8+A(1)*A(1)/BJ2)*OM2-2.*PI*II*AK*LAMBDA*	G 72
	1B(1)*(0.5+ACMA*CL(1)*C/PI2/B(1))*(CL(1)/PI2+ACMA/B(1))-ACMA/B(1)*CL	G 73
	2(1)*C*LAMBDA)*TN/AR	G 74
	AAL3=-((II*PI*AK*A(1)-ACMA/B(1)*CL(1)*C)*BJ2/AR2*LAMBDA*TN	G 75
	AAL4=-BJ2*TN/AR2*(II*AK*(O8+A(1)*A(1)/BJ2)*BJ2+A(1)+(1.+ACMA/PI*B(1)*CL(1)*C)*(CL(1)/PI2+ACMA/B(1))*B(1))*PI*LAMBDA	G 76
	A0=A0+.25*DBAR/CS*(-.5*AH1-.5*AH2-.5*AH3+.5*AH4*TN/AR)+.5*TN/AR*(-	G 77
	1.5*AAL1-.5*AAL2-.5*AAL3+.5*AAL4*TN/AR)	G 78
	A2=A2+.25*DBAR/CS*(.5*AH1+.5*AH2+.5*AH3-.5*AH4*TN/AR)+.5*TN/AR*(.5	G 79
	1*AAL1+.5*AAL2+.5*AAL3-.5*AAL4*TN/AR)	G 80
	A4=.25*DBAR/CS*AH4+.5*TN/AR*AAL4+.5*GJ(2)*TN*AR	G 81
		G 82
C	ADD ON ENGINE TERMS	G 83
	IF (NENG.EQ.0) GO TO 7	G 84
	DO 6 IJ=1,NENG	G 85
	IF (LOC(IJ).NE.1) GO TO 5	G 86
	AQAL=CPY(IJ)*OM2*TN/(1.-OM2*DPY(IJ))	G 87
	AQAL1=CPY(IJ)*OM2/(1.-OM2*DPY(IJ))	G 88
	A0=A0+.5*TN/AR*(-AQAL)+.25*(-AQAL1)	G 89
	A2=A2+.5*TN/AR*AQAL+.25*AQAL1	G 90
5	IF (LOC(IJ).NE.2) GO TO 6	G 91
	AQH=CPY(IJ)*CM2*AR*CS/(1.-DPY(IJ))	G 92
	AQAL=-OM2*ENM(IJ)*PYL(IJ)/AR*SN/(1.-BPY(IJ))	G 93
	AQAL1=.25*DBAR/AR	G 94
	A0=A0+.25*DBAR/CS*(AQH*AQAL1+AQAL*(-AQAL1*TN)*PYL(IJ))	G 95
	A2=A2+.25*DBAR/CS*(AQH*(-AQAL1)+AQAL*(AQAL1*TN)*PYL(IJ)+1.)	G 96
	A3=A3+.25*DBAR/CS*(.5*CS/AR+AQAL*(-.5/AR*SN*PYL(IJ)))	G 97
	A4=A4+.25*DBAR/CS*(AQH*SN+AQAL*CS)	G 98
		G 99
6	CONTINUE	G 100
7	W0=-((A2*W(2)+A(3)*W(3)+A(4)*AL(2))/A0	G 101
	W(1)=DBAR*.5*(W(2)-W0)/CS	G 102
C	COMPUTE AERODYNAMIC LOADS AT J=1	G 103
	Q1=(AH1+AH2+AH3-AH4*TN)*.5*(W(2)-W0)+AH4*AL(2)	G 104
	Q2=(AAL1+AAL2+AAL3-AAL4*TN)*.5*(W(2)-W0)+AAL4*AL(2)	G 105
8	DO 35 J=IMU,MU	G 106
C		G 107
	C=(1.+10.61*II*AK*B(J))/(1.+13.51*II*AK*B(J))*(1.+1.774*II*AK*B(J)	G 108
	1)/(1.+2.745*II*AK*B(J))	G 109
C	PRE CALCULATIONS FOR ENGINE LOADS	G 110
C		G 111
C	DETERMINE SLOPES	G 112
	IF (J.EQ.1) GO TO 10	G 113
	IF (J.EQ.MU) GO TO 11	G 114
	SH=(W(J+1)-W(J-1))*0.5	G 115
	SAL=-AL(J-1)*0.5	G 116
	IF (J.EQ.2) GO TO 9	G 117
	SHP=.5*(W(J)-W(J-2))	G 118
	GO TO 12	G 119
9	SHP=-AL(1)*AR*TN	G 120
	IF (ISYM.EQ.3) SHP=AR*AL(1)/TN	G 121
	GO TO 12	G 122
10	SH=-2.*AR*AL(J)*TN	G 123
	SAL=-AL(1)	G 124
	GO TO 12	G 125
11	SHP=.5*(W(MU)-W(MU1))	G 126
	SH=W(MU)-W(MU1)	G 127
	SAL=AL(MU)-AL(MU1)	G 128

APPENDIX F

12	CONTINUE	G 129
	IF (NENG.EQ.0) GO TO 18	G 130
	DO 17 IJ=1,NENG	G 131
	IF (J.GT.(LOC(IJ)+1).OR.J.LT.(LOC(IJ)-1)) GO TO 16	G 132
	D1=1.-OM2*BPY(IJ)	G 133
	D2=1.-OM2*DPY(IJ)	G 134
C		G 135
	IF (J.NE.LOC(IJ)) GO TO 13	G 136
	IF (J.EQ.MU) QMMU(IJ)=ENJ(IJ)*ENM(IJ)*OM2*AR*(AL(J)*SN+SH*CS/AR)*C	G 137
	IS/D2-OM2*ENM(IJ)*PYL(IJ)/AR*((AL(J)*CS-SH*SN/AR)*PYL(IJ)+W(J))*SN/	G 138
	2D1	G 139
	QH(IJ)=OM2*ENM(IJ)*((AL(J)*CS-SH*SN/AR)*PYL(IJ)+W(J))/D1	G 140
	QAL(IJ)=OM2*ENM(IJ)/(AR*AR)*((AL(J)*CS-SH*SN/AR)*PYL(IJ)+W(J))*PYL	G 141
	I(IJ)*CS/D1+ENJ(IJ)*ENM(IJ)*OM2*(AL(J)*SN+SH*CS/AR)*SN/D2	G 142
	IF (J.EQ.1) QM1(IJ)=-CM2*ENM(IJ)*PYL(IJ)/AR*(AL(1)/CS*PYL(IJ)+W(1)	G 143
	1)*SN/D1	G 144
	QMA(IJ)=QMB(IJ)=QMA1(IJ)=QMA2(IJ)=QH1(IJ)=QAL1(IJ)=QM2(IJ)=0.	G 145
	GO TO 17	G 146
13	IF (J.EQ.(LOC(IJ)-1)) GO TO 15	G 147
	QMB(IJ)=ENM(IJ)*ENJ(IJ)*OM2*AR*(AL(J-1)*SN+SHP*CS/AR)*CS/D2-OM2*EN	G 148
	1M(IJ)*PYL(IJ)/AR*((AL(J-1)*CS-SHP*SN/AR)*PYL(IJ)+W(J-1))*SN/D1	G 149
	IF (ISYM.NE.3.OR.J.GT.2) GO TO 14	G 150
	QH1(IJ)=OM2*ENM(IJ)*DBAR/CS*(W(2)-W0)*.5/D1	G 151
	QAL1(IJ)=OM2*ENM(IJ)*DBAR/AR*.5*(W(2)-W0)*PYL(IJ)/D1+CPY(IJ)*OM2*	G 152
	1(W(2)-W0)*TN/D2	G 153
	QM2(IJ)=CPY(IJ)*OM2*AR*(AL(2)*SN+SH/AR*CS)*CS/D2-OM2*ENM(IJ)*PYL(I	G 154
	1J)/AR*((AL(2)*CS-SH*SN/AR)*PYL(IJ)+W(2))*SN/D1	G 155
14	CONTINUE	G 156
	QMA(IJ)=QH(IJ)=QAL(IJ)=QMA1(IJ)=QM1(IJ)=QMA2(IJ)=0.	G 157
	GO TO 17	G 158
15	QMAA=ENM(IJ)*ENJ(IJ)*OM2*AR*CS/D2	G 159
	QMBB=-OM2*ENM(IJ)*PYL(IJ)/AR*PYL(IJ)	G 160
	QMA(IJ)=QMAA*(-W(J))/(2.*AR)*CS-QMBB*(W(J))/(2.*AR)*SN+W(J+1))*SN/D	G 161
	11	G 162
	QMA2(IJ)=QMAA+QMBB*SN/D1	G 163
	QMA1(IJ)=OM2*ENM(IJ)*PYL(IJ)*PYL(IJ)/(2.*AR*AR)*SN/D1	G 164
	QH1(IJ)=QAL1(IJ)=QM2(IJ)=.0	G 165
	GO TO 17	G 166
16	QH(IJ)=QAL(IJ)=QMA(IJ)=QMB(IJ)=QMA1(IJ)=QMA2(IJ)=QM1(IJ)=QMMU(IJ)=	G 167
	1QH1(IJ)=QAL1(IJ)=QM2(IJ)=0.	G 168
17	CONTINUE	G 169
C	AERODYNAMIC LOADS	G 170
18	BJ2=B(J)*B(J)	G 171
	ACMA=AC(J)-A(J)	G 172
	AQH=B(J)*(OM2*RHO*B(J)-II*CL(J)*AR*C*LAMBDA*AK)*W(J)+BJ2*(OM2*RHO*	G 173
	1A(J))/B(J)+II*PI*LAMBDA*AK*AR*(1.+CL(J)/PI*(CL(J)/PI2+ACMA/B(J))*C)	G 174
	2+CL(J)*LAMBDA*AR*B(J)*C)*AL(J)	G 175
	AQAL=BJ2/AR*(A(J)*RHO/AR*OM2+II*PI*AK*LAMBDA*ACMA/(B(J)*PI)*CL(J)*	G 176
	1C)*W(J)+BJ2/AR*(RHO*BJ2/AR*(08+A(J)*A(J)/BJ2)*CM2-PI2*II*AK*LAMBDA	G 177
	2*B(J)*(.5+ACMA*CL(J)/(PI2*B(J))*C)*(CL(J)/PI2+ACMA/B(J))-ACMA/B(J)	G 178
	3*CL(J)*C*LAMBDA)*AL(J)	G 179
C	ACCOUNT FOR SLOPES IN AERODYNAMIC LOADS	G 180
	AQH1=(CL(J)*(CL(J)/PI2+ACMA/B(J))*C-II*PI*AK*A(J))*BJ2*LAMBDA*TN	G 181
	AQH=AQH-(CL(J)*C+II*PI*AK*B(J))*B(J)*LAMBDA*SH*TN+AQH1*SAL	G 182
	AQAL1=-BJ2/(AR*AR)*TN*(II*AK*(08+A(J)*A(J)/BJ2)*BJ2+A(J)+(1.+ACMA/	G 183
	1(PI*B(J))*CL(J)*C*(CL(J)/PI2+ACMA/B(J))*B(J))*LAMBDA*PI	G 184
	AQAL=AQAL-(II*PI*AK*A(J)-ACMA/B(J))*CL(J)*C)*BJ2/(AR*AR)*LAMBDA*TN*	G 185
	1SH*AQAL1*SAL	G 186

APPENDIX F

C		G 187
C	PROCEED ALONG SPAN CALCULATING AL(J+1) AND W(J+2)	G 188
	JP1=J+1	G 189
	JP2=J+2	G 190
	JM1=J-1	G 191
	JM2=J-2	G 192
	T=EI(JP1)	G 193
	S=GJ(JP1)	G 194
	IF (J.EQ.1) GO TO 21	G 195
	IF (J.EQ.2) GO TO 24	G 196
	IF (J.EQ.MU1) GO TO 29	G 197
	IF (J.EQ.MU) GO TO 33	G 198
	S=S+.5*AQAL1	G 199
	AL(JP1)=-GJ(J)*AL(JM1)+(GJ(JP1)+GJ(J)-OM2*EM(J)*RGSQ(J)/(AR*AR))*A	G 200
	1L(J)+CM2*SW(J)*EM(J)/(AR*AR)*W(J)-AQAL	G 201
	W(JP2)=-EI(JM1)*W(JM2)+2.*(EI(J)+EI(JM1))*W(JM1)-(EI(JP1)+4.*EI(J)	G 202
	1+EI(JM1)-EM(J)*OM2)*W(J)+2.*(EI(JP1)+EI(J))*W(JP1)-EM(J)*SW(J)*OM2	G 203
	2*AL(J)+AQH	G 204
C		G 205
C	APPLY ENGINE LOADS	G 206
	IF (NENG.EQ.0) GO TO 20	G 207
	DO 19 IJ=1,NENG	G 208
	T=T+.5*QMA1(IJ)	G 209
	AL(JP1)=AL(JP1)-QAL(IJ)	G 210
19	W(JP2)=W(JP2)+QH(IJ)+.5*(QMB(IJ)-QMA(IJ))	G 211
20	AL(JP1)=AL(JP1)/S	G 212
	W(JP2)=(W(JP2)+.5*AQH1*AL(JP1))/T	G 213
	GO TO 35	G 214
21	S=S+AQAL1*.5	G 215
	AL(2)=(GJ(2)-.5*EM(1)*OM2*RGSQ(J)/(AR*AR))*AL(1)+.5*OM2*EM(1)*SW(1	G 216
	1)*W(1)/(AR*AR)-.5*AQAL+2.*EI(1)*TN*((W(2)-W(1))/AR+AL(1)*TN)	G 217
	W(3)=2.*(EI(1)+EI(2))*W(2)-(2.*EI(1)+EI(2)-.5*OM2*EM(1))*W(1)-.5*E	G 218
	1M(1)*SW(1)*OM2*AL(1)+.5*AQH+2.*AR*EI(1)*TN*AL(1)	G 219
	IF (NENG.EQ.0) GO TO 23	G 220
	DO 22 IJ=1,NENG	G 221
	T=T+QMA1(IJ)*.5	G 222
	AL(2)=AL(2)-QAL(IJ)*.5+QM1(IJ)*.5/AR*TN	G 223
22	W(3)=W(3)+.5*QH(IJ)-.5*QMA(IJ)	G 224
23	AL(2)=AL(2)/S	G 225
	W(3)=(W(3)-.5*AQH1*AL(2))/T	G 226
	GO TO 35	G 227
24	S=S+.5*AQAL1	G 228
	AL(3)=-GJ(2)*AL(1)+(GJ(2)+GJ(3)-EM(2)*OM2*RGSQ(2)/(AR*AR))*AL(2)+E	G 229
	1M(2)*CM2*SW(2)/(AR*AR)*W(2)-AQAL	G 230
	IF (ISYM.NE.3) GO TO 25	G 231
	W(4)=.5*EI(1)*(W(2)-2.*W(1)+W0)-2.*EI(2)*(W(3)-2.*W(2)+W(1))+EI(3)	G 232
	1*(W(4)-2.*W(3)+W(2))-EM(2)*OM2*(W(2)-AL(2)*SW(2))+(GJ(2)*(AL(2)-(W	G 233
	2(2)-W0)/AR+.5*TN)*AR-.5*EM(1)*OM2*(RGSQ(1)*TN/AR-SW(2)*DBAR/CS)*(W	G 234
	3(2)-W0)*.5)*.5*TN/AR+(-EI(1)*(W(2)-2.*W(1)+W0)+EI(2)*(W(3)-2.*W(2)	G 235
	4+W(1))-5*EM(1)*(W(1)-SW(1)*AL(1))*OM2)*.5*DBAR/CS	G 236
	W(4)=W(4)-AQH-.25*TN*AR*Q2-.25*DBAR*Q1/CS	G 237
	W(4)=-W(4)	G 238
	GO TO 26	G 239
25	CONTINUE	G 240
	W(4)=2.*(EI(1)+EI(2))*W(1)-(2.*EI(1)+4.*EI(2)+EI(3)-OM2*EM(2))*W(2	G 241
	1)+2.*(EI(2)+EI(3))*W(3)-OM2*EM(2)*SW(2)*AL(2)-2.*EI(1)*AR*TN*AL(1)	G 242
	2+AQH	G 243

APPENDIX F

26	CONTINUE	G 244
	IF (NENG.EQ.0) GO TO 28	G 245
	DO 27 IJ=1,NENG	G 246
	T=T+.5*QMA1(IJ)	G 247
	AL(3)=AL(3)-QAL(IJ)	G 248
	IF (ISYM.EQ.3) W(4)=W(4)+.25*TN*AR*QAL1(IJ)+.25*DBAR/CS*(QH1(IJ)*Q	G 249
	IM2(IJ))	G 250
27	W(4)=W(4)+QH(IJ)-.5*QMA(IJ)	G 251
28	AL(3)=AL(3)/S	G 252
	w(4)=(W(4)+.5*AQH1*AL(3))/T	G 253
	GO TO 35	G 254
29	S=S+.5*AQAL1	G 255
	AL(MU)=-GJ(MU1)*AL(MU2)+(GJ(MU1)+GJ(MU)-OM2*EM(MU1)/(AR*AR)*RGSQ(M	G 256
	IUI))*AL(MU1)+EM(MU1)*OM2/(AR*AR)*SW(MU1)*W(MU1)-AQAL	G 257
	IF (NENG.EQ.0) GO TO 31	G 258
	DO 30 IJ=1,NENG	G 259
30	AL(MU)=AL(MU)-QAL(IJ)	G 260
31	AL(MU)=AL(MU)/S	G 261
	E(1,N)=EI(MU2)*(W(MU1)-2.*W(MU2)+W(MU3))-2.*EI(MU1)*(W(MU)-2.*W(MU	G 262
	I1)+W(MU2))-OM2*EM(MU1)*(W(MU1)-SW(MU1)*AL(MU1))-AQH-AQH1*AL(MU)*.5	G 263
	IF (NENG.EQ.0) GO TO 35	G 264
	DO 32 IJ=1,NENG	G 265
32	E(1,N)=E(1,N)-QH(IJ)-.5*(QMB(IJ)-.5*(QMA(IJ)+QMA1(IJ))*(2.*W(MU)-W(G 266
	1MU1))))	G 267
	GO TO 35	G 268
33	E(2,N)=EI(MU1)*(W(MU)-2.*W(MU1)+W(MU2))-2.*EM(MU)*OM2*(W(MU)-AL(MU	G 269
	1)*SW(MU))-2.*AQH	G 270
	E(3,N)=GJ(MU)*(AL(MU)-AL(MU1))-2.*EM(MU)*(AL(MU)*RGSQ(MU)-SW(MU)*W	G 271
	1(MU))*OM2/(AR*AR)-.5*AQAL	G 272
	IF (NENG.EQ.0) GO TO 35	G 273
	DO 34 IJ=1,NENG	G 274
	E(2,N)=E(2,N)-.5*(QH(IJ)+QMB(IJ)+QMMU(IJ))	G 275
34	E(3,N)=E(3,N)-.5*QAL(IJ)	G 276
35	CONTINUE	G 277
36	CONTINUE	G 278
	RETURN	G 279
C		G 280
	END	G 281-

APPENDIX F

	SUBROUTINE DEUPPS (A,N,DET,MAX)	H	1
	COMPLEX A(MAX,N),SWAP,DET,CO,C1	H	2
	COMMON // IX,JX,IERROR,KOPT	H	3
	CO=(0.,0.)	H	4
	C1=(1.,0.)	H	5
	DET=C1	H	6
	NN=N-1	H	7
C	PIVOT SEARCH	H	8
	DO 7 I=1,NN	H	9
	CAVM=0.	H	10
	II=I	H	11
	DO 1 J=II,N	H	12
	SWAP=A(J,II)	H	13
	AR=REAL(SWAP)	H	14
	AI=AIMAG(SWAP)	H	15
	CAVA=ABS(AR)+ABS(AI)	H	16
	IF (CAVM.GE.CAVA) GO TO 1	H	17
	IROW=J	H	18
	CAVM=CAVA	H	19
1	CONTINUE	H	20
	IF (CAVM.EQ.0.) GO TO 8	H	21
C	ROW INTERCHANGE	H	22
	IF (IROW.EQ.II) GO TO 3	H	23
	DET=-DET	H	24
	DO 2 L=II,N	H	25
	SWAP=A(IROW,L)	H	26
	A(IROW,L)=A(II,L)	H	27
	A(II,L)=SWAP	H	28
2	CONTINUE	H	29
3	SWAP=A(II,II)	H	30
	DET=DET*SWAP	H	31
C	NORMALIZE PIVOT ROW	H	32
	K=II+1	H	33
	DO 4 L=K,N	H	34
4	A(II,L)=A(II,L)/SWAP	H	35
C	ELIMINATION	H	36
	DO 6 LI=K,N	H	37
	SWAP=A(LI,II)	H	38
	DO 5 L=K,N	H	39
	A(LI,L)=A(LI,L)-A(II,L)*SWAP	H	40
5	CONTINUE	H	41
6	CONTINUE	H	42
7	CONTINUE	H	43
	GO TO 9	H	44
8	DET=CO	H	45
	GO TO 10	H	46
9	DET=DET*A(N,N)	H	47
10	RETURN	H	48
	END	H	49-

APPENDIX F

	SUBROUTINE DIV	I	1
C		I	2
C	CUMPUTES DIVERGENCE SPEED	I	3
C		I	4
	REAL LAMBDA	I	5
	DIMENSION X(3), Y(3)	I	6
	COMPLEX E,OM,CDET,W,AL	I	7
	COMMON // IX,JX,IERROR,KOPT/CUM/OM,LAMBDA,RHO,EM(60),EI(61),GJ(61)	I	8
	1,A(60),B(60),SW(60),AR,RGSQ(60),MU,E(3,3),W(60),AL(60),NN,SWEEP,IP	I	9
	2PDCD,ITMAX,ISYM,CL(90),AC(90)/STATIC/IST,ALO,CMAC,EL,ISHAPE/PYLON/	I	10
	3BPY(10),CPY(10),DPY(10),ENJ(10),ENM(10),ENEI(10),ENGJ(10),PYL(10),	I	11
	4LOC(10),NENG	I	12
	ABSCISA(X3,X2,X1,Y3,Y2,Y1)=X3+((Y1*Y3-Y2*Y3)*(X3-X1)*(X2-X3))/(Y1*	I	13
	1Y2*(X1-X2)+Y1*Y3*(X3-X1)+Y2*Y3*(X2-X3))	I	14
	IF (IST.GE.10) GO TO 7	I	15
	LAMBDA=0.	I	16
	KOUNT=0	I	17
	IST=2	I	18
	NN=3	I	19
	PRINT 11	I	20
	LU=1	I	21
	DAM1=DAM	I	22
	LAMBDA=DAM1	I	23
	CALL CFI	I	24
	CALL DEUPPS (E,3,CDET,3)	I	25
	XP=REAL(CDET)	I	26
1	LAMBDA=LAMBDA+DAM1	I	27
	KOUNT=KOUNT+1	I	28
	CALL CFI	I	29
	CALL DEUPPS (E,3,CDET,3)	I	30
	X(1)=REAL(CDET)	I	31
	ALAM=LAMBDA*EL*EL*EL	I	32
	PRINT 10, ALAM,CDET,KOUNT	I	33
	FMFP=ABS(X(1)-XP)	I	34
	IF (FMFP.GE.ABS(X(1)).AND.FMFP.GE.ABS(XP)) GO TO 2	I	35
	XP=X(1)	I	36
	IF (KOUNT.GT.100) GO TO 6	I	37
	IF (LAMBDA.GT.DAMMAX) GO TO 6	I	38
	GO TO 1	I	39
2	Y(3)=LAMBDA	I	40
	Y(1)=LAMBDA-DAM1	I	41
	LAMBDA=LAMBDA-.5*DAM1	I	42
	Y(2)=LAMBDA	I	43
	CALL CFI	I	44
	CALL DEUPPS (E,3,CDET,3)	I	45
	X(3)=X(1)	I	46
	X(1)=XP	I	47
	X(2)=REAL(CDET)	I	48
	XO=X(1)	I	49
	ALAM=LAMBDA*EL*EL*EL	I	50
	PRINT 10, ALAM,CDET,KOUNT	I	51
	AM=Y(2)	I	52

APPENDIX F

3	LAMBDA=ABSCISA(Y(3),Y(2),Y(1),X(3),X(2),X(1))	I 53
	CALL CFI	I 54
	CALL DEUPPS (E,3,CDET,3)	I 55
	ALAM=LAMBDA*EL*EL*EL	I 56
	PRINT 10, ALAM,CDET,KOUNT	I 57
	X(1)=REAL(CDET)	I 58
	Y(1)=LAMBDA	I 59
	IF (ABS(LAMBDA-AM).LT.1.E-5) GO TO 5	I 60
	AM=LAMBDA	I 61
	IF (KCUNT.GT.100) GO TO 6	I 62
	IF (LAMBDA.GT.DAMMAX) GO TO 6	I 63
	LU=2	I 64
	DAM1=DAM1/4.	I 65
	KOUNT=KOUNT+1	I 66
	DO 4 I=LU,3	I 67
	LAMBDA=LAMBDA+DAM1	I 68
	CALL CFI	I 69
	CALL DEUPPS (E,3,CDET,3)	I 70
	X(I)=REAL(CDET)	I 71
	Y(I)=LAMBDA	I 72
4	CONTINUE	I 73
	GO TO 3	I 74
5	ALAM=LAMBDA*EL*EL*EL	I 75
	PRINT 8, ALAM,CDET,KCUNT	I 76
	RETURN	I 77
6	ALAM=LAMBDA*EL*EL*EL	I 78
	PRINT 9, KOUNT,ALAM,CDET	I 79
7	RETURN	I 80
C		I 81
8	FORMAT (//,20X,21HDIVERGENCE AT LAMBDA=,E16.8,5X,5HCDET=,2E16.8,5X 1,18HNO. OF ITERATIONS=,I4/)	I 82
9	FORMAT (//,20X,20HDIVERGENCE NOT FOUND,5X,6HKOUNT=,I4,5X,7HLAMBDA= 1,E16.8,5X,5HCDET=,2E16.8/)	I 84
		I 85
10	FORMAT (5X,E16.8,10X,E16.8,1X,E16.8,10X,I2)	I 86
11	FORMAT (8X,6HLAMBDA,20X,4HCDET,15X,10HITERATIONS)	I 87
	END	I 88-

APPENDIX F

	SUBROUTINE NATRL (ILMAX,OS,OE,O DEL)	J	1
C		J	2
C	COMPUTES NATURAL FREQUENCIES OF AIRCRAFT	J	3
C	ILMAX=NUMBER OF FREQUENCIES TO BE FOUND	J	4
C	OS=STARTING VALUE FOR SEARCH	J	5
C	OE=FINAL VALUE FOR SEARCH	J	6
C	O DEL=STEP SIZE TO BE USED IN SEARCH	J	7
C		J	8
	REAL LAMBDA	J	9
	COMPLEX OM,W,AL,E,CDET	J	10
	COMMON // IX,JX,IERROR,KOPT/CUM/OM,LAMBDA,RHO,EM(60),EI(61),GJ(61)	J	11
	1,A(60),B(60),SW(60),AR,RGSQ(60),MU,E(3,3),W(60),AL(60),NN,SWEEP,IP	J	12
	2ROCD,ITMAX,ISYM,CL(90),AC(90)/STATIC/IST,ALO,CMAC,EL,ISHAPE/PYLON/	J	13
	3BPY(10),CPY(10),DPY(10),FNJ(10),ENM(10),ENEI(10),ENGJ(10),PYL(10),	J	14
	4LOC(10),NENG/FREQ/OM1(5),DOM1,DAM,CMMAX1,TDAM,DAMMAX	J	15
	LAMBDA=0.	J	16
	NN=3	J	17
	ELD=1./(EL*EL)	J	18
	X=OS*ELD	J	19
	XD=O DEL*ELD	J	20
	XMAX=OE*ELD	J	21
	IM=1	J	22
	CM=CPLX(X,.0)	J	23
	PRINT 7, ISYM	J	24
	CALL CFI	J	25
	CALL DEUPPS (E,3,CDET,3)	J	26
	FP=REAL(CDET)	J	27
1	X=X+XD	J	28
	OM=CPLX(X,.0)	J	29
	IF (X.GT.XMAX) GO TO 5	J	30
	CALL CFI	J	31
	CALL DEUPPS (E,3,CDET,3)	J	32
	F=REAL(CDET)	J	33
	IF (IX.EQ.2) GO TO 2	J	34
	PRINT 8, FP,F,X	J	35
2	CONTINUE	J	36
	FMFP=ABS(F-FP)	J	37
	IF (FMFP.GE.ABS(F).AND.FMFP.GE.ABS(FP)) GO TO 3	J	38
	FP=F	J	39
	GO TO 1	J	40
3	IF (ABS(XD).LT.ABS(X)*.5E-2.AND.XD.GT.0.) GO TO 4	J	41
	XD=-.5*XD	J	42
	FP=F	J	43
	GO TO 1	J	44
4	CM1(IM)=X*EL*EL	J	45
	FP=F	J	46
	IF (IM.EQ.ILMAX) RETURN	J	47
	IM=IM+1	J	48
	XD=O DEL*ELD	J	49
	GO TO 1	J	50
5	PRINT 6, IM,OE	J	51
	RETURN	J	52
C		J	53
6	FORMAT (/,2X,25HSEARCHING FOR ROOT NUMBER,I2,27HNO ROOT FOUND OUT	J	54
	1TO OMEGA=,E16.8/)	J	55
7	FORMAT (/,1X,5HISYM=,I4)	J	56
8	FORMAT (3X,3HFP=,E16.8,4H F=,E16.8,4H X=,E16.8)	J	57
	END	J	58-

APPENDIX F

Input Data for Sample Problem

```
$OPTION ISYM=1,KOPT=2,ISHAPE=1,ILMAX=5,IMORDER=1,2,3,4,5$
$TRACE DAM=.1,IPROC=2,ITMAX=10,ISTOP=200,DAMMAX=4.,DOMI=.1$
$INOUT IX=2,JX=2,IY=2$
$PLAN SPAN=20.,A=30*-1.02,B=30*3.,SW=30*.6,RGSQ=30*2.61,BCH=30*3.,ZT=30*.05,
Q=5.796E9,1.449E8,.0,1.449E8,5.796E8,3*.0,4.32E8,SWEEP=.0,N=30,
CL=30*6.2831853,AC=30*-.5$
$ENGINE ENEI=.0,ENGJ=.0,ENJ=.0,ENI=.0,PYL=.0,LOC=0,WENG=0$
$DESIGN EIREF=2.4E8,EMREF=2.5,RHO=.00237,RHOBAR=5.1,BREF=3.,WTI=30*106.554,
LOW=3,NL=1,DB=0.,G=32.2$
$PARAM ISTIFF=1,AA=.032,7*.0,KVT=1,KV1=5,KV2=1,DEL=.01570796,MAX=100$
$NATFQ JS=.1,OE=60.,ODEL=.3$
```

APPENDIX F

Computer Output for Sample Problem

```

DIMENSIONAL INPUT
*****
IX=2      JX=2      N=30      IFORD= 1      MAX=100      SPAN= 2.00000000E+01      SHEEP= 0.
KV1,KV2,DEL 5 1 1.57079600E-02
IPROCD ITMAX ISTOP ISHAPE ISYM ISTART ILMAX KOPT
 2      10      200      1      1      3      5      2
NODAL PT.
 1      A      B      SW      RGSQ
 2      -1.020000E+00 3.000000E+00 6.000000E-01 2.610000E+00
 3      -1.020000E+00 3.000000E+00 6.000000E-01 2.610000E+00
 4      -1.020000E+00 3.000000E+00 6.000000E-01 2.610000E+00
 5      -1.020000E+00 3.000000E+00 6.000000E-01 2.610000E+00
 6      -1.020000E+00 3.000000E+00 6.000000E-01 2.610000E+00
 7      -1.020000E+00 3.000000E+00 6.000000E-01 2.610000E+00
 8      -1.020000E+00 3.000000E+00 6.000000E-01 2.610000E+00
 9      -1.020000E+00 3.000000E+00 6.000000E-01 2.610000E+00
10      -1.020000E+00 3.000000E+00 6.000000E-01 2.610000E+00
11      -1.020000E+00 3.000000E+00 6.000000E-01 2.610000E+00
12      -1.020000E+00 3.000000E+00 6.000000E-01 2.610000E+00
13      -1.020000E+00 3.000000E+00 6.000000E-01 2.610000E+00
14      -1.020000E+00 3.000000E+00 6.000000E-01 2.610000E+00
15      -1.020000E+00 3.000000E+00 6.000000E-01 2.610000E+00
16      -1.020000E+00 3.000000E+00 6.000000E-01 2.610000E+00
17      -1.020000E+00 3.000000E+00 6.000000E-01 2.610000E+00
18      -1.020000E+00 3.000000E+00 6.000000E-01 2.610000E+00
19      -1.020000E+00 3.000000E+00 6.000000E-01 2.610000E+00
20      -1.020000E+00 3.000000E+00 6.000000E-01 2.610000E+00
21      -1.020000E+00 3.000000E+00 6.000000E-01 2.610000E+00
22      -1.020000E+00 3.000000E+00 6.000000E-01 2.610000E+00
23      -1.020000E+00 3.000000E+00 6.000000E-01 2.610000E+00
24      -1.020000E+00 3.000000E+00 6.000000E-01 2.610000E+00
25      -1.020000E+00 3.000000E+00 6.000000E-01 2.610000E+00
26      -1.020000E+00 3.000000E+00 6.000000E-01 2.610000E+00
27      -1.020000E+00 3.000000E+00 6.000000E-01 2.610000E+00
28      -1.020000E+00 3.000000E+00 6.000000E-01 2.610000E+00
29      -1.020000E+00 3.000000E+00 6.000000E-01 2.610000E+00
30      -1.020000E+00 3.000000E+00 6.000000E-01 2.610000E+00

```

APPENDIX F

NODAL PT.	BCH	ZT	WTI
1	3.000000E+00	2.500000E-01	1.065540E+02
2	3.000000E+00	2.500000E-01	1.065540E+02
3	3.000000E+00	2.500000E-01	1.065540E+02
4	3.000000E+00	2.500000E-01	1.065540E+02
5	3.000000E+00	2.500000E-01	1.065540E+02
6	3.000000E+00	2.500000E-01	1.065540E+02
7	3.000000E+00	2.500000E-01	1.065540E+02
8	3.000000E+00	2.500000E-01	1.065540E+02
9	3.000000E+00	2.500000E-01	1.065540E+02
10	3.000000E+00	2.500000E-01	1.065540E+02
11	3.000000E+00	2.500000E-01	1.065540E+02
12	3.000000E+00	2.500000E-01	1.065540E+02
13	3.000000E+00	2.500000E-01	1.065540E+02
14	3.000000E+00	2.500000E-01	1.065540E+02
15	3.000000E+00	2.500000E-01	1.065540E+02
16	3.000000E+00	2.500000E-01	1.065540E+02
17	3.000000E+00	2.500000E-01	1.065540E+02
18	3.000000E+00	2.500000E-01	1.065540E+02
19	3.000000E+00	2.500000E-01	1.065540E+02
20	3.000000E+00	2.500000E-01	1.065540E+02
21	3.000000E+00	2.500000E-01	1.065540E+02
22	3.000000E+00	2.500000E-01	1.065540E+02
23	3.000000E+00	2.500000E-01	1.065540E+02
24	3.000000E+00	2.500000E-01	1.065540E+02
25	3.000000E+00	2.500000E-01	1.065540E+02
26	3.000000E+00	2.500000E-01	1.065540E+02
27	3.000000E+00	2.500000E-01	1.065540E+02
28	3.000000E+00	2.500000E-01	1.065540E+02
29	3.000000E+00	2.500000E-01	1.065540E+02
30	3.000000E+00	2.500000E-01	1.065540E+02

REDUCED STIFFNESS MATRIX

5.79600000E+09 1.44900000E+08 0.
 1.44900000E+08 5.79600000E+08 0.
 0. 0. 4.32000000E+08

DCMI= 1.00000000E-01 DAM= 1.00000000E-01 DAMMAX= 4.00000000E+00

RHO= 2.37000000E-03 RHOBAR= 5.10000000E+00 BREF= 3.00000000E+00
 EIREF= 2.40000000E+08 EMREF= 2.50000000E+00

APPENDIX F

NO ENGINES ON THE WINGS

ELEMENTS OF MATRIX AA (ISTIFF=1, ONE LAMINA PER MATRIX COLUMN)

3.20000000E-02

0.
0.
0.
0.
0.
0.
0.

NON-DIMENSIONAL INPUT

NODAL PT.	A	B	SW	RGSQ
1	-3.400000E-01	1.000000E+00	2.000000E-01	2.900000E-01
2	-3.400000E-01	1.000000E+00	2.000000E-01	2.900000E-01
3	-3.400000E-01	1.000000E+00	2.000000E-01	2.900000E-01
4	-3.400000E-01	1.000000E+00	2.000000E-01	2.900000E-01
5	-3.400000E-01	1.000000E+00	2.000000E-01	2.900000E-01
6	-3.400000E-01	1.000000E+00	2.000000E-01	2.900000E-01
7	-3.400000E-01	1.000000E+00	2.000000E-01	2.900000E-01
8	-3.400000E-01	1.000000E+00	2.000000E-01	2.900000E-01
9	-3.400000E-01	1.000000E+00	2.000000E-01	2.900000E-01
10	-3.400000E-01	1.000000E+00	2.000000E-01	2.900000E-01
11	-3.400000E-01	1.000000E+00	2.000000E-01	2.900000E-01
12	-3.400000E-01	1.000000E+00	2.000000E-01	2.900000E-01
13	-3.400000E-01	1.000000E+00	2.000000E-01	2.900000E-01
14	-3.400000E-01	1.000000E+00	2.000000E-01	2.900000E-01
15	-3.400000E-01	1.000000E+00	2.000000E-01	2.900000E-01
16	-3.400000E-01	1.000000E+00	2.000000E-01	2.900000E-01
17	-3.400000E-01	1.000000E+00	2.000000E-01	2.900000E-01
18	-3.400000E-01	1.000000E+00	2.000000E-01	2.900000E-01
19	-3.400000E-01	1.000000E+00	2.000000E-01	2.900000E-01
20	-3.400000E-01	1.000000E+00	2.000000E-01	2.900000E-01
21	-3.400000E-01	1.000000E+00	2.000000E-01	2.900000E-01
22	-3.400000E-01	1.000000E+00	2.000000E-01	2.900000E-01
23	-3.400000E-01	1.000000E+00	2.000000E-01	2.900000E-01
24	-3.400000E-01	1.000000E+00	2.000000E-01	2.900000E-01
25	-3.400000E-01	1.000000E+00	2.000000E-01	2.900000E-01
26	-3.400000E-01	1.000000E+00	2.000000E-01	2.900000E-01
27	-3.400000E-01	1.000000E+00	2.000000E-01	2.900000E-01
28	-3.400000E-01	1.000000E+00	2.000000E-01	2.900000E-01
29	-3.400000E-01	1.000000E+00	2.000000E-01	2.900000E-01
30	-3.400000E-01	1.000000E+00	2.000000E-01	2.900000E-01

ASPECT RATIO= 6.66666667E+00 MASS RATIO=1/KAPPA= 3.73077691E+01

APPENDIX F

NODAL PT.	EI	GJ	EM	CL	AC
1	6.56954189E-01	9.79310592E-02	1.71533217E+00	6.28318530E+00	-5.00000000E-01
2	6.56954189E-01	9.79310592E-02	1.71533217E+00	6.28318530E+00	-5.00000000E-01
3	6.56954189E-01	9.79310592E-02	1.71533217E+00	6.28318530E+00	-5.00000000E-01
4	6.56954189E-01	9.79310592E-02	1.71533217E+00	6.28318530E+00	-5.00000000E-01
5	6.56954189E-01	9.79310592E-02	1.71533217E+00	6.28318530E+00	-5.00000000E-01
6	6.56954189E-01	9.79310592E-02	1.71533217E+00	6.28318530E+00	-5.00000000E-01
7	6.56954189E-01	9.79310592E-02	1.71533217E+00	6.28318530E+00	-5.00000000E-01
8	6.56954189E-01	9.79310592E-02	1.71533217E+00	6.28318530E+00	-5.00000000E-01
9	6.56954189E-01	9.79310592E-02	1.71533217E+00	6.28318530E+00	-5.00000000E-01
10	6.56954189E-01	9.79310592E-02	1.71533217E+00	6.28318530E+00	-5.00000000E-01
11	6.56954189E-01	9.79310592E-02	1.71533217E+00	6.28318530E+00	-5.00000000E-01
12	6.56954189E-01	9.79310592E-02	1.71533217E+00	6.28318530E+00	-5.00000000E-01
13	6.56954189E-01	9.79310592E-02	1.71533217E+00	6.28318530E+00	-5.00000000E-01
14	6.56954189E-01	9.79310592E-02	1.71533217E+00	6.28318530E+00	-5.00000000E-01
15	6.56954189E-01	9.79310592E-02	1.71533217E+00	6.28318530E+00	-5.00000000E-01
16	6.56954189E-01	9.79310592E-02	1.71533217E+00	6.28318530E+00	-5.00000000E-01
17	6.56954189E-01	9.79310592E-02	1.71533217E+00	6.28318530E+00	-5.00000000E-01
18	6.56954189E-01	9.79310592E-02	1.71533217E+00	6.28318530E+00	-5.00000000E-01
19	6.56954189E-01	9.79310592E-02	1.71533217E+00	6.28318530E+00	-5.00000000E-01
20	6.56954189E-01	9.79310592E-02	1.71533217E+00	6.28318530E+00	-5.00000000E-01
21	6.56954189E-01	9.79310592E-02	1.71533217E+00	6.28318530E+00	-5.00000000E-01
22	6.56954189E-01	9.79310592E-02	1.71533217E+00	6.28318530E+00	-5.00000000E-01
23	6.56954189E-01	9.79310592E-02	1.71533217E+00	6.28318530E+00	-5.00000000E-01
24	6.56954189E-01	9.79310592E-02	1.71533217E+00	6.28318530E+00	-5.00000000E-01
25	6.56954189E-01	9.79310592E-02	1.71533217E+00	6.28318530E+00	-5.00000000E-01
26	6.56954189E-01	9.79310592E-02	1.71533217E+00	6.28318530E+00	-5.00000000E-01
27	6.56954189E-01	9.79310592E-02	1.71533217E+00	6.28318530E+00	-5.00000000E-01
28	6.56954189E-01	9.79310592E-02	1.71533217E+00	6.28318530E+00	-5.00000000E-01
29	6.56954189E-01	9.79310592E-02	1.71533217E+00	6.28318530E+00	-5.00000000E-01
30	6.56954189E-01	9.79310592E-02	1.71533217E+00	6.28318530E+00	-5.00000000E-01

ISVM= 1

ESTIMATES OF NAT. FREQ. 2.12031250E+00 5.04531250E+00
 1.19265625E+01 1.65765625E+01 2.30265625E+01

REAL PART	OMEGA	IMAGINARY PART	LAMBDA	REAL PART	DETERMINANT	IMAGINARY PART	NO. ITERATIONS
2.12019144E+00	0.	0.06365696E-01	0.	-7.56948891E-04	0.	8.68636836E-08	3
2.21709892E+00	1.06365696E-01	1.67928671E-01	1.00000000E-01	4.23072504E-07	0.	2.77472633E-05	3
2.34202768E+00	1.67928671E-01	2.26631224E-01	2.00000000E-01	-5.98807394E-05	-2.77472633E-05	-5.22190153E-06	2
2.53865870E+00	2.26631224E-01	2.00546729E-01	3.00000000E-01	-2.52286468E-05	-5.22190153E-06	-5.87186135E-08	2
3.04674568E+00	2.00546729E-01	-3.73819215E-01	4.00000000E-01	-4.92740931E-06	-5.87186135E-08	-4.21611283E-06	9
3.0877212E+00	-3.73819215E-01		5.00000000E-01	1.50058558E-05	-4.21611283E-06		6

OMEGA= 2.5387

LAMBDA= .4342

FLUTTER INSTABILITY ENCOUNTERED AT LAMBDA= .4342

APPENDIX F

OMEGA		LAMBDA		DETERMINANT		NO. ITERATIONS
REAL PART	IMAGINARY PART	REAL PART	IMAGINARY PART	REAL PART	IMAGINARY PART	
5.02739671E+00	0.	1.00000000E-01	0.	1.22817573E-03	0.	3
4.78890809E+00	1.39339768E-01	1.00000000E-01	1.39339768E-01	1.84646760E-04	-3.74597765E-05	3
4.48224180E+00	2.32572193E-01	2.00000000E-01	2.32572193E-01	-1.12542634E-06	5.44974429E-07	3
4.08171240E+00	3.18581985E-01	3.00000000E-01	3.18581985E-01	4.86714229E-04	6.89487055E-05	2
3.35060583E+00	4.88055300E-01	4.00000000E-01	4.88055300E-01	3.85220254E-05	3.43285133E-06	5
3.07139735E+00	1.21171209E+00	5.00000000E-01	1.21171209E+00	-4.83569769E-05	-1.09204048E-04	5
LAMBDA EXCEEDS .53492						

OMEGA		LAMBDA		DETERMINANT		NO. ITERATIONS
REAL PART	IMAGINARY PART	REAL PART	IMAGINARY PART	REAL PART	IMAGINARY PART	
1.19135428E+01	0.	1.00000000E-01	0.	-4.36235019E-03	0.	3
1.19357822E+01	1.50119270E-01	1.00000000E-01	1.50119270E-01	1.68069886E-04	-8.53525682E-05	2
1.19596681E+01	2.14485307E-01	2.00000000E-01	2.14485307E-01	2.09175677E-04	-1.29446611E-04	2
1.19852701E+01	2.65530383E-01	3.00000000E-01	2.65530383E-01	1.59312150E-05	-9.57548451E-06	2
1.20126683E+01	3.10097829E-01	4.00000000E-01	3.10097829E-01	5.07014213E-06	-5.13302333E-06	2
1.20419692E+01	3.50859501E-01	5.00000000E-01	3.50859501E-01	1.18854929E-06	-3.65118273E-06	2
LAMBDA EXCEEDS .53492						

OMEGA		LAMBDA		DETERMINANT		NO. ITERATIONS
REAL PART	IMAGINARY PART	REAL PART	IMAGINARY PART	REAL PART	IMAGINARY PART	
1.65175340E+01	0.	1.00000000E-01	0.	8.29254515E-03	0.	3
1.64609518E+01	5.68725993E-02	1.00000000E-01	5.68725993E-02	5.61470150E-05	7.20596144E-07	3
1.64014260E+01	8.42139704E-02	2.00000000E-01	8.42139704E-02	-5.23270508E-04	1.99386514E-05	2
1.63390476E+01	1.07272678E-01	3.00000000E-01	1.07272678E-01	-2.33289533E-05	3.30762927E-06	2
1.62737578E+01	1.28077626E-01	4.00000000E-01	1.28077626E-01	9.89257237E-06	2.99421579E-06	2
1.62055437E+01	1.47290246E-01	5.00000000E-01	1.47290246E-01	2.04843607E-05	3.04557599E-06	2
LAMBDA EXCEEDS .53492						

OMEGA		LAMBDA		DETERMINANT		NO. ITERATIONS
REAL PART	IMAGINARY PART	REAL PART	IMAGINARY PART	REAL PART	IMAGINARY PART	
2.30110627E+01	0.	1.00000000E-01	0.	-2.85216870E-02	0.	3
2.29905865E+01	1.48309211E-01	1.00000000E-01	1.48309211E-01	-1.45336415E-05	-4.72530278E-07	3
2.29699582E+01	2.11712582E-01	2.00000000E-01	2.11712582E-01	6.47730386E-03	-2.85766947E-04	2
2.29492861E+01	2.61650026E-01	3.00000000E-01	2.61650026E-01	6.29885510E-04	3.59184642E-07	2
2.29284326E+01	3.04786543E-01	4.00000000E-01	3.04786543E-01	2.92462618E-04	1.28319320E-06	2
2.29074518E+01	3.43667837E-01	5.00000000E-01	3.43667837E-01	1.77738391E-04	1.68793634E-06	2
LAMBDA EXCEEDS .53492						

***** PRELIMINARY DESIGN OCCURS AT LAMBDA= 4.34916194E-01 AND OMEGA= 2.53866202E+00 ON BRANCH NO. 1 *****

APPENDIX F

POSITION	DEFLECTION		DEFORMATION SHAPE		TWIST	PHASE
	MAGNITUDE	PHASE	MAGNITUDE	PHASE		
1	0.	0.	0.	0.	0.	0.
2	2.86551529E-01	-1.73750403E-03	8.49500096E+00	8.49500096E+00	3.13101852E+00	3.13101852E+00
3	1.00000000E+00	0.	1.63587203E+01	1.63587203E+01	3.13087466E+00	3.13087466E+00
4	1.99787673E+00	1.60793027E-03	2.29841899E+01	2.29841899E+01	3.13056846E+00	3.13056846E+00
5	3.14578254E+00	3.29073159E-03	2.78400208E+01	2.78400208E+01	3.13002957E+00	3.13002957E+00
6	4.32181392E+00	5.07815788E-03	3.05157754E+01	3.05157754E+01	3.12914779E+00	3.12914779E+00
7	5.42062061E+00	6.96102788E-03	3.07579338E+01	3.07579338E+01	3.12772924E+00	3.12772924E+00
8	6.35670255E+00	8.90766102E-03	2.84936466E+01	2.84936466E+01	3.12538783E+00	3.12538783E+00
9	7.06664586E+00	1.08619299E-02	2.38404229E+01	2.38404229E+01	3.12121663E+00	3.12121663E+00
10	7.51010375E+00	1.27334842E-02	1.71011392E+01	1.71011392E+01	3.11244210E+00	3.11244210E+00
11	7.66944385E+00	1.43798218E-02	8.74656599E+00	8.74656599E+00	3.08444752E+00	3.08444752E+00
12	7.54809789E+00	1.55756797E-02	8.13216538E-01	8.13216538E-01	6.44417567E-01	6.44417567E-01
13	7.16775766E+00	1.59598066E-02	1.03763702E+01	1.03763702E+01	4.47800968E-02	4.47800968E-02
14	6.56465445E+00	1.49380300E-02	1.96951872E+01	1.96951872E+01	2.16514437E-02	2.16514437E-02
15	5.78523411E+00	1.14947342E-02	2.79189669E+01	2.79189669E+01	1.33632881E-02	1.33632881E-02
16	4.88159912E+00	3.79243001E-03	3.44084772E+01	3.44084772E+01	8.82243713E-03	8.82243713E-03
17	3.90715440E+00	-1.17860303E-02	3.86463978E+01	3.86463978E+01	5.62189546E-03	5.62189546E-03
18	2.91307359E+00	-4.33392789E-02	4.02757590E+01	4.02757590E+01	2.83661421E-03	2.83661421E-03
19	1.94712977E+00	-1.13165027E-01	3.91281022E+01	3.91281022E+01	-1.16593916E-04	-1.16593916E-04
20	1.06382149E+00	-3.09420115E-01	3.52378466E+01	3.52378466E+01	-3.89393239E-03	-3.89393239E-03
21	4.66136469E-01	-1.20023344E+00	2.88416052E+01	2.88416052E+01	-9.72878770E-03	-9.72878770E-03
22	8.02734111E-01	-2.39163560E+00	2.03627613E+01	2.03627613E+01	-2.11462372E-02	-2.11462372E-02
23	1.41607058E+00	-2.65881858E+00	1.03857595E+01	1.03857595E+01	-5.60671890E-02	-5.60671890E-02
24	1.99068390E+00	-2.74929593E+00	8.48556423E-01	8.48556423E-01	-2.10795616E+00	-2.10795616E+00
25	2.50727039E+00	-2.79368763E+00	1.13306963E+01	1.13306963E+01	-3.06512851E+00	-3.06512851E+00
26	2.97564101E+00	-2.82140531E+00	2.14804609E+01	2.14804609E+01	-3.09570173E+00	-3.09570173E+00
27	3.41098547E+00	-2.84218410E+00	3.02200736E+01	3.02200736E+01	-3.10574152E+00	-3.10574152E+00
28	3.82793940E+00	-2.85957086E+00	3.69310482E+01	3.69310482E+01	-3.11032348E+00	-3.11032348E+00
29	4.23740377E+00	-2.87440679E+00	4.11458434E+01	4.11458434E+01	-3.11249332E+00	-3.11249332E+00
30	4.64458347E+00	-2.88608968E+00	4.25786612E+01	4.25786612E+01	-3.11315880E+00	-3.11315880E+00

FLUTTER SPEED= 1.35465473E+03

APPENDIX F

NODAL PT.	EI	GJ	EM	CL	AC
1	6.56662323E-01	9.85150199E-02	1.715333217E+00	6.28318530E+00	-5.0000000E-01
2	6.56662323E-01	9.85150199E-02	1.715333217E+00	6.28318530E+00	-5.0000000E-01
3	6.56662323E-01	9.85150199E-02	1.715333217E+00	6.28318530E+00	-5.0000000E-01
4	6.56662323E-01	9.85150199E-02	1.715333217E+00	6.28318530E+00	-5.0000000E-01
5	6.56662323E-01	9.85150199E-02	1.715333217E+00	6.28318530E+00	-5.0000000E-01
6	6.56662323E-01	9.85150199E-02	1.715333217E+00	6.28318530E+00	-5.0000000E-01
7	6.56662323E-01	9.85150199E-02	1.715333217E+00	6.28318530E+00	-5.0000000E-01
8	6.56662323E-01	9.85150199E-02	1.715333217E+00	6.28318530E+00	-5.0000000E-01
9	6.56662323E-01	9.85150199E-02	1.715333217E+00	6.28318530E+00	-5.0000000E-01
10	6.56662323E-01	9.85150199E-02	1.715333217E+00	6.28318530E+00	-5.0000000E-01
11	6.56662323E-01	9.85150199E-02	1.715333217E+00	6.28318530E+00	-5.0000000E-01
12	6.56662323E-01	9.85150199E-02	1.715333217E+00	6.28318530E+00	-5.0000000E-01
13	6.56662323E-01	9.85150199E-02	1.715333217E+00	6.28318530E+00	-5.0000000E-01
14	6.56662323E-01	9.85150199E-02	1.715333217E+00	6.28318530E+00	-5.0000000E-01
15	6.56662323E-01	9.85150199E-02	1.715333217E+00	6.28318530E+00	-5.0000000E-01
16	6.56662323E-01	9.85150199E-02	1.715333217E+00	6.28318530E+00	-5.0000000E-01
17	6.56662323E-01	9.85150199E-02	1.715333217E+00	6.28318530E+00	-5.0000000E-01
18	6.56662323E-01	9.85150199E-02	1.715333217E+00	6.28318530E+00	-5.0000000E-01
19	6.56662323E-01	9.85150199E-02	1.715333217E+00	6.28318530E+00	-5.0000000E-01
20	6.56662323E-01	9.85150199E-02	1.715333217E+00	6.28318530E+00	-5.0000000E-01
21	6.56662323E-01	9.85150199E-02	1.715333217E+00	6.28318530E+00	-5.0000000E-01
22	6.56662323E-01	9.85150199E-02	1.715333217E+00	6.28318530E+00	-5.0000000E-01
23	6.56662323E-01	9.85150199E-02	1.715333217E+00	6.28318530E+00	-5.0000000E-01
24	6.56662323E-01	9.85150199E-02	1.715333217E+00	6.28318530E+00	-5.0000000E-01
25	6.56662323E-01	9.85150199E-02	1.715333217E+00	6.28318530E+00	-5.0000000E-01
26	6.56662323E-01	9.85150199E-02	1.715333217E+00	6.28318530E+00	-5.0000000E-01
27	6.56662323E-01	9.85150199E-02	1.715333217E+00	6.28318530E+00	-5.0000000E-01
28	6.56662323E-01	9.85150199E-02	1.715333217E+00	6.28318530E+00	-5.0000000E-01
29	6.56662323E-01	9.85150199E-02	1.715333217E+00	6.28318530E+00	-5.0000000E-01
30	6.56662323E-01	9.85150199E-02	1.715333217E+00	6.28318530E+00	-5.0000000E-01

ELEMENTS OF MATRIX AA (ISTIFF=1, ONE LAMINA PER MATRIX COLUMN)

3.2000000E-02
 0.
 0.
 0.
 1.5707600E-02
 0.
 0.
 0.

REAL PART	OMEGA	IMAGINARY PART	LAMBDA	REAL PART	DETERMINANT	NO. ITERATIONS
3.13341510E+00	-7.01611940E-02	4.34916194E-01	1.03881680E-06	-1.81684838E-07	7	
2.63640984E+00	2.46064902E-01	3.34916194E-01	-3.34800666E-05	-6.17921539E-06	5	
FLUTTER INSTABILITY ENCOUNTERED AT LAMBDA= .41273				OMEGA= 3.0231		

APPENDIX F

POSITION	DEFLECTION		DEFORMATION SHAPE		TWIST	PHASE
	MAGNITUDE	PHASE	MAGNITUDE	PHASE		
1	0.	0.	0.	0.	0.	0.
2	6.68748045E-04	3.134232257E+00	2.88133200E-01		-2.61231148E+00	
3	1.00000000E+00	0.	5.75815807E-01		-2.61221863E+00	
4	4.00467484E+00	-9.35743222E-06	8.61909481E-01		-2.61188143E+00	
5	1.00160371E+01	-1.35505922E-05	1.14390103E+00		-2.61102172E+00	
6	2.00368502E+01	-1.64667486E-05	1.4172192E+00		-2.60923454E+00	
7	3.50701047E+01	-1.88810051E-05	1.67456283E+00		-2.60595514E+00	
8	5.61192649E+01	-2.10085709E-05	1.90524338E+00		-2.60038607E+00	
9	8.41886412E+01	-2.28851975E-05	2.09457350E+00		-2.59134454E+00	
10	1.20283916E+02	-2.44663652E-05	2.22333530E+00		-2.57693979E+00	
11	1.65412843E+02	-2.56615448E-05	2.26745092E+00		-2.55384764E+00	
12	2.20586160E+02	-2.63481641E-05	2.19819982E+00		-2.51549139E+00	
13	2.86818716E+02	-2.63780280E-05	1.98425252E+00		-2.44667426E+00	
14	3.65130868E+02	-2.55803934E-05	1.60166949E+00		-2.30358946E+00	
15	4.56550152E+02	-2.37635082E-05	1.09626568E+00		-1.91626898E+00	
16	5.62113264E+02	-2.07153505E-05	1.00245893E+00		-8.82437409E-01	
17	6.82868383E+02	-1.62039442E-05	2.06067000E+00		-1.93606859E-01	
18	8.19877843E+02	-9.97744415E-06	3.86584250E+00		3.28333932E-02	
19	9.74221215E+02	-1.76410514E-06	6.30492316E+00		1.31146010E-01	
20	1.14699880E+03	8.72779900E-06	9.44271226E+00		1.84073850E-01	
21	1.33933556E+03	2.18100582E-05	1.33845429E+01		2.16429480E-01	
22	1.55238555E+03	3.78145767E-05	1.82554025E+01		2.37884740E-01	
23	1.78733687E+03	5.70933648E-05	2.41958322E+01		2.52934882E-01	
24	2.04541711E+03	8.00184460E-05	3.13611313E+01		2.63937797E-01	
25	2.32789940E+03	1.06981660E-04	3.99214588E+01		2.72243083E-01	
26	2.63610913E+03	1.38394343E-04	5.00622426E+01		2.78675609E-01	
27	2.97143118E+03	1.74686858E-04	6.19847172E+01		2.83765870E-01	
28	3.33531800E+03	2.16307974E-04	7.59065310E+01		2.87869169E-01	
29	3.72929824E+03	2.63724052E-04	9.20623989E+01		2.91231457E-01	
30	4.15498632E+03	3.17418055E-04	1.10704796E+02		2.94027703E-01	

FLUTTER SPEED= 1.31964891E+03

APPENDIX F

NODAL PT.	EI	GJ	EM	CL	AC
1	6.55787447E-01	1.00264597E-01	1.71533217E+00	6.28318530E+00	-5.0000000E-01
2	6.55787447E-01	1.00264597E-01	1.71533217E+00	6.28318530E+00	-5.0000000E-01
3	6.55787447E-01	1.00264597E-01	1.71533217E+00	6.28318530E+00	-5.0000000E-01
4	6.55787447E-01	1.00264597E-01	1.71533217E+00	6.28318530E+00	-5.0000000E-01
5	6.55787447E-01	1.00264597E-01	1.71533217E+00	6.28318530E+00	-5.0000000E-01
6	6.55787447E-01	1.00264597E-01	1.71533217E+00	6.28318530E+00	-5.0000000E-01
7	6.55787447E-01	1.00264597E-01	1.71533217E+00	6.28318530E+00	-5.0000000E-01
8	6.55787447E-01	1.00264597E-01	1.71533217E+00	6.28318530E+00	-5.0000000E-01
9	6.55787447E-01	1.00264597E-01	1.71533217E+00	6.28318530E+00	-5.0000000E-01
10	6.55787447E-01	1.00264597E-01	1.71533217E+00	6.28318530E+00	-5.0000000E-01
11	6.55787447E-01	1.00264597E-01	1.71533217E+00	6.28318530E+00	-5.0000000E-01
12	6.55787447E-01	1.00264597E-01	1.71533217E+00	6.28318530E+00	-5.0000000E-01
13	6.55787447E-01	1.00264597E-01	1.71533217E+00	6.28318530E+00	-5.0000000E-01
14	6.55787447E-01	1.00264597E-01	1.71533217E+00	6.28318530E+00	-5.0000000E-01
15	6.55787447E-01	1.00264597E-01	1.71533217E+00	6.28318530E+00	-5.0000000E-01
16	6.55787447E-01	1.00264597E-01	1.71533217E+00	6.28318530E+00	-5.0000000E-01
17	6.55787447E-01	1.00264597E-01	1.71533217E+00	6.28318530E+00	-5.0000000E-01
18	6.55787447E-01	1.00264597E-01	1.71533217E+00	6.28318530E+00	-5.0000000E-01
19	6.55787447E-01	1.00264597E-01	1.71533217E+00	6.28318530E+00	-5.0000000E-01
20	6.55787447E-01	1.00264597E-01	1.71533217E+00	6.28318530E+00	-5.0000000E-01
21	6.55787447E-01	1.00264597E-01	1.71533217E+00	6.28318530E+00	-5.0000000E-01
22	6.55787447E-01	1.00264597E-01	1.71533217E+00	6.28318530E+00	-5.0000000E-01
23	6.55787447E-01	1.00264597E-01	1.71533217E+00	6.28318530E+00	-5.0000000E-01
24	6.55787447E-01	1.00264597E-01	1.71533217E+00	6.28318530E+00	-5.0000000E-01
25	6.55787447E-01	1.00264597E-01	1.71533217E+00	6.28318530E+00	-5.0000000E-01
26	6.55787447E-01	1.00264597E-01	1.71533217E+00	6.28318530E+00	-5.0000000E-01
27	6.55787447E-01	1.00264597E-01	1.71533217E+00	6.28318530E+00	-5.0000000E-01
28	6.55787447E-01	1.00264597E-01	1.71533217E+00	6.28318530E+00	-5.0000000E-01
29	6.55787447E-01	1.00264597E-01	1.71533217E+00	6.28318530E+00	-5.0000000E-01
30	6.55787447E-01	1.00264597E-01	1.71533217E+00	6.28318530E+00	-5.0000000E-01

ELEMENTS OF MATRIX AA (STIFF=1, ONE LAMINA PER MATRIX COLUMN)

3.20000000E-02
0.
0.
0.
3.14159200E-02
0.
0.
0.

REAL PART	OMEGA	IMAGINARY PART	LAMBDA	REAL PART	DETERMINANT	NO. ITERATIONS
3.05446293E+00		2.16055571E-01	4.12729159E-01	-5.71294871E-06	-1.18748524E-07	6
3.10807616E+00		-3.65855970E-01	5.12729159E-01	-1.99519585E-05	6.76551012E-06	6
					OMEGA= 3.0744	

FLUTTER INSTABILITY ENCOUNTERED AT LAMBDA= .4986

APPENDIX F

POSITION	DEFLECTION		DEFORMATION SHAPE		TWIST	PHASE
	MAGNITUDE	PHASE	MAGNITUDE	PHASE		
1	0.	0.	0.	0.	0.	0.
2	1.12587368E-03	0.	7.23891316E-01	0.	2.20506329E+00	2.20506329E+00
3	1.00000000E+00	0.	1.44642340E+00	0.	2.20541822E+00	2.20541822E+00
4	4.00712248E+00	-8.32679840E-04	2.16559371E+00	0.	2.20569602E+00	2.20569602E+00
5	1.00244240E+01	-1.13901705E-03	2.87811166E+00	0.	2.20542262E+00	2.20542262E+00
6	2.00560790E+01	-1.30353103E-03	3.57876319E+00	0.	2.20392345E+00	2.20392345E+00
7	3.51065541E+01	-1.40983952E-03	4.25981018E+00	0.	2.20030209E+00	2.20030209E+00
8	5.61809379E+01	-1.48903095E-03	4.91047790E+00	0.	2.19339650E+00	2.19339650E+00
9	8.42854418E+01	-1.55667022E-03	5.51662915E+00	0.	2.18169744E+00	2.18169744E+00
10	1.20428107E+02	-1.62246299E-03	6.06080234E+00	0.	2.16320554E+00	2.16320554E+00
11	1.65619754E+02	-1.69361105E-03	6.52293924E+00	0.	2.13518932E+00	2.13518932E+00
12	2.20875205E+02	-1.77620375E-03	6.88242618E+00	0.	2.09378610E+00	2.09378610E+00
13	2.87214817E+02	-1.87587003E-03	7.12268596E+00	0.	2.03336848E+00	2.03336848E+00
14	3.65666369E+02	-1.99811178E-03	7.24080356E+00	0.	1.94563852E+00	1.94563852E+00
15	4.57267327E+02	-2.14848532E-03	7.26688309E+00	0.	1.81876238E+00	1.81876238E+00
16	5.63067526E+02	-2.33270390E-03	7.29977234E+00	0.	1.63834197E+00	1.63834197E+00
17	6.84132321E+02	-2.55669645E-03	7.55722681E+00	0.	1.39560621E+00	1.39560621E+00
18	8.21546223E+02	-2.82663938E-03	8.39337593E+00	0.	1.10695380E+00	1.10695380E+00
19	9.76417086E+02	-3.14897526E-03	1.01941772E+01	0.	8.21422980E-01	8.21422980E-01
20	1.14988086E+03	-3.53041090E-03	1.32178990E+01	0.	5.84710337E-01	5.84710337E-01
21	1.34310696E+03	-3.97791886E-03	1.75894310E+01	0.	4.08435350E-01	4.08435350E-01
22	1.55730434E+03	-4.49872308E-03	2.34010164E+01	0.	2.82139591E-01	2.82139591E-01
23	1.79372821E+03	-5.1002811E-03	3.07725016E+01	0.	1.91666851E-01	1.91666851E-01
24	2.05368760E+03	-5.79026647E-03	3.98630399E+01	0.	1.25869567E-01	1.25869567E-01
25	2.33855365E+03	-6.57653088E-03	5.08673132E+01	0.	7.70944629E-02	7.70944629E-02
26	2.64976885E+03	-7.46708165E-03	6.40106672E+01	0.	4.02563302E-02	4.02563302E-02
27	2.98885715E+03	-8.47003925E-03	7.95459724E+01	0.	1.19630122E-02	1.19630122E-02
28	3.35743507E+03	-9.59359623E-03	9.77520375E+01	0.	-1.00872674E-02	-1.00872674E-02
29	3.75722391E+03	-1.08459705E-02	1.18933049E+02	0.	-2.74896890E-02	-2.74896890E-02
30	4.19006303E+03	-1.22353542E-02	1.43418656E+02	0.	-4.13736674E-02	-4.13736674E-02

FLUTTER SPEED= 1.37772783E+03

APPENDIX F

NODAL PT.	EI	GJ	EM	CL	AC
1	6.54331719E-01	1.03172887E-01	1.71533217E+00	6.28318530E+00	-5.00000000E-01
2	6.54331719E-01	1.03172887E-01	1.71533217E+00	6.28318530E+00	-5.00000000E-01
3	6.54331719E-01	1.03172887E-01	1.71533217E+00	6.28318530E+00	-5.00000000E-01
4	6.54331719E-01	1.03172887E-01	1.71533217E+00	6.28318530E+00	-5.00000000E-01
5	6.54331719E-01	1.03172887E-01	1.71533217E+00	6.28318530E+00	-5.00000000E-01
6	6.54331719E-01	1.03172887E-01	1.71533217E+00	6.28318530E+00	-5.00000000E-01
7	6.54331719E-01	1.03172887E-01	1.71533217E+00	6.28318530E+00	-5.00000000E-01
8	6.54331719E-01	1.03172887E-01	1.71533217E+00	6.28318530E+00	-5.00000000E-01
9	6.54331719E-01	1.03172887E-01	1.71533217E+00	6.28318530E+00	-5.00000000E-01
10	6.54331719E-01	1.03172887E-01	1.71533217E+00	6.28318530E+00	-5.00000000E-01
11	6.54331719E-01	1.03172887E-01	1.71533217E+00	6.28318530E+00	-5.00000000E-01
12	6.54331719E-01	1.03172887E-01	1.71533217E+00	6.28318530E+00	-5.00000000E-01
13	6.54331719E-01	1.03172887E-01	1.71533217E+00	6.28318530E+00	-5.00000000E-01
14	6.54331719E-01	1.03172887E-01	1.71533217E+00	6.28318530E+00	-5.00000000E-01
15	6.54331719E-01	1.03172887E-01	1.71533217E+00	6.28318530E+00	-5.00000000E-01
16	6.54331719E-01	1.03172887E-01	1.71533217E+00	6.28318530E+00	-5.00000000E-01
17	6.54331719E-01	1.03172887E-01	1.71533217E+00	6.28318530E+00	-5.00000000E-01
18	6.54331719E-01	1.03172887E-01	1.71533217E+00	6.28318530E+00	-5.00000000E-01
19	6.54331719E-01	1.03172887E-01	1.71533217E+00	6.28318530E+00	-5.00000000E-01
20	6.54331719E-01	1.03172887E-01	1.71533217E+00	6.28318530E+00	-5.00000000E-01
21	6.54331719E-01	1.03172887E-01	1.71533217E+00	6.28318530E+00	-5.00000000E-01
22	6.54331719E-01	1.03172887E-01	1.71533217E+00	6.28318530E+00	-5.00000000E-01
23	6.54331719E-01	1.03172887E-01	1.71533217E+00	6.28318530E+00	-5.00000000E-01
24	6.54331719E-01	1.03172887E-01	1.71533217E+00	6.28318530E+00	-5.00000000E-01
25	6.54331719E-01	1.03172887E-01	1.71533217E+00	6.28318530E+00	-5.00000000E-01
26	6.54331719E-01	1.03172887E-01	1.71533217E+00	6.28318530E+00	-5.00000000E-01
27	6.54331719E-01	1.03172887E-01	1.71533217E+00	6.28318530E+00	-5.00000000E-01
28	6.54331719E-01	1.03172887E-01	1.71533217E+00	6.28318530E+00	-5.00000000E-01
29	6.54331719E-01	1.03172887E-01	1.71533217E+00	6.28318530E+00	-5.00000000E-01
30	6.54331719E-01	1.03172887E-01	1.71533217E+00	6.28318530E+00	-5.00000000E-01

ELEMENTS OF MATRIX AA (ISTIFF=1, ONE LAMINA PER MATRIX COLUMN)

3.20000000E-02
 0.
 0.
 0.
 4.71238800E-02
 0.
 0.
 0.

ISVM= 1

ESTIMATES OF NAT. FREQ. 2.12031250E+00 5.15781250E+00
 1.20390625E+01 1.67640625E+01 2.35890625E+01

APPENDIX F

REAL PART	OMEGA	IMAGINARY PART	LAMBDA	REAL PART	DETERMINANT	IMAGINARY PART	NO. ITERATIONS
2.11830225E+00	0.	0.	0.	-8.02616956E-04	0.	0.	3
2.21042340E+00	1.05771132E-01	1.05771132E-01	1.00000000E-01	2.12260137E-07	6.10742688E-08	6.10742688E-08	3
2.32508544E+00	1.66802733E-01	1.66802733E-01	2.00000000E-01	-5.09832508E-05	-2.16647754E-05	-2.16647754E-05	2
2.49598420E+00	2.25288291E-01	2.25288291E-01	3.00000000E-01	-2.71360615E-05	-3.52708354E-06	-3.52708354E-06	2
2.83072357E+00	2.76484197E-01	2.76484197E-01	4.00000000E-01	-1.54419273E-05	-1.37728104E-06	-1.37728104E-06	3
3.15392364E+00	-2.47869126E-01	-2.47869126E-01	5.00000000E-01	2.56337201E-05	-8.48617450E-06	-8.48617450E-06	8

FLUTTER INSTABILITY ENCOUNTERED AT LAMBDA= .45273 OMEGA= 2.4960

REAL PART	OMEGA	IMAGINARY PART	LAMBDA	REAL PART	DETERMINANT	IMAGINARY PART	NO. ITERATIONS
5.15418112E+00	0.	0.	0.	1.31935425E-03	0.	0.	3
4.92478584E+00	1.38681941E-01	1.38681941E-01	1.00000000E-01	1.70314819E-04	-3.18737088E-05	-3.18737088E-05	3
4.63414959E+00	2.30474623E-01	2.30474623E-01	2.00000000E-01	-3.55180383E-06	2.20688905E-07	2.20688905E-07	3
4.26569110E+00	3.14372531E-01	3.14372531E-01	3.00000000E-01	3.94923049E-04	5.97730522E-05	5.97730522E-05	2
3.71605246E+00	4.03958459E-01	4.03958459E-01	4.00000000E-01	1.59341131E-04	5.61588870E-06	5.61588870E-06	3
3.16263785E+00	1.07276972E+00	1.07276972E+00	5.00000000E-01	-2.83447161E-05	7.35810670E-05	7.35810670E-05	5

LAMBDA EXCEEDS .55273

REAL PART	OMEGA	IMAGINARY PART	LAMBDA	REAL PART	DETERMINANT	IMAGINARY PART	NO. ITERATIONS
1.20364305E+01	0.	0.	0.	-4.60797206E-03	0.	0.	3
1.20598625E+01	1.45411824E-01	1.45411824E-01	1.00000000E-01	1.89853660E-04	-1.15669610E-04	-1.15669610E-04	2
1.20849139E+01	2.07661550E-01	2.07661550E-01	2.00000000E-01	2.60396914E-04	-1.17631230E-04	-1.17631230E-04	2
1.21116612E+01	2.56932373E-01	2.56932373E-01	3.00000000E-01	2.16981226E-05	-8.48952857E-06	-8.48952857E-06	2
1.21401890E+01	2.99848579E-01	2.99848579E-01	4.00000000E-01	8.08727647E-06	-4.54610298E-06	-4.54610298E-06	2
1.21706093E+01	3.38991463E-01	3.38991463E-01	5.00000000E-01	3.19985469E-06	-3.24824533E-06	-3.24824533E-06	2

LAMBDA EXCEEDS .55273

REAL PART	OMEGA	IMAGINARY PART	LAMBDA	REAL PART	DETERMINANT	IMAGINARY PART	NO. ITERATIONS
1.67590737E+01	0.	0.	0.	9.09599843E-03	0.	0.	3
1.67018505E+01	6.03787137E-02	6.03787137E-02	1.00000000E-01	6.6428552E-05	5.53793950E-07	5.53793950E-07	3
1.66418341E+01	8.92442424E-02	8.92442424E-02	2.00000000E-01	-6.30493309E-04	2.47365848E-05	2.47365848E-05	2
1.65789922E+01	1.13565154E-01	1.13565154E-01	3.00000000E-01	-3.14759388E-05	3.60553116E-06	3.60553116E-06	2
1.65132928E+01	1.35545601E-01	1.35545601E-01	4.00000000E-01	8.54378215E-06	3.09967068E-06	3.09967068E-06	2
1.64447173E+01	1.55922350E-01	1.55922350E-01	5.00000000E-01	2.15558926E-05	3.08548951E-06	3.08548951E-06	2

LAMBDA EXCEEDS .55273

APPENDIX F

OMEGA		LAMBDA		DETERMINANT		NO. ITERATIONS
REAL PART	IMAGINARY PART	REAL PART	IMAGINARY PART	REAL PART	IMAGINARY PART	
2.35520690E+01	0.	0.	0.	-3.21318582E-02	0.	3
2.35330514E+01	1.49697504E-01	1.00000000E-01	0.	-8.47850534E-06	-3.87657067E-07	3
2.35138509E+01	2.13533373E-01	2.00000000E-01	0.	7.00165634E-03	-3.22519199E-04	2
2.34946189E+01	2.63712399E-01	3.00000000E-01	0.	6.80799927E-04	-1.53514123E-06	2
2.34752333E+01	3.06981795E-01	4.00000000E-01	0.	3.17402120E-04	4.53353664E-07	2
2.34557337E+01	3.45921935E-01	5.00000000E-01	0.	1.93287406E-04	1.17379235E-06	2

LAMBDA EXCEEDS .55273

MINIMUM FLUTTER SPEED FOR PRELIMINARY DESIGN OCCURS AT LAMBDA= 4.52728606E-01 AND OMEGA= 2.49598298E+00 ON BRANCH NO. 1

DEFORMATION SHAPE

POSITION	DEFLECTION		TWIST		PHASE
	MAGNITUDE	PHASE	MAGNITUDE	PHASE	
1	0.	0.	0.	0.	0.
2	2.86953139E-01	-1.61677387E-03	8.08100966E+00	3.13557204E+00	3.13557204E+00
3	1.00000000E+00	0.	1.5636039E+01	3.13544860E+00	3.13544860E+00
4	1.99510270E+00	0.	1.8712248E+01	3.13518100E+00	3.13518100E+00
5	3.13641097E+00	3.06654004E-03	2.64980769E+01	3.13470459E+00	3.13470459E+00
6	4.30079400E+00	4.73381602E-02	2.90525104E+01	3.13391864E+00	3.13391864E+00
7	5.38201099E+00	6.49133322E-03	2.92915196E+01	3.13266464E+00	3.13266464E+00
8	6.29411263E+00	8.30974734E-03	2.71436638E+01	3.13053655E+00	3.13053655E+00
9	6.97375907E+00	1.01365750E-02	2.27186143E+01	3.12676409E+00	3.12676409E+00
10	7.38124988E+00	1.18863954E-02	1.63026782E+01	3.11880727E+00	3.11880727E+00
11	7.50017971E+00	1.34226669E-02	8.34206221E+00	3.09338065E+00	3.09338065E+00
12	7.33752505E+00	1.45260133E-02	7.46046953E-01	6.0798417E-01	6.0798417E-01
13	6.91189823E+00	1.48375658E-02	9.89084946E+00	4.45620375E-02	4.45620375E-02
14	6.26743371E+00	1.37523724E-02	1.87877358E+01	2.35203426E-02	2.35203426E-02
15	5.45158744E+00	1.02037679E-02	2.66446666E+01	1.59957370E-02	1.59957370E-02
16	4.51927297E+00	2.18235538E-03	3.28506686E+01	1.18794419E-02	1.18794419E-02
17	3.52657412E+00	-1.44909146E-02	3.69100092E+01	8.97738715E-03	8.97738715E-03
18	2.52715668E+00	-4.99570916E-02	3.84793964E+01	6.44356196E-03	6.44356196E-03
19	1.57182319E+00	-1.36122047E-01	3.73951898E+01	3.74005588E-03	3.74005588E-03
20	7.29561029E-01	-4.37876053E-01	3.36874536E+01	2.55546341E-04	2.55546341E-04
21	4.34559286E-01	-1.90480629E+00	2.75796366E+01	-5.16765034E-03	-5.16765034E-03
22	9.84926010E-01	-2.59414001E+00	1.9474117E+01	-1.58420259E-02	-1.58420259E-02
23	1.55949727E+00	-2.73870981E+00	9.92743932E+00	-4.86443637E-02	-4.86443637E-02
24	2.05646290E+00	-2.79274541E+00	7.84265621E-01	-2.14756210E+00	-2.14756210E+00
25	2.47816297E+00	-2.81967562E+00	1.08670517E+01	-3.06569608E+00	-3.06569608E+00
26	2.84030754E+00	-2.83656351E+00	2.06029305E+01	-3.09430254E+00	-3.09430254E+00
27	3.16158938E+00	-2.84973584E+00	2.89868517E+01	-3.10367482E+00	-3.10367482E+00
28	3.45943108E+00	-2.86155741E+00	3.54317489E+01	-3.10793617E+00	-3.10793617E+00
29	3.74708684E+00	-2.87230262E+00	3.94830287E+01	-3.10994470E+00	-3.10994470E+00
30	4.03158899E+00	-2.88088780E+00	4.08619675E+01	-3.11055694E+00	-3.11055694E+00

FLUTTER SPEED= 1.38211696E+03

APPENDIX F

POSITION	DEFLECTION		DEFORMATION SHAPE		TWIST	PHASE
	MAGNITUDE	PHASE	MAGNITUDE	PHASE		
1	0.	0.	0.	0.	0.	0.
2	1.13807704E-03	2.71966866E+00	7.15676478E-01	2.27366737E+00	2.27366737E+00	2.27366737E+00
3	1.00000000E+00	0.	1.43001848E+00	2.27400939E+00	2.27400939E+00	2.27400939E+00
4	4.00725473E+00	-8.10475452E-04	2.14103574E+00	2.27428623E+00	2.27428623E+00	2.27428623E+00
5	1.00248734E+01	-1.10838034E-03	2.84542510E+00	2.27405486E+00	2.27405486E+00	2.27405486E+00
6	2.00571021E+01	-1.26818525E-03	3.53792156E+00	2.27268487E+00	2.27268487E+00	2.27268487E+00
7	3.51084860E+01	-1.37137455E-03	4.21067976E+00	2.26933810E+00	2.26933810E+00	2.26933810E+00
8	5.61842121E+01	-1.44830028E-03	4.85273191E+00	2.26292669E+00	2.26292669E+00	2.26292669E+00
9	8.42906631E+01	-1.51421466E-03	5.44960761E+00	2.25203447E+00	2.25203447E+00	2.25203447E+00
10	1.20435997E+02	-1.57868001E-03	5.98327004E+00	2.23477779E+00	2.23477779E+00	2.23477779E+00
11	1.65631451E+02	-1.64883562E-03	6.43265462E+00	2.20856668E+00	2.20856668E+00	2.20856668E+00
12	2.20892304E+02	-1.73075241E-03	6.77536586E+00	2.16970098E+00	2.16970098E+00	2.16970098E+00
13	2.87239637E+02	-1.83006747E-03	6.99166080E+00	2.11270185E+00	2.11270185E+00	2.11270185E+00
14	3.65702269E+02	-1.95230844E-03	7.07307376E+00	2.02927076E+00	2.02927076E+00	2.02927076E+00
15	4.57319120E+02	-2.10306968E-03	7.04047445E+00	1.90700329E+00	1.90700329E+00	1.90700329E+00
16	5.63142023E+02	-2.28811166E-03	6.97963637E+00	1.72933836E+00	1.72933836E+00	1.72933836E+00
17	6.84239005E+02	-2.51341741E-03	7.09774685E+00	1.48261049E+00	1.48261049E+00	1.48261049E+00
18	8.21698095E+02	-2.78522326E-03	7.58827723E+00	1.17872001E+00	1.17872001E+00	1.17872001E+00
19	9.76631695E+02	-3.11003311E-03	9.37873496E+00	8.71625157E-01	8.71625157E-01	8.71625157E-01
20	1.15018155E+03	-3.49462117E-03	1.22330617E+01	6.17516341E-01	6.17516341E-01	6.17516341E-01
21	1.34352437E+03	-3.94602617E-03	1.64324241E+01	4.31307035E-01	4.31307035E-01	4.31307035E-01
22	1.55787816E+03	-4.47153855E-03	2.20494565E+01	3.00309217E-01	3.00309217E-01	3.00309217E-01
23	1.79450929E+03	-5.07868166E-03	2.91900377E+01	2.07894872E-01	2.07894872E-01	2.07894872E-01
24	2.05474032E+03	-5.77518746E-03	3.80038423E+01	1.41466897E-01	1.41466897E-01	1.41466897E-01
25	2.33995880E+03	-6.56866702E-03	4.86779845E+01	9.26515042E-02	9.26515042E-02	9.26515042E-02
26	2.65162682E+03	-7.46807594E-03	6.14307202E+01	5.60217187E-02	5.60217187E-02	5.60217187E-02
27	2.99129166E+03	-8.48067485E-03	7.65076828E+01	2.80253901E-02	2.80253901E-02	2.80253901E-02
28	3.36059744E+03	-9.61498510E-03	9.41800425E+01	6.28687593E-03	6.28687593E-03	6.28687593E-03
29	3.76125784E+03	-1.08792397E-02	1.14743850E+02	-1.08218133E-02	-1.08218133E-02	-1.08218133E-02
30	4.19527006E+03	-1.22816257E-02	1.38520090E+02	-2.44432084E-02	-2.44432084E-02	-2.44432084E-02

FLUTTER SPEED= 1.44456187E+03

APPENDIX F

NODAL PT.	EI	GJ	EM	CL	AC
1	6.49693476E-01	1.12415164E-01	1.71533217E+00	6.28318530E+00	-5.00000000E-01
2	6.49693476E-01	1.12415164E-01	1.71533217E+00	6.28318530E+00	-5.00000000E-01
3	6.49693476E-01	1.12415164E-01	1.71533217E+00	6.28318530E+00	-5.00000000E-01
4	6.49693476E-01	1.12415164E-01	1.71533217E+00	6.28318530E+00	-5.00000000E-01
5	6.49693476E-01	1.12415164E-01	1.71533217E+00	6.28318530E+00	-5.00000000E-01
6	6.49693476E-01	1.12415164E-01	1.71533217E+00	6.28318530E+00	-5.00000000E-01
7	6.49693476E-01	1.12415164E-01	1.71533217E+00	6.28318530E+00	-5.00000000E-01
8	6.49693476E-01	1.12415164E-01	1.71533217E+00	6.28318530E+00	-5.00000000E-01
9	6.49693476E-01	1.12415164E-01	1.71533217E+00	6.28318530E+00	-5.00000000E-01
10	6.49693476E-01	1.12415164E-01	1.71533217E+00	6.28318530E+00	-5.00000000E-01
11	6.49693476E-01	1.12415164E-01	1.71533217E+00	6.28318530E+00	-5.00000000E-01
12	6.49693476E-01	1.12415164E-01	1.71533217E+00	6.28318530E+00	-5.00000000E-01
13	6.49693476E-01	1.12415164E-01	1.71533217E+00	6.28318530E+00	-5.00000000E-01
14	6.49693476E-01	1.12415164E-01	1.71533217E+00	6.28318530E+00	-5.00000000E-01
15	6.49693476E-01	1.12415164E-01	1.71533217E+00	6.28318530E+00	-5.00000000E-01
16	6.49693476E-01	1.12415164E-01	1.71533217E+00	6.28318530E+00	-5.00000000E-01
17	6.49693476E-01	1.12415164E-01	1.71533217E+00	6.28318530E+00	-5.00000000E-01
18	6.49693476E-01	1.12415164E-01	1.71533217E+00	6.28318530E+00	-5.00000000E-01
19	6.49693476E-01	1.12415164E-01	1.71533217E+00	6.28318530E+00	-5.00000000E-01
20	6.49693476E-01	1.12415164E-01	1.71533217E+00	6.28318530E+00	-5.00000000E-01
21	6.49693476E-01	1.12415164E-01	1.71533217E+00	6.28318530E+00	-5.00000000E-01
22	6.49693476E-01	1.12415164E-01	1.71533217E+00	6.28318530E+00	-5.00000000E-01
23	6.49693476E-01	1.12415164E-01	1.71533217E+00	6.28318530E+00	-5.00000000E-01
24	6.49693476E-01	1.12415164E-01	1.71533217E+00	6.28318530E+00	-5.00000000E-01
25	6.49693476E-01	1.12415164E-01	1.71533217E+00	6.28318530E+00	-5.00000000E-01
26	6.49693476E-01	1.12415164E-01	1.71533217E+00	6.28318530E+00	-5.00000000E-01
27	6.49693476E-01	1.12415164E-01	1.71533217E+00	6.28318530E+00	-5.00000000E-01
28	6.49693476E-01	1.12415164E-01	1.71533217E+00	6.28318530E+00	-5.00000000E-01
29	6.49693476E-01	1.12415164E-01	1.71533217E+00	6.28318530E+00	-5.00000000E-01
30	6.49693476E-01	1.12415164E-01	1.71533217E+00	6.28318530E+00	-5.00000000E-01

ELEMENTS OF MATRIX AA (ISTIFF=1, ONE LAMINA PER MATRIX COLUMN)

3.20000000E-02
 0.
 0.
 0.
 7.85398000E-02
 0.
 0.
 0.

REAL PART	OMEGA	IMAGINARY PART	LAMBDA	REAL PART	DETERMINANT	NO. ITERATIONS
3.21841433E+00	1.57464195E-01	1.57464195E-01	4.94561883E-01	-2.23212523E-07	1.88902855E-07	4
3.19922212E+00	-3.72920481E-01	-3.72920481E-01	5.94561883E-01	-2.40781654E-05	8.56313881E-06	5

FLUTTER INSTABILITY ENCOUNTERED AT LAMBDA= .52425 OMEGA= 3.2127

APPENDIX F

POSITION	DEFLECTION		DEFORMATION SHAPE		MAGNITUDE	TWIST	PHASE
	MAGNITUDE	PHASE	MAGNITUDE	PHASE			
1	0.	0.	0.	0.	0.	0.	0.
2	1.16399354E-03	2.71803841E+00	7.00438369E-01		7.00438369E-01	2.25086217E+00	
3	1.00000000E+00	0.	0.		1.39958971E+00	2.25120832E+00	
4	4.00741444E+00	-8.31701534E-04	-8.31701534E-04		2.09553476E+00	2.25148957E+00	
5	1.00254208E+01	-1.13724210E-03	-1.13724210E-03		2.78508840E+00	2.25125923E+00	
6	2.00583580E+01	-1.30107903E-03	-1.30107903E-03		3.46317410E+00	2.24988178E+00	
7	3.51108702E+01	-1.40693213E-03	-1.40693213E-03		4.1222829E+00	2.24651274E+00	
8	5.61882568E+01	-1.48605443E-03	-1.48605443E-03		4.75168064E+00	2.24005700E+00	
9	8.42970057E+01	-1.55421832E-03	-1.55421832E-03		5.33759476E+00	2.22909101E+00	
10	1.20445546E+02	-1.62137423E-03	-1.62137423E-03		5.86262207E+00	2.21172538E+00	
11	1.65645261E+02	-1.69500364E-03	-1.69500364E-03		6.30655094E+00	2.18536982E+00	
12	2.20911787E+02	-1.78150942E-03	-1.78150942E-03		6.64799521E+00	2.14633855E+00	
13	2.87266660E+02	-1.88686703E-03	-1.88686703E-03		6.86831933E+00	2.08920316E+00	
14	3.65739316E+02	-2.01695712E-03	-2.01695712E-03		6.96006519E+00	2.00580171E+00	
15	4.57369515E+02	-2.17774615E-03	-2.17774615E-03		6.94441723E+00	1.88405942E+00	
16	5.63210207E+02	-2.37538789E-03	-2.37538789E-03		6.90514268E+00	1.70809595E+00	
17	6.84330892E+02	-2.61462808E-03	-2.61462808E-03		7.04159140E+00	1.46515897E+00	
18	8.21821510E+02	-2.90709222E-03	-2.90709222E-03		7.70064858E+00	1.16694864E+00	
19	9.7696907E+02	-3.25480657E-03	-3.25480657E-03		9.28242082E+00	8.64880559E-01	
20	1.15040192E+03	-3.66665772E-03	-3.66665772E-03		1.20566170E+01	6.12893474E-01	
21	1.34381714E+03	-4.15019154E-03	-4.15019154E-03		1.61390065E+01	4.26797313E-01	
22	1.55826537E+03	-4.71321640E-03	-4.71321640E-03		2.16048639E+01	2.95077428E-01	
23	1.79501883E+03	-5.36378920E-03	-5.36378920E-03		2.85588483E+01	2.0172364E-01	
24	2.0540729E+03	-6.11018848E-03	-6.11018848E-03		3.71471280E+01	1.34521669E-01	
25	2.34082690E+03	-6.96088194E-03	-6.96088194E-03		4.75521389E+01	8.50088793E-02	
26	2.65275014E+03	-7.92448853E-03	-7.92448853E-03		5.99867629E+01	4.78042369E-02	
27	2.99273664E+03	-9.00973516E-03	-9.00973516E-03		7.46907406E+01	1.93367944E-02	
28	3.36244514E+03	-1.02254082E-02	-1.02254082E-02		9.19288950E+01	-2.78936011E-03	
29	3.76364656E+03	-1.15802957E-02	-1.15802957E-02		1.11990496E+02	-2.02198242E-02	
30	4.19823833E+03	-1.30831492E-02	-1.30831492E-02		1.35189318E+02	-3.41113924E-02	

FLUTTER SPEED= 1.48728870E+03

APPENDIX F

NODAL PT.	EI	GJ	EM	CL	AC
1	6.46522378E-01	1.18712676E-01	1.71533217E+00	6.28318530E+00	-5.00000000E-01
2	6.46522378E-01	1.18712676E-01	1.71533217E+00	6.28318530E+00	-5.00000000E-01
3	6.46522378E-01	1.18712676E-01	1.71533217E+00	6.28318530E+00	-5.00000000E-01
4	6.46522378E-01	1.18712676E-01	1.71533217E+00	6.28318530E+00	-5.00000000E-01
5	6.46522378E-01	1.18712676E-01	1.71533217E+00	6.28318530E+00	-5.00000000E-01
6	6.46522378E-01	1.18712676E-01	1.71533217E+00	6.28318530E+00	-5.00000000E-01
7	6.46522378E-01	1.18712676E-01	1.71533217E+00	6.28318530E+00	-5.00000000E-01
8	6.46522378E-01	1.18712676E-01	1.71533217E+00	6.28318530E+00	-5.00000000E-01
9	6.46522378E-01	1.18712676E-01	1.71533217E+00	6.28318530E+00	-5.00000000E-01
10	6.46522378E-01	1.18712676E-01	1.71533217E+00	6.28318530E+00	-5.00000000E-01
11	6.46522378E-01	1.18712676E-01	1.71533217E+00	6.28318530E+00	-5.00000000E-01
12	6.46522378E-01	1.18712676E-01	1.71533217E+00	6.28318530E+00	-5.00000000E-01
13	6.46522378E-01	1.18712676E-01	1.71533217E+00	6.28318530E+00	-5.00000000E-01
14	6.46522378E-01	1.18712676E-01	1.71533217E+00	6.28318530E+00	-5.00000000E-01
15	6.46522378E-01	1.18712676E-01	1.71533217E+00	6.28318530E+00	-5.00000000E-01
16	6.46522378E-01	1.18712676E-01	1.71533217E+00	6.28318530E+00	-5.00000000E-01
17	6.46522378E-01	1.18712676E-01	1.71533217E+00	6.28318530E+00	-5.00000000E-01
18	6.46522378E-01	1.18712676E-01	1.71533217E+00	6.28318530E+00	-5.00000000E-01
19	6.46522378E-01	1.18712676E-01	1.71533217E+00	6.28318530E+00	-5.00000000E-01
20	6.46522378E-01	1.18712676E-01	1.71533217E+00	6.28318530E+00	-5.00000000E-01
21	6.46522378E-01	1.18712676E-01	1.71533217E+00	6.28318530E+00	-5.00000000E-01
22	6.46522378E-01	1.18712676E-01	1.71533217E+00	6.28318530E+00	-5.00000000E-01
23	6.46522378E-01	1.18712676E-01	1.71533217E+00	6.28318530E+00	-5.00000000E-01
24	6.46522378E-01	1.18712676E-01	1.71533217E+00	6.28318530E+00	-5.00000000E-01
25	6.46522378E-01	1.18712676E-01	1.71533217E+00	6.28318530E+00	-5.00000000E-01
26	6.46522378E-01	1.18712676E-01	1.71533217E+00	6.28318530E+00	-5.00000000E-01
27	6.46522378E-01	1.18712676E-01	1.71533217E+00	6.28318530E+00	-5.00000000E-01
28	6.46522378E-01	1.18712676E-01	1.71533217E+00	6.28318530E+00	-5.00000000E-01
29	6.46522378E-01	1.18712676E-01	1.71533217E+00	6.28318530E+00	-5.00000000E-01
30	6.46522378E-01	1.18712676E-01	1.71533217E+00	6.28318530E+00	-5.00000000E-01

ELEMENTS OF MATRIX AA (ISTIFF=1, ONE LAMINA PER MATRIX COLUMN)

3.20000000E-02
 0.
 0.
 0.
 9.42477600E-02
 0.
 0.
 0.

ISYM= 1

ESTIMATES OF NAT. FREQ. 2.11562500E+00 5.52812500E+00
 1.23156250E+01 1.75656250E+01 2.50656250E+01

APPENDIX F

REAL PART	OMEGA	IMAGINARY PART	LAMBDA	REAL PART	IMAGINARY PART	NO. ITERATIONS
2.11114662E+00	0.	1.04418361E-01	0.	-9.35170950E-04	0.	3
2.19212119E+00	1.04418361E-01	1.64113703E-01	1.00000000E-01	2.14174853E-05	1.36318605E-05	2
2.28486134E+00	1.64113703E-01	2.20809236E-01	2.00000000E-01	-2.72675121E-05	-1.12780192E-05	2
2.40958477E+00	2.20809236E-01	2.79973950E-01	3.00000000E-01	-1.73303813E-05	-1.53917545E-06	2
2.59644613E+00	2.79973950E-01	3.22953937E-01	4.00000000E-01	-2.27377588E-05	2.30400742E-06	2
2.97323333E+00	3.22953937E-01	-2.39945365E-01	5.00000000E-01	-2.65832554E-05	-3.37484343E-06	3
3.27189848E+00	-2.39945365E-01		6.00000000E-01	5.96482579E-06	-1.78603333E-06	8

FLUTTER INSTABILITY ENCOUNTERED AT LAMBDA= .55812 OMEGA= 2.5964

REAL PART	OMEGA	IMAGINARY PART	LAMBDA	REAL PART	IMAGINARY PART	NO. ITERATIONS
5.51324831E+00	0.	1.36917068E-01	0.	1.58870701E-03	0.	3
5.30604896E+00	1.36917068E-01	2.25027830E-01	1.00000000E-01	1.35717362E-04	-2.02372770E-05	3
5.05192051E+00	2.25027830E-01	3.04824028E-01	2.00000000E-01	-7.26837474E-06	-1.55756444E-07	3
4.74626684E+00	3.04824028E-01	3.79282906E-01	3.00000000E-01	2.46966370E-04	4.11729409E-05	2
4.36340478E+00	3.79282906E-01	4.61422830E-01	4.00000000E-01	4.14634842E-04	5.40037408E-05	2
3.77831957E+00	4.61422830E-01	1.17501814E+00	5.00000000E-01	2.06894655E-04	8.89463669E-06	3
3.25899663E+00	1.17501814E+00		6.00000000E-01	-2.41091814E-05	-1.61839335E-05	7

LAMBDA EXCEEDS .65812

REAL PART	OMEGA	IMAGINARY PART	LAMBDA	REAL PART	IMAGINARY PART	NO. ITERATIONS
1.23005106E+01	0.	1.32099619E-01	0.	-5.35807589E-03	0.	3
1.23251883E+01	1.32099619E-01	1.88489152E-01	1.00000000E-01	2.48021562E-04	-2.21083272E-04	2
1.23512467E+01	1.88489152E-01	2.32919047E-01	2.00000000E-01	4.49771315E-04	-8.27813521E-05	2
1.23787694E+01	2.32919047E-01	2.71380735E-01	3.00000000E-01	4.41123470E-05	-4.96714151E-06	2
1.24078316E+01	2.71380735E-01	3.06193136E-01	4.00000000E-01	2.02489729E-05	-2.53152091E-06	2
1.24385408E+01	3.06193136E-01	3.38555965E-01	5.00000000E-01	1.17397283E-05	-1.76568208E-06	2
1.24710070E+01	3.38555965E-01		6.00000000E-01	7.39555391E-06	-1.43109757E-06	2

LAMBDA EXCEEDS .65812

REAL PART	OMEGA	IMAGINARY PART	LAMBDA	REAL PART	IMAGINARY PART	NO. ITERATIONS
1.75107678E+01	0.	7.11770986E-02	0.	1.19427521E-02	0.	3
1.74540688E+01	7.11770986E-02	1.04607281E-01	1.00000000E-01	8.31677122E-05	1.25029085E-07	3
1.73948377E+01	1.04607281E-01	1.32612431E-01	2.00000000E-01	-1.02472379E-03	3.89035620E-05	2
1.73331655E+01	1.32612431E-01	1.57944316E-01	3.00000000E-01	-6.73012374E-05	4.13012260E-06	2
1.72689675E+01	1.57944316E-01	1.81574085E-01	4.00000000E-01	-3.59523533E-06	3.14043434E-06	2
1.72022346E+01	1.81574085E-01	2.03946149E-01	5.00000000E-01	1.77383396E-05	2.93690368E-06	2
1.71329176E+01	2.03946149E-01		6.00000000E-01	2.83944716E-05	3.02637878E-06	2

LAMBDA EXCEEDS .65812

OMEGA		LAMBDA		DETERMINANT		NO. ITERATIONS
REAL PART	IMAGINARY PART	REAL PART	IMAGINARY PART	REAL PART	IMAGINARY PART	
2.50524396E+01	0.	-4.32843755E-02	0.	0.	0.	3
2.50370218E+01	1.52664369E-01	2.99827701E-03	1.00000000E-01	2.60641652E-03	2.60641652E-03	2
2.50214918E+01	2.17406608E-01	8.36376486E-03	2.00000000E-01	-4.39028539E-04	-4.39028539E-04	2
2.50059575E+01	2.68076313E-01	3.00000000E-01	3.00000000E-01	-8.77334202E-06	-8.77334202E-06	2
2.49903248E+01	3.11598296E-01	4.00000000E-01	4.00000000E-01	3.82408670E-04	-2.91437200E-06	2
2.49746296E+01	3.50628139E-01	5.00000000E-01	5.00000000E-01	2.33900976E-04	-9.94990727E-07	2
2.49588783E+01	3.86515255E-01	6.00000000E-01	6.00000000E-01	1.60612100E-04	-3.66891231E-07	2

LAMBDA EXCEEDS .65812

MINIMUM FLUTTER SPEED FOR PRELIMINARY DESIGN OCCURS AT LAMBDA= 5.58117358E-01 AND OMEGA= 2.59644503E+00 ON BRANCH NO. 1

APPENDIX F

DEFORMATION SHAPE

POSITION	DEFLECTION		MAGNITUDE		TWIST	PHASE
	MAGNITUDE	PHASE	MAGNITUDE	PHASE		
1	0.	0.	0.	0.	0.	0.
2	2.88005348E-01	-1.95582207E-03	7.08915032E+00	3.12336265E+00	3.12336265E+00	3.12336265E+00
3	1.00000000E+00	0.	1.36593962E+01	3.12336265E+00	3.12336265E+00	3.12336265E+00
4	1.98782490E+00	0.	1.92078347E+01	3.12293572E+00	3.12293572E+00	3.12293572E+00
5	3.11180805E+00	3.76482292E-03	2.32906945E+01	3.12238270E+00	3.12238270E+00	3.12238270E+00
6	4.24558280E+00	5.85251961E-03	2.55618392E+01	3.12144629E+00	3.12144629E+00	3.12144629E+00
7	5.28056902E+00	8.09559088E-03	2.58036694E+01	3.11990267E+00	3.11990267E+00	3.11990267E+00
8	6.12966373E+00	1.0475617E-02	2.39480124E+01	3.11730911E+00	3.11730911E+00	3.11730911E+00
9	6.72978715E+00	1.29603803E-02	2.00853748E+01	3.11263048E+00	3.11263048E+00	3.11263048E+00
10	7.04304867E+00	1.54742551E-02	1.44619917E+01	3.10271878E+00	3.10271878E+00	3.10271878E+00
11	7.05642543E+00	1.78971320E-02	7.46686929E+00	3.07119790E+00	3.07119790E+00	3.07119790E+00
12	6.7799720E+00	2.00161214E-02	6.41909959E+01	8.30018873E-01	8.30018873E-01	8.30018873E-01
13	6.24373646E+00	2.14525602E-02	8.62861804E+00	4.75440728E-02	4.75440728E-02	4.75440728E-02
14	5.49354931E+00	2.15062382E-02	1.65027986E+01	2.03980687E-02	2.03980687E-02	2.03980687E-02
15	4.58617940E+00	1.87988628E-02	2.34780077E+01	1.08636967E-02	1.08636967E-02	1.08636967E-02
16	3.58414607E+00	1.03399468E-02	2.90096249E+01	5.74952845E-03	5.74952845E-03	5.74952845E-03
17	2.55088838E+00	-1.14594959E-02	3.26537382E+01	2.22842190E-03	2.22842190E-03	2.22842190E-03
18	1.54781969E+00	-7.19812088E-02	3.40997609E+01	-7.72464509E-04	-7.72464509E-04	-7.72464509E-04
19	6.46656174E-01	-3.25233110E-01	3.31951152E+01	-3.91434705E-03	-3.91434705E-03	-3.91434705E-03
20	3.72653498E-01	-2.15185215E+00	2.99585077E+01	-7.92106287E-03	-7.92106287E-03	-7.92106287E-03
21	9.78995190E-01	-2.69657122E+00	2.45805949E+01	-1.41324738E-02	-1.41324738E-02	-1.41324738E-02
22	1.51053150E+00	-2.78204181E+00	1.74122302E+01	-2.63396629E-02	-2.63396629E-02	-2.63396629E-02
23	1.90734471E+00	-2.80126693E+00	8.94439648E+00	-6.36265187E-02	-6.36265187E-02	-6.36265187E-02
24	2.17624557E+00	-2.79832816E+00	7.29420458E+01	-1.95976934E+00	-1.95976934E+00	-1.95976934E+00
25	2.33662480E+00	-2.78515938E+00	9.59091509E+00	-3.06082411E+00	-3.06082411E+00	-3.06082411E+00
26	2.41333044E+00	-2.76685753E+00	1.82889962E+01	-3.09446843E+00	-3.09446843E+00	-3.09446843E+00
27	2.43240335E+00	-2.74634888E+00	2.58033146E+01	-3.10537684E+00	-3.10537684E+00	-3.10537684E+00
28	2.41759315E+00	-2.72533664E+00	3.15928826E+01	-3.11029709E+00	-3.11029709E+00	-3.11029709E+00
29	2.38763358E+00	-2.70405207E+00	3.52425464E+01	-3.11259765E+00	-3.11259765E+00	-3.11259765E+00
30	2.35441885E+00	-2.68049771E+00	3.64896349E+01	-3.11329250E+00	-3.11329250E+00	-3.11329250E+00

FLUTTER SPEED= 1.53457667E+03

REFERENCES

1. Yates, E. Carson, Jr.: Flutter and Unsteady-Lift Theory. Performance and Dynamics of Aerospace Vehicles, NASA SP-258, 1971, pp. 289-374.
2. Yates, E. Carson, Jr.: Modified-Strip-Analysis Method for Predicting Wing Flutter at Subsonic to Hypersonic Speeds. J. Aircraft, vol. 3, no. 1, Jan.-Feb. 1966, pp. 25-29.
3. Yates, E. Carson, Jr.: Calculation of Flutter Characteristics for Finite-Span Swept or Unswept Wings at Subsonic and Supersonic Speeds by a Modified Strip Analysis. NACA RM L57L10, 1958.
4. Goland, Martin: The Flutter of a Uniform Cantilever Wing. J. Appl. Mech., vol. 12, no. 4, Dec. 1945, pp. A-197 - A-208.
5. Goland, Martin; and Luke, Y. L.: The Flutter of a Uniform Wing With Tip Weights. J. Appl. Mech., vol. 15, no. 1, Mar. 1948, pp. 13-20.
6. Barmby, J. G.; Cunningham, H. J.; and Garrick, I. E.: Study of Effects of Sweep on the Flutter of Cantilever Wings. NACA Rep. 1014, 1951. (Supersedes NACA TN 2121.)
7. Peterson, Leonard: SADSAM User's Manual. MSR-10, MacNeal-Schwendler Corp., Dec. 1970.
8. Ashton, J. E.; Halpin, J. C.; and Petit, P. H.: Primer on Composite Materials: Analysis. Technomic Pub. Co., Inc., c.1969, pp. 16-21.
9. Bisplinghoff, Raymond L.; and Ashley, Holt: Principles of Aeroelasticity. John Wiley & Sons, Inc., c.1962, pp. 392-393.
10. Cooper, Paul A.; and Stroud, W. Jefferson: Selective Reinforcement of Wing Structure for Flutter Prevention. J. Aircraft, vol. 9, no. 11, Nov. 1972, pp. 797-799.
11. Yates, E. Carson, Jr.: Subsonic and Supersonic Flutter Analysis of a Highly Tapered Swept-Wing Planform, Including Effects of Density Variation and Finite Wing Thickness and Comparison With Experiments. NASA TN D-4230, 1967. (Supersedes NASA TM X-764.)
12. Yates, E. Carson, Jr.: Flutter Prevention at Low Mass-Density Ratios With Application to the Finite-Span Noncavitating Hydrofoil. AIAA Paper No. 68-472, Apr.-May 1968.
13. Reissner, Eric; and Stein, Manuel: Torsion and Transverse Bending of Cantilever Plates. NACA TN 2369, 1951.

**TABLE I.- FLUTTER SPEED COMPARISONS FOR UNIFORM
CANTILEVER RECTANGULAR STRAIGHT WING
OF ASPECT RATIO 6.67**

Program or reference	Description	Flutter speed, km/hr	Percent difference with exact solution	Flutter frequency, Hz
4 and 5	Exact analysis	494	---	11.25
COMBOF	10 finite-difference stations	484.2	-2.0	11.20
COMBOF	15 finite-difference stations	483.4	-2.1	11.24
COMBOF	20 finite-difference stations	483.1	-2.2	11.26
COMBOF	25 finite-difference stations	483.1	-2.2	11.27
SADSAM, ref. 7	1 finite element	447.1	-9.5	----
SADSAM, ref. 7	10 finite elements	472.5	-4.4	----

**TABLE II.- FLUTTER SPEED COMPARISONS FOR THE SYMMETRIC
FLUTTER OF UNIFORM RECTANGULAR STRAIGHT WING
OF ASPECT RATIO 6.67 AND WITH ATTACHED
FUSELAGE AND TIP WEIGHTS**

Program or reference	Case (a)	Description	Flutter speed, km/hr	Flutter frequency, Hz	Branch
5	1	Exact analysis	1054	3.05	First torsion
COMBOF	1	31 finite-difference stations	1049	3.05	First torsion
SADSAM, ref. 7	1	10 finite elements	1049	3.01	First torsion
COMBOF	1	31 finite-difference stations	994	1.81	First bending
SADSAM	1	10 finite elements	990	1.81	First bending
COMBOF	1	31 finite-difference stations	943	16.48	Second bending
SADSAM	1	10 finite elements	961	16.2	Second bending
5	2	Exact analysis	826	3.05	First torsion
COMBOF	2	31 finite-difference stations	821	3.02	First torsion
SADSAM	2	10 finite elements	837	3.00	First torsion

^aCase 1: center of gravity of tip weights coincides with elastic axis

Case 2: center of gravity of tip weights located aft of elastic axis

TABLE III.- FLUTTER SPEED COMPARISONS FOR UNIFORM
CANTILEVER RECTANGULAR SWEEP WING
OF ASPECT RATIO 12.4

Sweep angle, deg	Flutter speed, km/hr			Percent difference with experiment
	Reference 6		COMBOF	
	Experimental	Analytical		
0	368	346	354	-3.8
30	378	368	370	-2.1
45	433	426	423	-2.3
60	563	568	541	-2.1

TABLE IV.- PROPERTIES OF BORON-EPOXY COMPOSITE, UNIFORM,
CANTILEVERED, RECTANGULAR STRAIGHT WING
OF ASPECT RATIO 6.67

Elastic moduli:

$$E_l = 276 \text{ GN/m}^2$$

$$E_t = 27.6 \text{ GN/m}^2$$

$$\nu_{lt} = 0.25$$

$$G_{lt} = 10.3 \text{ GN/m}^2$$

Wing properties:

$$a = -0.34$$

$$b = 1.0$$

$$x_\alpha = 0.2$$

$$r_\alpha^2 = 0.29$$

$$C_{l_\alpha} = 2\pi$$

$$a_c = -0.5$$

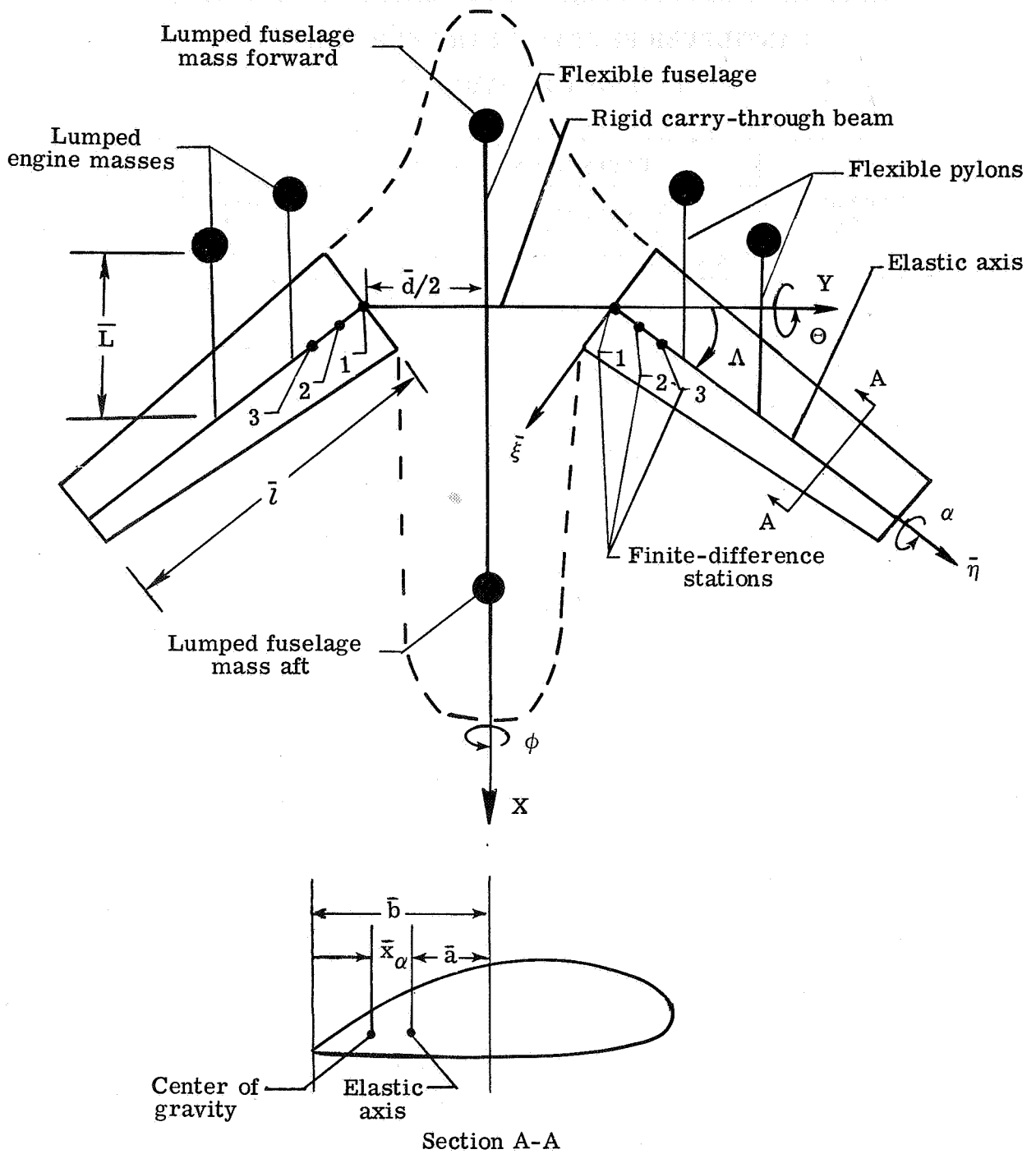


Figure 1.- Aircraft model.

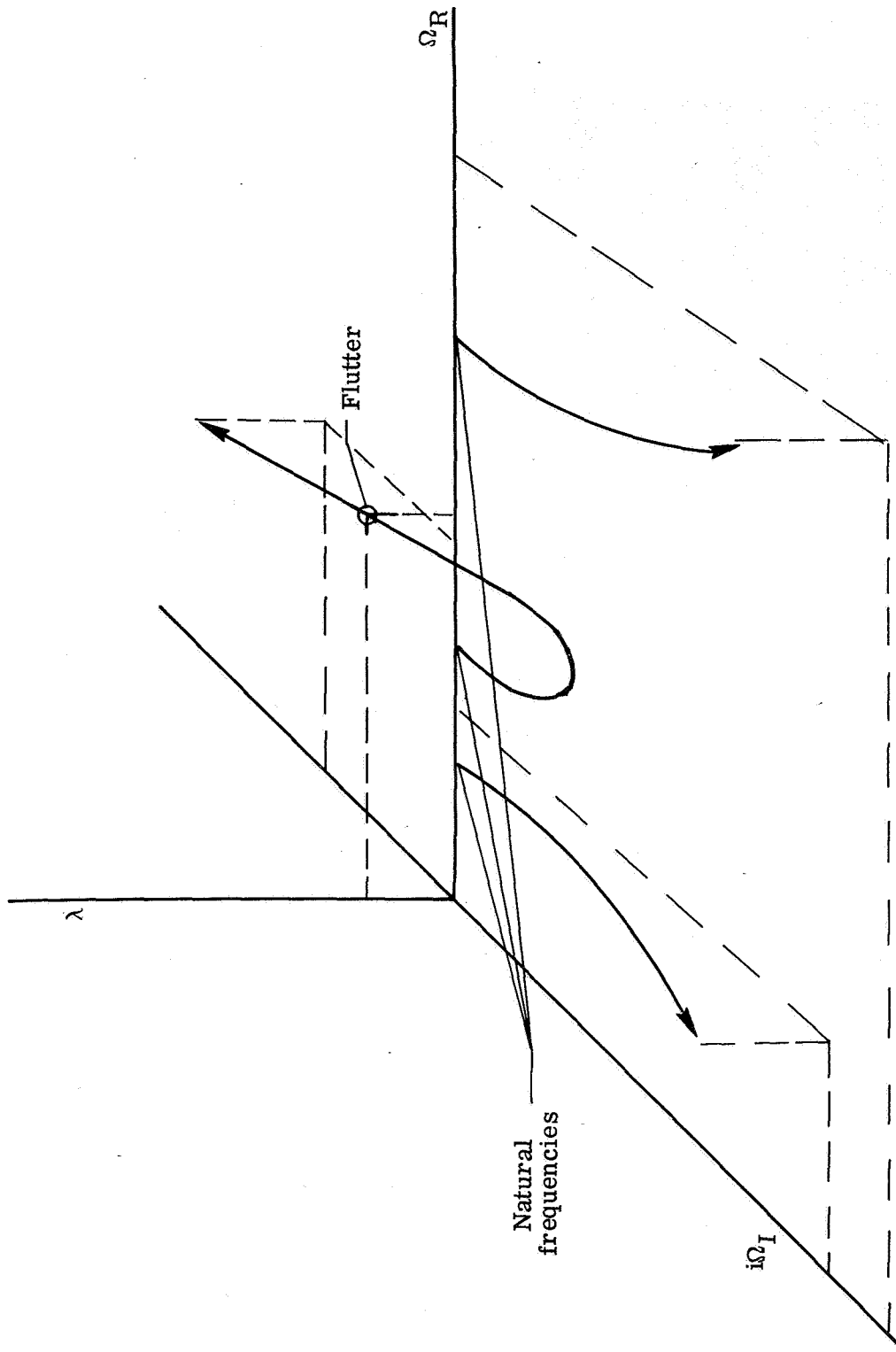


Figure 2.- Root locus branches. $\Omega = \Omega_R + i\Omega_I = \text{Frequency}$.

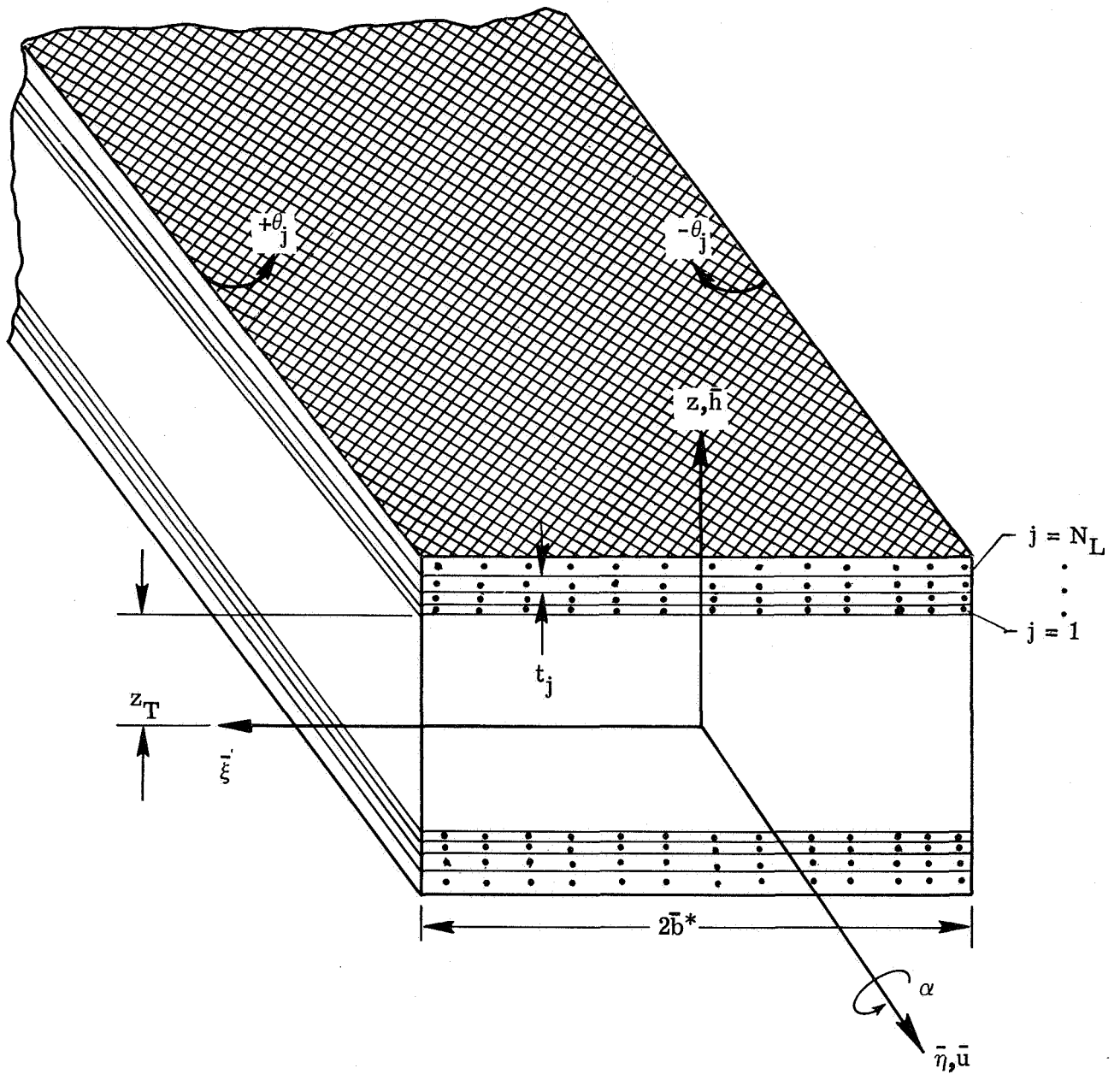


Figure 3.- Laminated, balanced ply, filamentary composite wing box.

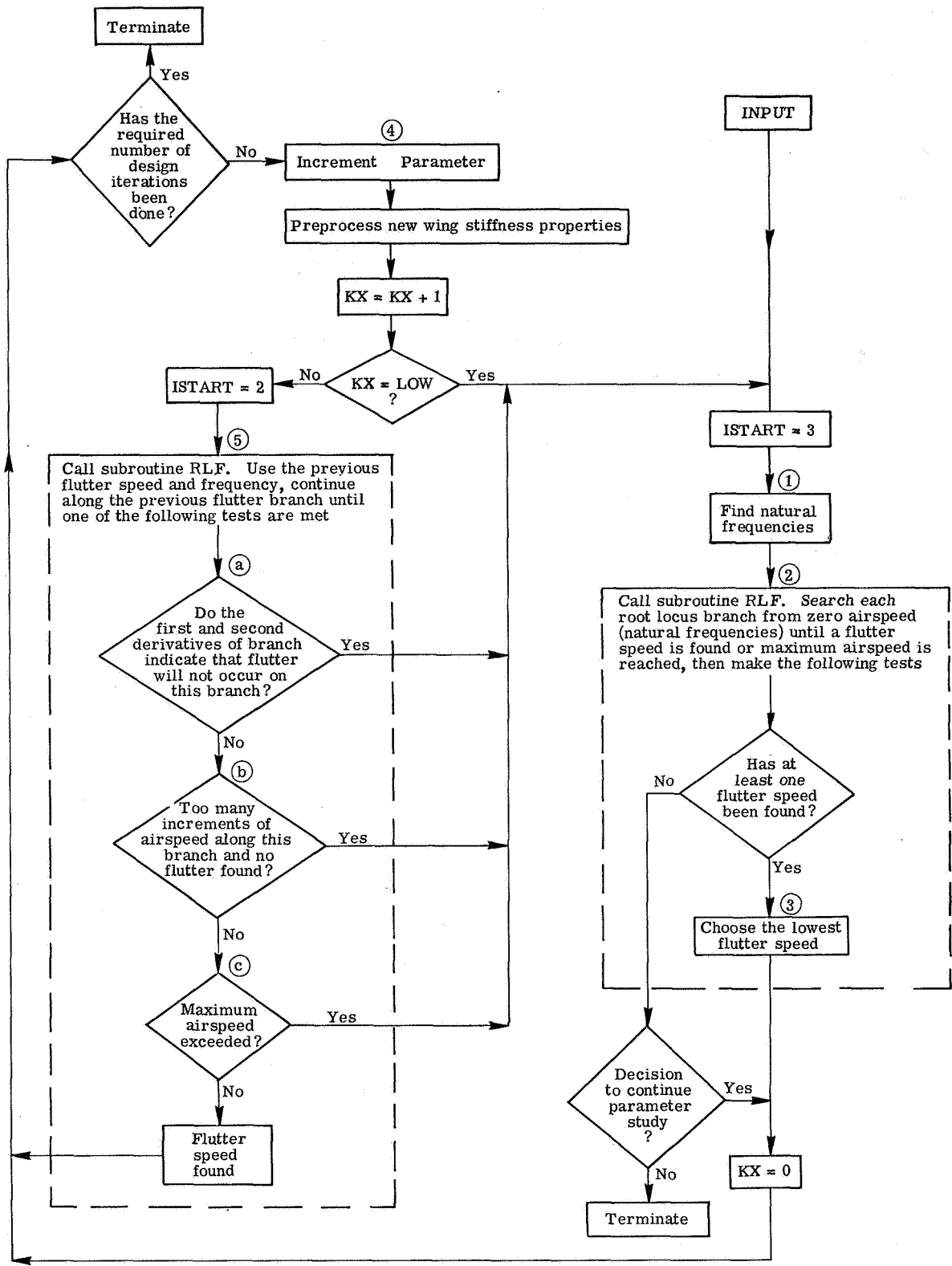


Figure 4.- Flow diagram of COMBOF.

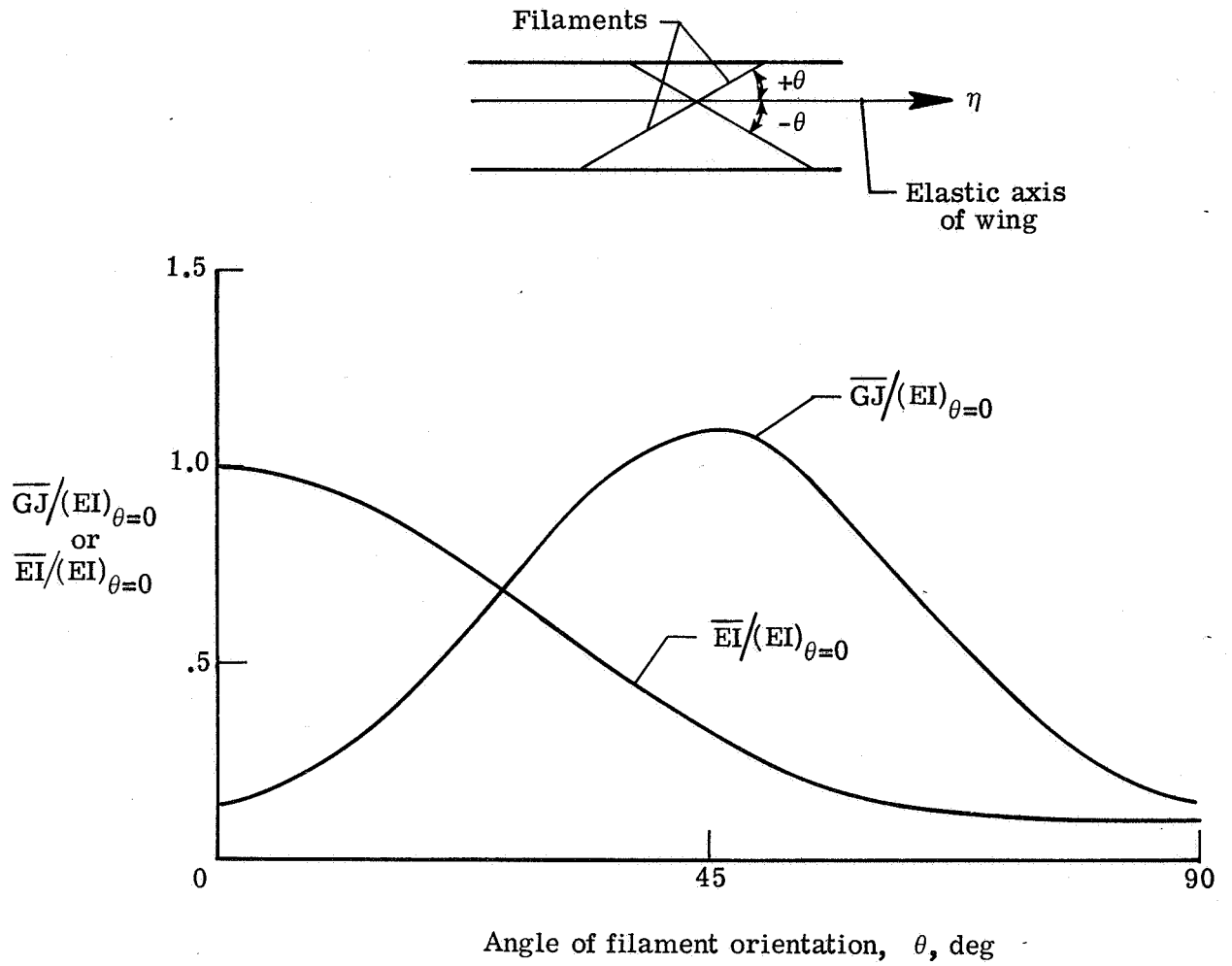


Figure 5.- Variation of GJ and EI with filament orientation for uniform wing.

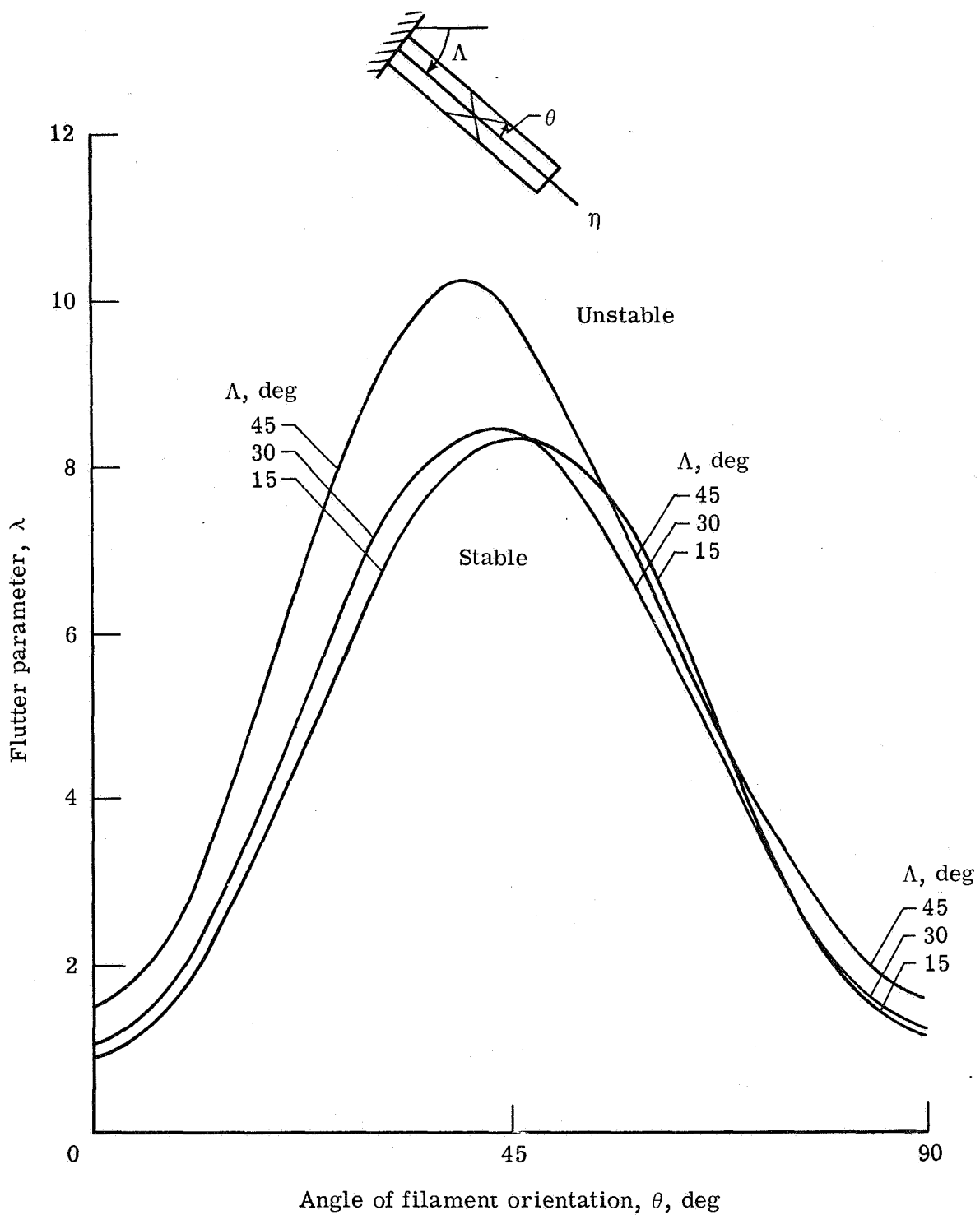


Figure 6.- Effect of filament orientation on flutter speed of several swept cantilever wings for $m/m_r \kappa = 8$.

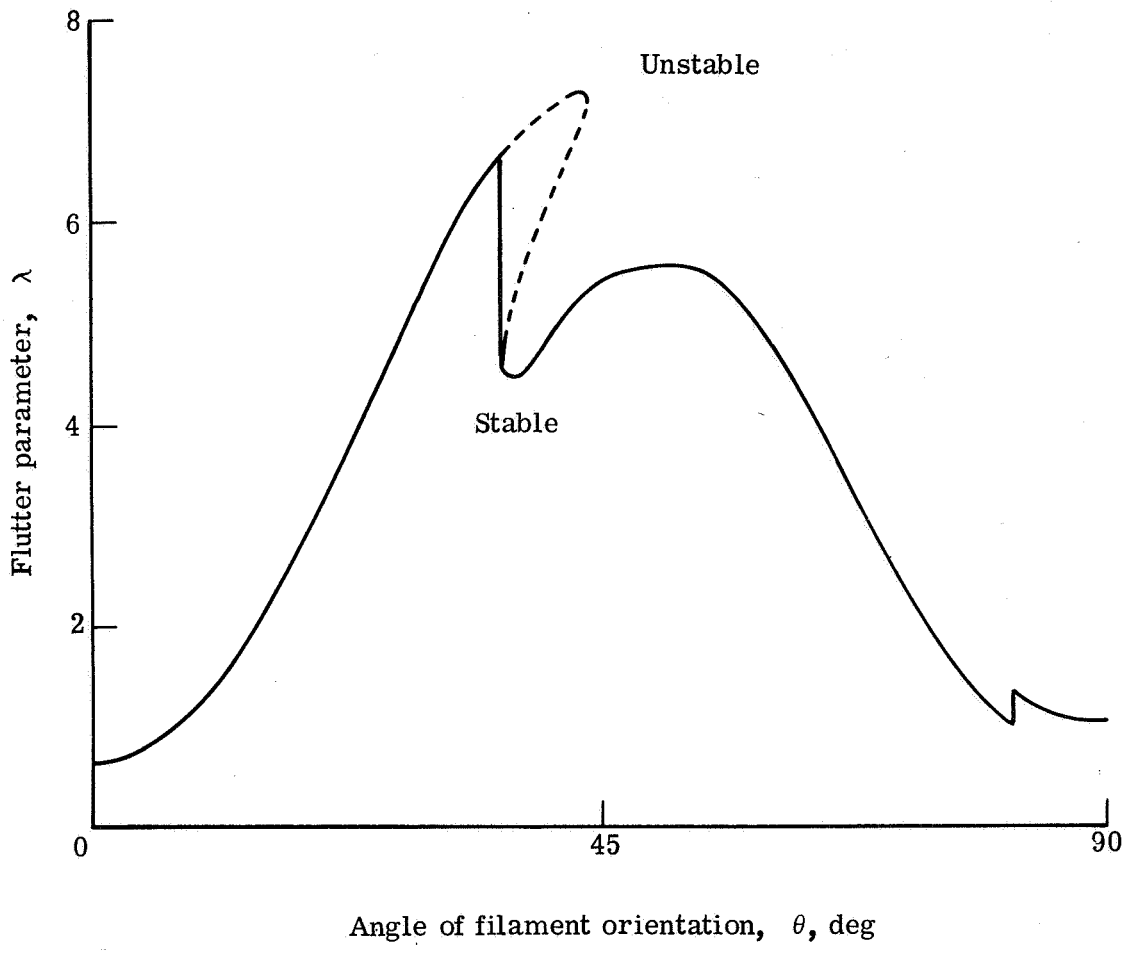


Figure 7.- Effect of filament orientation on the flutter speed of uniform rectangular straight cantilever wing with aspect ratio of 6.67 and $m/m_r \kappa = 64$.

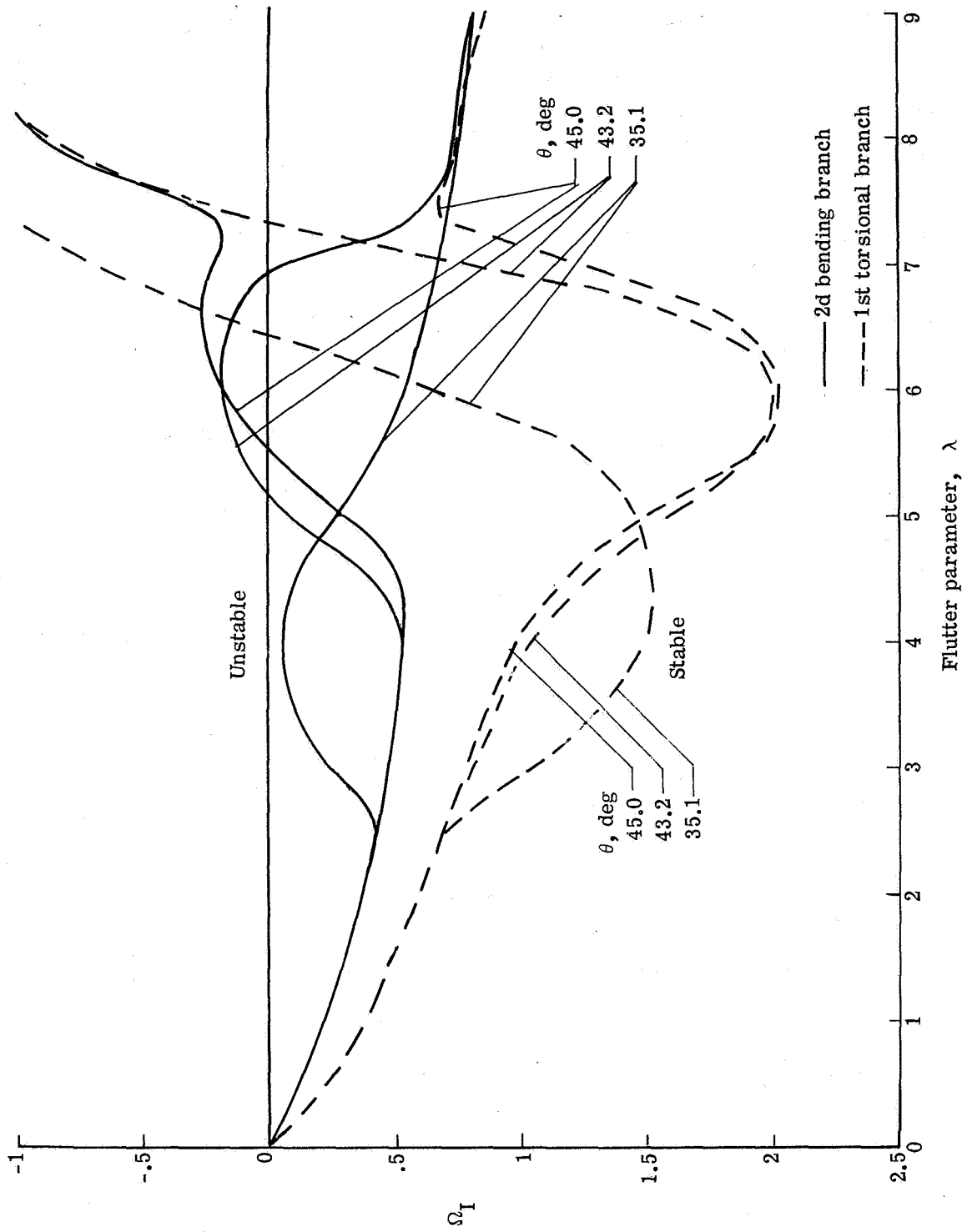


Figure 8.- Projection of root locus branches on imaginary plane at filament orientations near discontinuity of lowest flutter speed of uniform rectangular straight wing of aspect ratio 6.67 and $m/m_r \kappa = 64$.

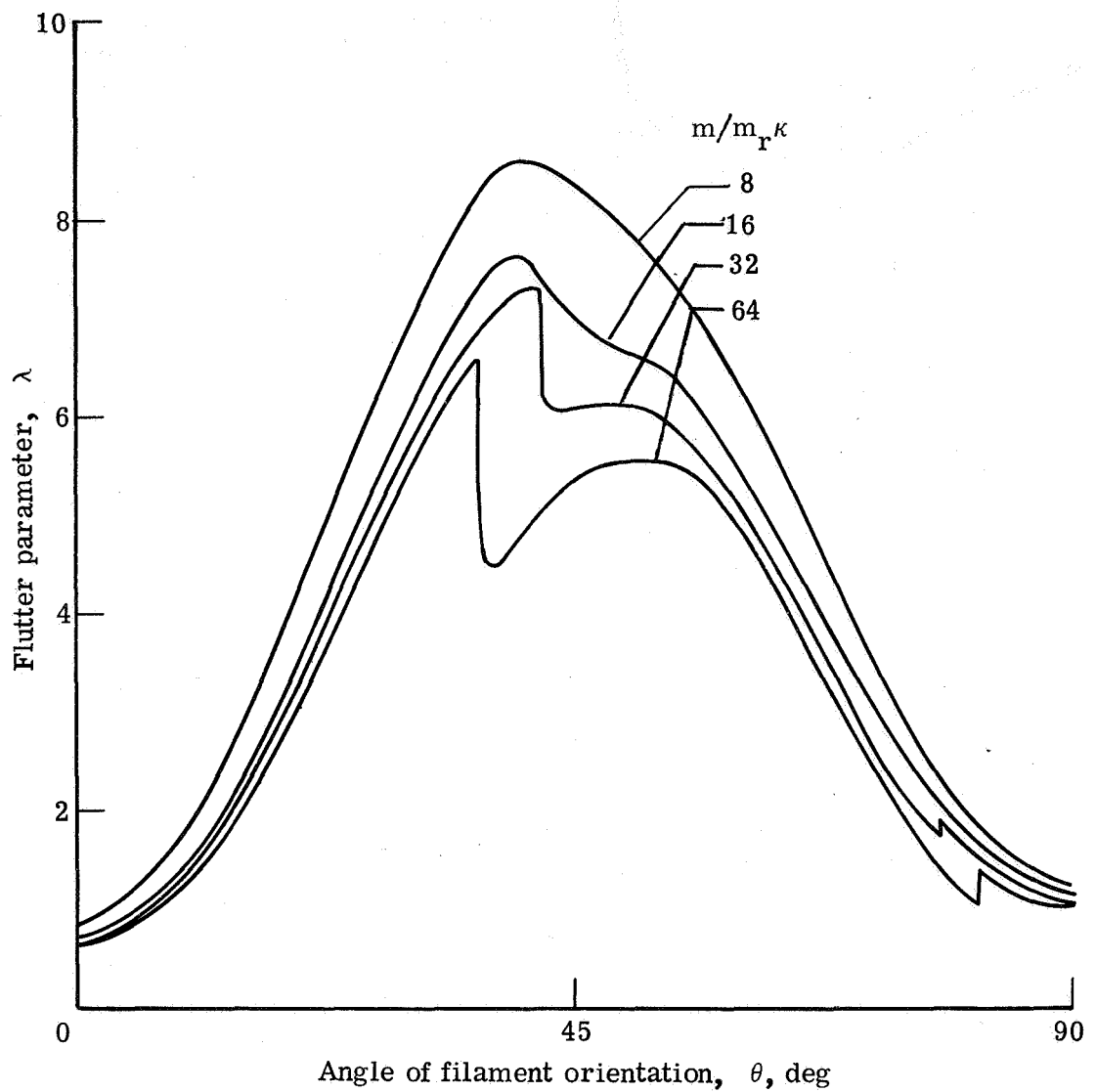


Figure 9.- Effect of filament orientation on flutter speed for uniform cantilever rectangular straight wings of aspect ratio 6.67 over a range of mass ratios.

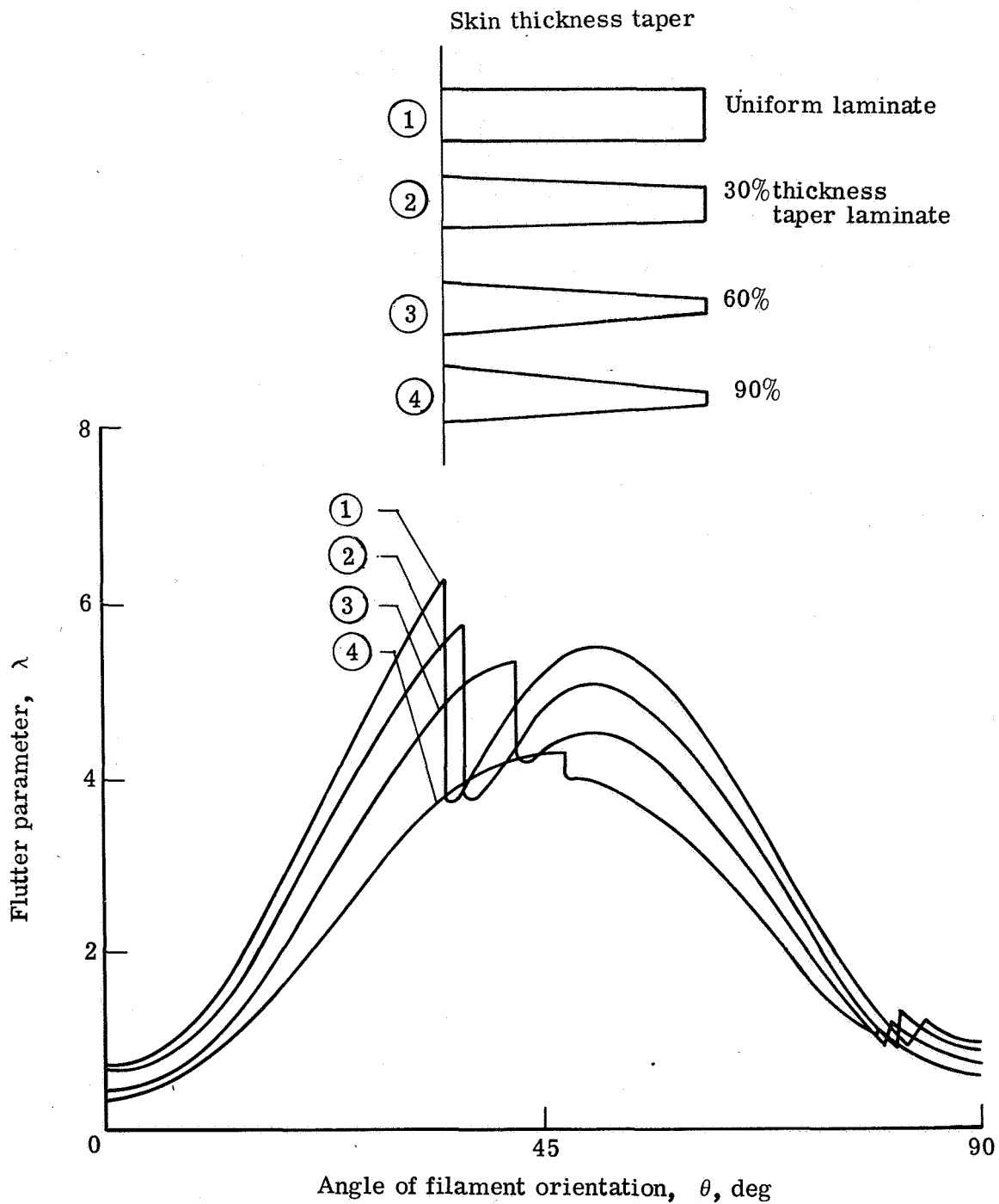


Figure 10.- Effect of filament orientation on flutter speed of variable lamina thickness cantilever rectangular straight wings of aspect ratio 6.67 and $m/m_r \kappa = 8$.

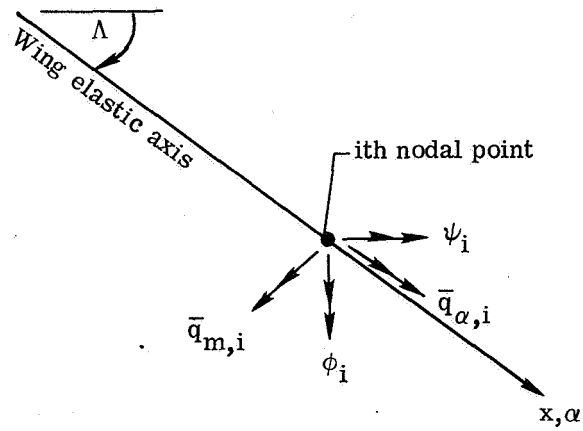
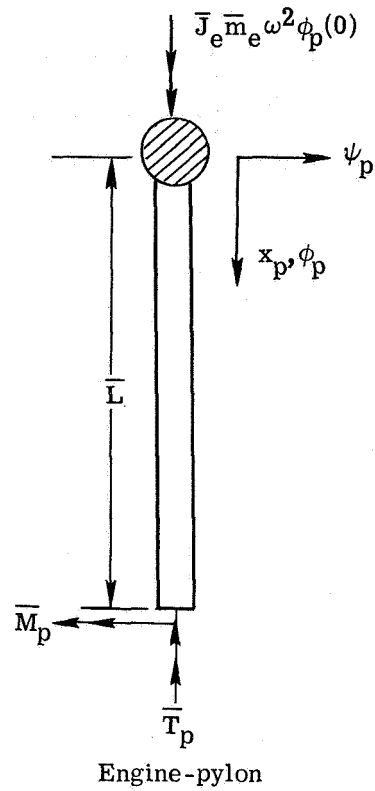


Figure 11.- Engine loads applied to wing elastic axis.

1. Report No. NASA TN D-7539	2. Government Accession No.	3. Recipient's Catalog No.	
4. Title and Subtitle FLUTTER ANALYSIS OF SWEEP-WING SUBSONIC AIRCRAFT WITH PARAMETER STUDIES OF COMPOSITE WINGS		5. Report Date September 1974	
		6. Performing Organization Code	
7. Author(s) J. M. Housner and Manuel Stein		8. Performing Organization Report No. L-9260	
		10. Work Unit No. 501-22-03-06	
9. Performing Organization Name and Address NASA Langley Research Center Hampton, Va. 23665		11. Contract or Grant No.	
		13. Type of Report and Period Covered Technical Note	
12. Sponsoring Agency Name and Address National Aeronautics and Space Administration Washington, D.C. 20546		14. Sponsoring Agency Code	
		15. Supplementary Notes	
16. Abstract <p>This paper presents a computer program which has been developed for the flutter analysis, including the effects of rigid-body roll, pitch, and plunge, of swept-wing subsonic aircraft with a flexible fuselage and engines mounted on flexible pylons. The program utilizes a direct flutter solution in which the flutter determinant is derived by using finite differences, and the root locus branches of the determinant are searched for the lowest flutter speed. In addition, a preprocessing subroutine is included which evaluates the variable bending and twisting stiffness properties of the wing by using a laminated, balanced ply, filamentary composite plate theory. The program has been substantiated by comparisons with existing flutter solutions.</p> <p>The program has been applied to parameter studies which examine the effect of filament orientation upon the flutter behavior of wings belonging to the following three classes: wings having different angles of sweep, wings having different mass ratios, and wings having variable skin thicknesses. These studies demonstrated that the program can perform a complete parameter study in one computer run. The program is designed to detect abrupt changes in the lowest flutter speed and mode shape as the parameters are varied.</p>			
17. Key Words (Suggested by Author(s)) Subsonic flutter Composite wing		18. Distribution Statement Unclassified - Unlimited STAR Category 32	
19. Security Classif. (of this report) Unclassified	20. Security Classif. (of this page) Unclassified	21. No. of Pages 106	22. Price* \$ 4.00

NATIONAL AERONAUTICS AND SPACE ADMINISTRATION
WASHINGTON, D.C. 20546

OFFICIAL BUSINESS
PENALTY FOR PRIVATE USE \$300

SPECIAL FOURTH-CLASS RATE
BOOK

POSTAGE AND FEES PAID
NATIONAL AERONAUTICS AND
SPACE ADMINISTRATION
451



POSTMASTER: If Undeliverable (Section 158
Postal Manual) Do Not Return

"The aeronautical and space activities of the United States shall be conducted so as to contribute . . . to the expansion of human knowledge of phenomena in the atmosphere and space. The Administration shall provide for the widest practicable and appropriate dissemination of information concerning its activities and the results thereof."

—NATIONAL AERONAUTICS AND SPACE ACT OF 1958

NASA SCIENTIFIC AND TECHNICAL PUBLICATIONS

TECHNICAL REPORTS: Scientific and technical information considered important, complete, and a lasting contribution to existing knowledge.

TECHNICAL NOTES: Information less broad in scope but nevertheless of importance as a contribution to existing knowledge.

TECHNICAL MEMORANDUMS: Information receiving limited distribution because of preliminary data, security classification, or other reasons. Also includes conference proceedings with either limited or unlimited distribution.

CONTRACTOR REPORTS: Scientific and technical information generated under a NASA contract or grant and considered an important contribution to existing knowledge.

TECHNICAL TRANSLATIONS: Information published in a foreign language considered to merit NASA distribution in English.

SPECIAL PUBLICATIONS: Information derived from or of value to NASA activities. Publications include final reports of major projects, monographs, data compilations, handbooks, sourcebooks, and special bibliographies.

TECHNOLOGY UTILIZATION PUBLICATIONS: Information on technology used by NASA that may be of particular interest in commercial and other non-aerospace applications. Publications include Tech Briefs, Technology Utilization Reports and Technology Surveys.

Details on the availability of these publications may be obtained from:

**SCIENTIFIC AND TECHNICAL INFORMATION OFFICE
NATIONAL AERONAUTICS AND SPACE ADMINISTRATION
Washington, D.C. 20546**